α2δ-1 Signaling Drives Pathological Synaptogenesis, Cell Death and Epileptogenic Circuit Reorganization in a Model of Insult-Induced Cortical Malformation

A thesis submitted by

Lauren Andresen Lau

in partial fulfillment of the requirements

for the degree of

Doctor of Philosophy

In

Neuroscience

Tufts University

August 2017

Adviser: Chris Dulla, PhD

Abstract

Developmental cortical malformations (DCM) are a common cause of pharmacoresistent epilepsy. DCMs are a group of diverse disorders, associated with varied seizure phenotypes and co-morbidities, including cognitive impairments and developmental delays. DCMs can result from genetic mutations, as well as pre- and peri-natal insults. Hypoxia, viral infection, and traumatic injury are the most common environmental causes of DCMs, and are associated with the sub-syndromes polymicrogyria, schizencephaly, and focal cortical dysplasia Type IIId. To understand how neonatal brain insult leads to cortical malformation and network dysfunction, we utilized the neonatal freeze lesion (FL) model. A freezing insult is delivered to the skull on the day of birth, inducing a focal hypoxic insult. A cortical malformation develops, along with hyperexcitability and spontaneous seizures. We found here that thrombospondin (TSP) is upregulated following FL. During normal development, TSP drives excitatory synapse formation. The neuronal receptor for TSP-mediated synaptogenesis is the calcium channel subunit $\alpha 2\delta$-1, which is also upregulated following FL. We hypothesize that increased TSP/$\alpha 2\delta$-1 signaling may lead to exuberant excitation in the FL cortex. The drug gabapentin (GBP) blocks $\alpha 2\delta$-1-mediated synaptogenesis, and in several models, prevents injury-induced hyperexcitability and cell death. We found that GBP treatment prevented excitatory synaptogenesis, network hyperexcitability and cell death following FL. GBP has multiple targets, however, and it is unknown whether its neuroprotective effects are mediated by its actions on $\alpha 2\delta$-1. To

address this, we genetically deleted α2δ-1 and examined FL-induced pathology using electrophysiological and anatomical approaches. Deletion of α2δ-1 reduced FL-driven cell death, malformation, excitatory synaptogenesis, and network hyperexcitability. Genetic deletion of α2δ-1 also eliminated gabapentin's neuroprotective effects and the majority of its effects on network physiology. GBP did have a mild α2δ-1-independent effect on excitatory synaptogenesis. Our studies show that α2δ-1 activity contributes to FL pathophysiology and that gabapentin acts at α2δ-1 to provide neuroprotection and to prevent injury-induced synaptogenesis and epileptiform network formation. This suggests that inhibiting α2δ-1 signaling may have therapeutic promise to reduce cell death and epileptogenic network reorganization associated with neonatal injury and developmental cortical malformations.

Acknowledgments

During my time as a graduate student at Tufts, I have been fortunate to meet and work with many wonderful people who have contributed to my growth as a person, and as a scientist. I would like to begin by thanking my adviser, Dr. Chris Dulla, for his support, guidance and encouragement throughout my graduate studies. Chris provided a fun, stimulating environment in which to conduct research and has taught me to be an enthusiastic scientist, and to push forward through challenges. I feel so grateful to have been his student. I would also like to thank all the Dulla lab members, past and present. In particular, I would like to thank Amaro and David for being the pioneering members of the lab with me. I would also like to thank Liz, Jen, Jenny, Moritz, Dave, Danielle and Kyle, who have all been so helpful and have made the lab an enjoyable place to be.

I would like to thank my thesis committee members, Dr. Jamie Maguire, Dr. Rob Jackson, and Dr. Yongjie Yang, for all the guidance they have provided. I would also like to acknowledge my external examiner, Dr. Alex Rotenberg and am grateful for his time and expertise in serving on my defense committee. I would also like to thank the rest of the Tufts Neuroscience faculty, in particular, Dr. Michele Jacob, for our collaborative work on the CURE infantile spasm project, and Dr. Alexei Degterev, for his help exploring cell death mechanisms associated with this project. I would also like to thank the members of the Neuroscience program, in particular Jackie, Alex, Drew and Laura who started this journey with me.

Outside of Tufts, I would like to thank all my friends and family, who have enriched my life in so many ways and remind me of the important things outside of lab. I would like to thank my parents for their ever present love and support, which has gotten me to this point. I need to thank my husband, Allen, who has made all things possible. Finally, I thank my son, Lucas, who has brought such joy to my life.

Table of Contents

List of Tables

List of Figures

List of Copyrighted Materials Produced by the Author

This volume contains figures reproduced from the copyrighted publication:

> Andresen L, Hampton D, Taylor-Weiner A, Morel L, Yang Y, Maguire J, Dulla CG (2014) Gabapentin attenuates hyperexcitability in the freeze-lesion model of developmental cortical malformation. Neurobiology of disease 71:305-316.

I have obtained written permission from the rights holder to reproduce these copyrighted materials in my dissertation.

List of Abbreviations

aCSF	Artificial Cerebrospinal Fluid
AMPA	4-isoxazolepropionic acid
CCC	Cation Chloride Co-transporter
CFP	Cyan Fluorescent Protein
CNS	Central Nervous System
DCM	Developmental Cortical Malformations
EAAT	Excitatory Amino Acid Transporter
EEG	Electroencephalogram
FCD	Focal Cortical Dysplasia
fEPSP	Field Excitatory Post-synaptic Potential
FGF	Fibroblast Growth Factor
FL	Freeze Lesion
FRET	Forster Resonance Energy Transfer
FS	Fast Spiking
GABA	γ-Aminobutyric acid
GAT	GABA Transporter
GBP	Gabapentin
GFAP	Glial Fibrillary Acid Protein
HCN	Hyperpolarization-activated Non-selective Cation
I.P.	Intraperitoneal
IEI	Inter-event Interval
K(IR)	Inwardly Rectifying Potassium
KA	Kainic Acid

KO	Knockout
KS	Kolmogorov-Smirnov
LGE	Lateral Ganglionic Eminence
LIS	Lissencephaly
LSPS	Laser-scanning Photostimulation
MAM	Methylazoxymethanol
mEPSC	Miniature Excitatory Post-synaptic Potential
MGE	Medial Ganglionic Eminence
mIPSC	Miniature Inhibitory Post-synaptic Potential
MZ	Microgyrial Zone
NGF	Nerve Growth Factor
NMDA	N-methyl-d-aspartate
OF	Open Field
P	Postnatal day
PAF-AH	Platelet-activating Factor Acetylhydrolase
PB	Phenobarbital
PMG	Polymicrogyria
PMZ	Paramicrogyrial Zone
PNH	Periventricular Nodular Heterotopia
PNS	Peripheral Nervous System
RPM	Rotations Per Minute
SBH	Subcortical Band Heterotopia
SEM	Standard Error Mean
SVZ	Subventricular Zone

TH	Threshold
TSC	Tuberous Sclerosis Complex
TSP	Thrombospondin
TUNEL	Terminal Deoxynucleotidyl Transferase dUTP Nick End Labeling
VGCC	Voltage-gated Calcium Channel
YFP	Yellow Fluorescent Protein

Chapter 1: Introduction

1.1: Epilepsy and Developmental Cortical Malformation

Epilepsy is characterized by recurrent, unprovoked seizures and is the fourth most common neurological disorder in the United States (after migraine, stroke and Alzheimer's disease) (Hirtz et al., 2007). Epilepsy represents a spectrum of disorders, with a range of seizure types and severity, etiologies and co-morbidities. It can affect people of all ages, but the onset is most often in childhood or late adulthood (Hauser et al., 1980). Despite decades of research and the development of many new anticonvulsant drugs, about one third of patients still do not have good seizure control with currently available treatment options (Kwan and Brodie, 2000). Poor seizure control is associated with decreased quality of life and increased risk of sudden unexplained death in epilepsy (Golyala and Kwan, 2017; Jacoby and Baker, 2008; Tomson et al., 2008).

Malformations of cortical development are increasingly being recognized as a common cause of epilepsy in childhood and are often found in patients with pharmaco-resistant epilepsy. Focal cortical dysplasia is the most common indication for pediatric epilepsy surgery (Krsek et al., 2008). Epilepsy surgery can be effective for achieving seizure freedom for patients with drug-resistant focal epilepsy, with success rates varying from 25-85% depending on the subtype of epilepsy, surgery location and age of the patient (Ryvlin et al., 2014). However, not all patients are candidates for surgical resection (if there is no lesion identified by MRI or the lesion is in an unfavorable region for surgery) and there is often considerable delay for drug-resistance epilepsy patients to be referred for surgery (Dalic and Cook, 2016). Overall, the epilepsies require more

research aimed at understanding the underlying pathophysiological mechanisms of epileptogenesis, which will impact therapy development for seizure control, disease modification, and cures. The work of this thesis has focused on elucidating key signaling events in the pathophysiology of a model of developmental cortical malformation; we will therefore briefly review the normal developmental program of the cortex and the current clinical classifications of developmental cortical malformations.

Normal Cortical Development

In order to understand pathological conditions of development, such as those seen with malformations of cortical development, we should first consider normal cortical development in both humans and rodents. The cerebral cortex is a modular structure that is formed by the induction of neurons in the neuroepithelial sheet, which then need to differentiate, migrate and organize into the mature cortex. Modules of neurons are generated by gradients of extracellular signaling molecules and transcription factors. The cortex is composed of six layers of neurons, which have distinct cell types and connectivity patterns. These vertical layers span the cortex; the cortex is further organized into functionally distinct areas, such as those for motor control, and visual and auditory processing.

The development of the cortex begins in the embryonic cerebral vesicle, at the rostral end of the neural tube. Neurogenesis begins at embryonic day 33 (E33) in humans (Bystron et al., 2006) and E10 in mice (Garcia-Moreno et al., 2007) in the ventricular zone. A gradient of fibroblast growth factor (FGF) signaling begins area patterning (Fukuchi-Shimogori and Grove, 2001). Radial glia are then induced by a set of genes,

which includes *GLAST, FOXG1*, *LHX2*, *PAX6* and *EMX2* (Gotz et al., 1998; Molyneaux et al., 2007). Radial glia play an important role as both scaffolds for neuronal migration and as key neuronal progenitors (Barry et al., 2014; Gotz and Barde, 2005). Progenitors also begin to accumulate in the new subventricular zone (SVZ). Intermediate neuronal precursors express a different set of transcription factors, including *TBR2*, *NGN2*, *CUX1* and *CUX2*, but not *GLAST* or *PAX6* (Gotz and Barde, 2005). These progenitors will primarily form glutamatergic, pyramidal neurons. In contrast, most GABAergic interneurons are generated by precursors in the medial and lateral ganglionic eminences (MGE and LGE) (Wonders and Anderson, 2006).

Neurons must then migrate to the proper location within the developing cortex. Glutamatergic neurons migrate radially, following the radial glia, while interneurons will first migrate tangentially, then radially. The cortical plate is formed in an inside-out manner, such that the earliest-born neurons will first form the future layer VI and the last-born neurons migrate past the existing layers to form layer II (Angevine and Sidman, 1961; Rakic, 1974). In humans, the peak of neuronal migration into the cortex occurs between the third and fifth months of gestation, and is complete by the third trimester (Gressens, 2000; Rakic et al., 1994; Sidman and Rakic, 1973). In rodents, neuronal migration is complete in the first post-natal week (Ignacio et al., 1995). The cortex then goes through a period of synaptogenesis and neuronal maturation, followed by refinement carried out by apoptosis and synaptic pruning. Perturbations in any aspect of this set of complex and overlapping processes can result in varied disorders and diseases.

Developmental Cortical Malformations

Developmental cortical malformations (DCM) are a group of diverse disorders that all involve a disruption of cortical development that lead to anatomical changes in the cerebral cortex. It is estimated that 25% to 40% of intractable childhood epilepsy can be attributed to a DCM (Leventer et al., 2008). DCMs represent a spectrum of disorders, with diverse etiologies. Genetic mutations are increasingly being recognized as causes of cortical malformations; Table 1 summarizes the main genes associated with various subtypes of DCM.

Classification of DCMs is based on the first developmental stage that is disrupted, the underlying genes or pathways that are disturbed or, when the biological pathways involved are unknown, based on imaging features. DCMs are classified into 3 groups: Group I is 'Malformations secondary to abnormal neuronal or glial proliferation or apoptosis', Group II is 'Malformation secondary to abnormal neuronal migration, and Group III is 'Malformations secondary to abnormal postmigrational development' (Barkovich et al., 2012). Here we consider the most common disorders in each group.

Group I includes microcephaly and megalencephaly, (defined as abnormally small or large brains, respectively) and tuberous sclerosis. Tuberous sclerosis complex (TSC) is an autosomal dominant disorder caused by mutations in either the *TSC1* or *TSC2* gene, leading to tumor formation in multiple organs (Crino et al., 2006). The clinical features of TSC are highly variable depending on the effected organ systems; however, up to 90% of patients have brain abnormalities and epilepsy (Chu-Shore et al., 2010). Epilepsy in TSC is typically associated with cortical tubers, and surgical resection can sometimes

eliminate seizure (Wong, 2008). Dysfunction of mTOR signaling is heavily implicated in driving TSC pathology and mTOR inhibitors have been shown to reverse many TSC-associated pathologies (Carson et al., 2012; Krueger et al., 2013; Zeng et al., 2008). Several causative genes of microcephaly have been identified, which affect pathways involving neurogenesis and the cell cycle phase of mitosis (Thornton and Woods, 2009). Microcephaly may also be caused by environmental factors that alter neurogenesis, such as Zika virus infection (Garcez et al., 2016). The underlying pathways resulting in megalencephaly are not well defined, therefore disorders in this group are usually clinically defined (Barkovich et al., 2012); however, mutations in the PI3K-AKT3-mTOR pathway have been implicated in some forms of megalencephaly (Lee et al., 2012). Group I malformations are often associated with developmental delay, intellectual disability and pharmacoresistant, early-life seizures (Guerrini and Dobyns, 2014).

Group II disorders include heterotopia, subcortical heterotopia, lissencephaly, and cobblestone malformations. Heterotopia is defined as a group of cells found in the wrong location, within the tissue of origin; heterotopic neurons come in many forms and sizes, with the most common form being periventricular nodular heterotopia (PNH). The majority of patients with PNH present with partial seizures, which are often intractable (Dubeau et al., 1995). Mutations in the *FLNA* gene have been identified in roughly 80% of familial cases, and 20% of sporadic PNH (Fox et al., 1998; Lange et al., 2015; Sheen et al., 2001). The gene product Filamin A is a large, actin-binding protein, which is necessary for proper cell motility (Baldassarre et al., 2009; Cunningham et al., 1992).

Subcortical band heterotopia (SBH), also known as double cortex, is characterized by bands of grey matter within the white matter between the cortex and lateral ventricles. Nearly all SBH patients have epilepsy, which is often intractable and many patients also present with intellectual disability (Barkovich and Lindan, 1994). SBH is most often caused by mutations in the *DCX* gene (Matsumoto et al., 2001), which encodes a microtubule-associated protein that is expressed in migrating neuroblasts (Gleeson et al., 2000). Both of these disorders arise from abnormal neuronal migration. The etiology of other forms of heterotopia remains poorly defined.

Lissencephaly (LIS), or smooth brain, is characterized by absent or decreased gyration, cortical thickening, and a smooth cortical surface. Several types of LIS are recognized, with a range of severities and pathological features. Many children with LIS present with developmental disabilities and infantile spasms, and go on to have mixed seizure types, which are often intractable (Barkovich et al., 2012). Rare forms of severe lissencephaly syndromes are also associated with a high mortality rate (Barkovich et al., 2012). The most common cause of LIS is deletion or mutations in the *LIS1* gene (Dobyns et al., 1993; Pilz et al., 1998); however several genetic causes of LIS have been identified (Barkovich et al., 2012; Parrini et al., 2016). *LIS1* encodes a regulatory subunit of platelet-activating factor acetylhydrolase (PAF-AH), which causes neuronal migratory defects when mutated (Hirotsune et al., 1998).

Cobblestone malformations, also known as cobblestone lissencephaly, are characterized by a smooth, pebbled appearance of the cortex with a thickened cortex and abnormal white matter. In addition to epilepsy, cobblestone malformations are associated with

eye abnormalities, muscular dystrophy, intellectual disability, and early death (Pang et al., 2008). Several genetic causes of cobblestone malformations have been identified, all of which are involved in the glycosylation of alpha dystroglycan, which normally act to maintain cell stability through its interaction with multiple proteins in the extraceulluar matrix (Pang et al., 2008). Deficits in this pathway allow for over-migration of neurons in the cortex.

Group III disorders include polymicrogyria, schizencephaly and focal cortical dysplasia. Polymicrogyria (PMG) is characterized by excessive folding of the cortical mantle. This generates irregular cortical gyration characterized by small gyri separated by shallow sulci (Crome, 1952). PMG is a spectrum and the extent of the misfolded cortex can vary from small areas of microgyric cortex to wide swaths of the cortex displaying the characteristic uneven, irregular appearance. PMG is associated with epilepsy and cognitive delays and can be caused by insult (hypoperfusion of the neonatal brain (Barkovich et al., 1995)), infection (Barkovich et al., 1995), and genetic mutation (Jansen and Andermann, 2005; Stutterd and Leventer, 2014). PMG that presents with deep clefts is classified as schizencephaly (Barkovich and Kjos, 1992).

Focal cortical dysplasia (FCD) was first identified by histological analysis of brain tissue resected from patients with pharmacoresistant epilepsy, which revealed a malformation of the cortex which contained “large, bizarre neurons” (Taylor et al., 1971). FCD represents a spectrum of anatomical disruptions that can be characterized based on the severity of malformation, and it can be focal or multi-focal. FCDs may be caused by prenatal and perinatal insults, such as asphyxia, bleeding or stroke (Barkovich et al.,

2012; Krsek et al., 2010) or by mutations in genes regulating PI3K-AKT3-mTOR signaling (Iffland and Crino, 2017); however, in many cases the underlying cause of FCD is unknown. FCD patients normally present with seizures, developmental delay and focal neurological deficits (Leventer et al., 2008). Surgical resection of the area of malformation is often used to treat FCDs, as the resultant epilepsy is often intractable and the lesions are often easily identified radiologically.

Genes Associated with DCMs	
DCM Subtype	**Associated Genes**
Group I:	
Tuberous Sclerosis	**TSC1, TSC2**
Megalencephaly	AKT3, PIK3CA, MTOR
Microcephaly	MCPH1, CDK5RAP2, ASPM, CENPJ, SIL, SLC25A19
Group II:	
Periventricular Nodular Heterotopia	**FLNA,** ARFGEF2
Subcortical Heterotopia	**DCX,** LIS1
Lissencephaly	**LIS1,** DCX, TUBA1A, ARX, RELN
Cobblestone Lissencephaly	Fukutin, POMT1, POMT2, POMGnT1
Group III:	
Polymicrogyria	GPR56, EMX2, TUBA1A, TUBA8, TUBB2B, TUBB3
Focal Cortical Dysplasia	MTOR, DEPDC5, NPRL2, NPRL3, PIK3CA, TSC1/2
*Highly prevelant gene mutations are indicated in bold	

Table 1.1: Gene Mutations Associated with DCMs

1.2: Neonatal Freeze Lesion Model

The desire to understand DCMs has resulted in the generation of a number of useful animal models. In this study, we made use of the neonatal freeze lesion (FL) as a model of DCM associated with neonatal injury (such as PMG, schizencephaly, and FCD type IIId). FL recapitulated many of the key features of PMG and FCD type IIID, including etiology, anatomical reorganization and spontaneous seizures. A number of other valuable acquired models exist, including the methylazoxymethanol (MAM) model of prenatal teratogen exposure, the in utero irradiation model, in utero camustine (BCNU) and neonatal focal ibotenate (Benardete and Kriegstein, 2002; Luhmann, 2015; Moroni et al., 2011; Redecker et al., 1998; Takano et al., 2004). Additionally, genetic models of tuberous sclerosis, lissencephaly, and heteroptopia exist and have contributed greatly to our understanding of DCM pathogenesis (Wong, 2009; Wong and Roper, 2016). While a number of genes linked to polymicrogyria and FCD have been identified (Iffland and Crino, 2017; Kuzniecky, 2015; Stutterd and Leventer, 2014), a genetic animal model that replicates the structural and seizure phenotypes of human PMG or FCD remains to be identified.

History of the Freeze Lesion Model

Briefly, the FL model is based on the finding that placing a freezing probe on the surface of the skull on or near the day of birth results in the generation of a microgyrus in the rodent brain. The resultant microgyrus is a focal, four-layer structure surrounded by histologically normal six-layered cortex. Over decades of use, researchers have determined that this relatively simple, neonatal insult results in the generation of a

hyperexcitable cortical network surrounding the microgyrus and recent studies have demonstrated that spontaneous seizure occur in animals after FL (Sun et al., 2016).

The earliest report demonstrating that cortical freezing can create an epileptic focus dates back to Openchowski (1883), who found that local cooling of the cortex in adult rabbit and dog can lead to recurrent seizures. However, as with many injury models, only a minority of animals with this type of adult freeze lesion goes on to develop spontaneous seizures. Focal lesions created by cortical cooling in the adult cat have also been shown to be epileptogeneic (Hanna and Stalmaster, 1973; Smith and Purpura, 1960; Stalmaster and Hanna, 1972). In these studies, the epileptiform activity emerged within an hour of the freezing injury. In some animals the epileptiform activity was progressive and led to the formation of a seizure focus, but often the epileptiform activity would gradual diminish after the first week. The neonatal freeze lesion model was first introduced in rats by Dvorak and Feit (1977; Dvorak et al., 1978).

In general, inducing a freeze lesion is carried out with a relatively simple surgical procedure. Rodents, either mice or rats, are utilized on day of birth (postnatal day 0; P0) or one day later (P1). Animals are anesthetized via hypothermia and a small incision is made in the scalp to reveal the skull. Then a cooled metal bar (-60 to -100^{o}C) is briefly (≈ 5 seconds) touched to the calvarium. Cortical cooling of the rodent cortex during the neonatal period reliably drives the formation of a focal cortical malformation consisting of a four-layered microgyrus, similar to the histology observed in human polymicrogyria. In the first hours and days after freezing, the cortex is marked by a necrotic area. The four-layered cortex begins to emerge 4 days after freezing and is fully formed 10 days

after freezing (Dvorak and Feit, 1977). The area immediately adjacent to the lesion (paramicrogyrial zone—PMZ) has disrupted neurofilament staining, with abnormal placement and orientation of the glutamatergic processes (Humphreys et al., 1991). The PMZ was shown to be a region of hyperexcitability (Jacobs et al., 1996; Luhmann et al., 1996), establishing the utility of the FL model for examining mechanisms of epileptogenesis associated with malformations of cortical development.

Structure of the Freeze Lesion

Human polymicrogyria has many histopathological signatures, but is often characterized as a four-layered, over folded cortex. Four layered polymicrogyria is associated with late fetal insults (>24 weeks post-conception)(Barth, 1987). The microgyrus generated by freeze lesion is strikingly similar to this 4-layered structure (Fig. 1.1). Layer i of the microgyrus, the molecular layer, is continuous with normal cortical layer I, contains few neurons, and follows the entire infolding of the microgyrus. Layer ii of the microgyrus, an infolded layer rich in neurons, makes up the bulk of the migrogyrus, and is thought to contain mainly neurons normally found in layer II/III (Dvorak et al., 1978). Layer iii of the microgyrus is a neuron free area that consists mainly of axons passing under the microgyrus and reactive astrocytes (Bordey et al., 2001). Layer iv of the microgyrus is very thin and contains layer IV-VI neurons spared during the freeze lesion surgery (Humphreys et al., 1991). In the microgyrus, as well as the PMZ, there are many reactive astrocytes, as indicated by heavy glial fibrillary acid protein (GFAP) labeling (Bordey et al., 2001; Rosen et al., 1992). Unlike neurons, astrocytes undergo a large amount of injury-induced proliferation (Bordey et al., 2001). Overall, the microgyrus created by

freeze lesion has many structure, etiological, and cellular similarities to human polymicrogyria-associated with early life cortical insult.

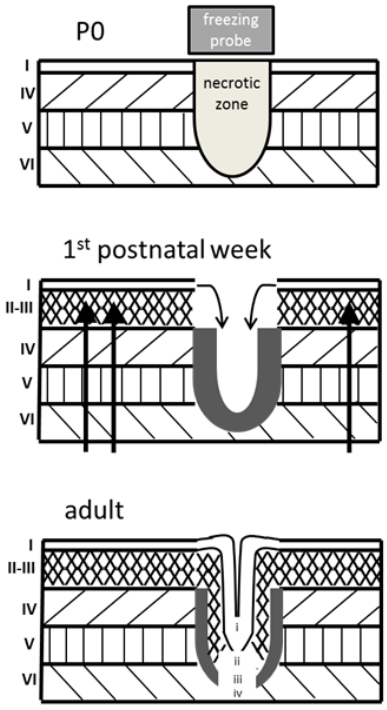

Figure 1.1. Schematic of Freeze Lesion formation

Illustration of the result of freeze lesion on P0 in newborn rodent pup, showing the loss of deep layer cells and the eventual formation of a 4-layer microgyrus (denoted by lower case letters) and the surrounding 6-layered cortex (denoted by upper case letters) as upper layer cells migrate into the cortex

In vivo Seizure Activity

For many years, it was believed that spontaneous seizures did not occur in the FL model. A number of robust and high quality studies attempted to identify seizures in FL animals to no avail (Kellinghaus et al., 2007; Scantlebury et al., 2004). However, recent work finds that an altered FL protocol, where multiple freezing injuries are performed on

embryonic day 18, does result in spontaneous seizure in ~70% of multiple FL animals (Kamada et al., 2013). Sun et al. (2016) have also shown non-convulsive, spike-wave seizures in FL mice. In this study, roughly 90 percent of animals had at least one spontaneous seizure event over the course of 24 hours, and a subset of animals presented with a chronic seizure state, consisting of bursts of rhythmic high-amplitude spike-wave activity that persisted throughout the recording session. FL animals also show disrupted cortical and subcortical synchrony, with the reduction in synchronous burst activity being greatest near the lesion (Williams et al., 2016).

In vitro Epileptiform Activity in the FL Model

Besides the anatomical similarities to human DCMs, the FL model has gained traction as a preclinical tool because in vitro epileptiform activity can be readily evoked in acute brain slices from FL animals. In vitro epileptiform activity refers to abnormal prolonged, high amplitude network discharges with a significant high frequency component. Extracellular recording of field excitatory post-synaptic potentials (fEPSPs) reveal epileptiform activity as multiple population spikes superimposed on a large post-synaptic potential. This type of activity approximates abnormal epileptiform activity recorded interictally in human EEG defined as “distinctive waves or complexes, distinguished from background activity and resembling those recorded in human subjects suffering from epileptic disorder”(Chatrian et al., 1974). Epileptiform EEG activity is highly associated with epileptic disorders and has long-standing clinical diagnostic utility.

Pioneering work done by Jacobs and Prince established the presence and characteristics of epileptiform activity in the FL model. Through careful extracellular recording of FL rat cortical brain slices, a number of key aspects of hyperexcitability in the FL model were established. Epileptiform activity can be evoked robustly by stimulation of ascending cortical axons approximately 14 days after FL, although some epileptiform activity can be seen 11 days after FL (Jacobs et al., 1996). Lowering the magnesium levels in the artificial cerebrospinal fluid (aCSF) in the FL cortex can evoke abnormal network activity before P11 (Bell and Jacobs, 2014), suggesting abnormalities may exist before epileptiform activity can be evoked under physiological conditions. Evoked epileptiform activity is all-or-none, indicative of initiation of uncontrolled network activity, and relies on NMDA receptor activation (Luhmann et al., 1996). Greater than 80% of FL animals have at least 1 brain slice that generates epileptiform activity when assayed within 40 days of lesion. After 40 days post-lesion, the number of animals that demonstrate epileptiform activity decreases, although less so for FL performed on P1 as compared to P0 (Jacobs et al., 1999). Epileptiform fEPSPs persisted to some degree even in animals as old as 6 months of age. This emphasizes the long-lasting changes in network activity seen in the FL model.

The stimulation parameters used are critical to evoking epileptiform activity. Only low amplitude stimulation (1-2 times threshold, the minimum amount required to evoke a fEPSP) produces epileptiform responses. Greater stimulation intensity results in brief, short latency responses, similar to fEPSPs evoked in control cortical brain slices. Higher intensity stimulation is thought to evoke enhanced feed-forward inhibition, thus

inhibiting the production of epileptiform activity (Jacobs et al., 1999). Epileptiform activity is also most robustly evoked when simulation occurs with low frequency. If stimulation occurs more frequently than 0.4 Hz, epileptiform activity is not maintained. The site of stimulation is also critical to evoking epileptiform activity. Stimulation of the white matter beneath the microgyrus fails to evoke epileptiform activity. Epileptiform activity can be evoked from the border of the microgyrus to approximately 2mm away.

There is also great regional specificity in the area of cortex which generates and propagates epileptiform activity in the FL brain. When stimulation is delivered to the white matter below the PMZ, epileptiform activity firsts initiates above the site of stimulation and propagates both medially (towards the microgyrus) and laterally (away from the microgyrus). Epileptiform activity then travels laterally for approximately 2-4 mm medially until it reaches the microgyrus, where it is attenuated. Studies of the laminar distribution of epileptiform activity demonstrate that activity is largely initiated synchronously through all cortical layers in the PMZ, but that the highest amplitude activity occurs in layer II/III. Interestingly, the microgyrus does not generate or propagate epileptiform activity, perhaps due to altered ascending input (Jacobs et al., 1996). In fact, the microgyrus can be surgically isolated from the adjacent cortical slice and epileptiform activity persists in the PMZ (Jacobs et al., 1996). This shows that the microgyrus is not required for epileptiform activity, but rather that abnormal circuitry within the PMZ drives network hyperexcitability.

Innovations in imaging and multi-electrode recording have confirmed these findings and added a new level of understanding. Glutamate imaging studies (Dulla et al., 2013) of

stimulus-evoked epileptiform activity show that white matter stimulation evoked the earliest excitatory glutamate events in the PMZ near the wall of the microgyrus. This skewed distribution of glutamatergic activity suggests that the area nearest the lesion in the PMZ initiates stimulus-evoked epileptiform activity. This activity then spreads laterally away from the micgrogyrus (Dulla et al., 2013), similar to results from multi-electrode recordings. Interestingly, voltage-sensitive dye imaging of spontaneous network activity induced by removal of magnesium from the aCSF originates from within the migrogyrus itself (Redecker et al., 2005). Removal of Mg^{2+} eliminates the voltage block of NMDA receptors and is generally used as a model of ictal activity. This suggests that different modes of abnormal activity (ictal vs interictal) may originate from distinct locations within the malformed cortex.

Changes in Network Connectivity in the FL Model

In order to understand how epileptiform activity is generated in the FL cortex, a number of exciting studies have probed changes in synaptic, cellular, and network connectivity. Multiple studies show that excitatory input, as well as inhibitory input, is increased in the PMZ. The increase in inhibitory input, however, appears to rely on enhanced excitation as pharmacological blockade of excitatory neurotransmission normalizes inhibitory currents to typical levels. Studies of neonatal cortical networks following FL also support enhanced excitation, even before the onset of hyperexcitability (Zsombok and Jacobs, 2007). Interestingly, dual whole cell recording suggest that there may also be changes in unitary IPSCs from fast-spiking interneurons onto layer V excitatory cells, which may contribute to network hyperexcitability, although further studies are

required to understand how this result fits into the greater picture of local cortical network activity in the FL model (Sun et al., 2005).

Laser-scanning photostimulation (LSPS) has also been used to investigate changes in network connectivity in the FL model. LSPS utilizes combined whole-cell patch clamp recording and glutamate uncaging (Brill and Huguenard, 2010) to selectively activate neurons with temporal and spatial precision while recoding their outputs onto a recorded neuron. This allows for mapping of the spatial distribution of synaptically connected neurons, the kinetic properties of those connections, and many other properties of interest. LSPS revealed increased excitation onto layer V neurons in the FL cortex from both layer II/III and V excitatory neurons. This increase in excitation occurred due to elevated connectivity probability with no change in connection strength. These changes in excitation were unique to layer V excitatory neurons and were not seen in layer II/III neurons. In the same study, inhibition was again found to be increased in layer V but not layer II/III excitatory neurons, but here the increase was driven by enhancement of inhibitory current amplitude with no change in the probability of connectivity.

Glutamate imaging has also been used to map the spatial projections of glutamatergic input in the FL cortex. Interestingly, after FL, excitatory inputs are more predominant in layer II/III, while in sham or naïve cortex ascending cortical input arrives largely at deeper cortical layers (Dulla et al., 2013) . These studies are in agreement with anatomical studies showing large scale reorganization of ascending projections into the cortex following FL (Jacobs et al., 1999). If ascending input into the cortex arrives at the

wrong location in the cortical lamina, it is not surprising the resultant network activity is greatly disrupted. Together these studies largely implicate enhanced excitation onto layer V pyramidal neurons as a prime suspect in the generation of epileptiform network activity. Of note, FL and the associated changes in cortical network structure disrupt synaptic plasticity in the malformed cortex (Peters et al., 2004) in line with the known behavioral deficits reported in FL animals (Fitch et al., 1994). Future studies using high-speed, high-resolution imaging and other emerging technologies will help shed light on how the cortical network is disrupted by FL and how those changes in structure manifest as alterations in network activity.

Molecular Changes in the FL Model Relevant to Epilepsy

A number of excellent studies have examined mechanistic and molecular changes that occur in the FL model. Great emphasis has been given to neurotransmitter systems as well as changes in the electrical properties of neurons. Here we will attempt to summarize and synthesize work over the last 3 decades examining the molecular changes that may drive pathology in the FL model.

Glutamate Signaling

. Aberrant neuronal excitability can directly drive hyperexcitable network activity and contribute to seizures. Glutamate is the main excitatory neurotransmitter in the brain and exerts its effects through several ionotropic and metabotropic receptors which are critical for normal neuronal signaling. Glutamate transporters are essential for the reuptake of released glutamate and confine the duration and spread of the glutamate signal. A number of studies implicate alterations in glutamate receptors, transporters,

and handling in the pathophysiology of FL. Pathological alterations in glutamatergic signaling are of great interest as they can directly drive network hyperexcitability. Seizure induces elevations in extracellular glutamate and can contribute to excitotoxic cell damage. Increases in glutamate receptors or loss of glutamate transporters both could contribute to the formation of a hyperexcitable network. Here we discuss the changes in components of the glutamatergic system following FL, and how these may be central to the generation of epileptiform activity in the FL cortex.

Glutamate Receptors

The main postsynaptic ionotropic glutamate receptors are α-amino-3-hydroxy-5-methyl-4-isoxazolepropionic acid (AMPA), kainite, and N-methyl-d-aspartate (NMDA) receptors. AMPA receptors are responsible for fast excitatory neurotransmission. NMDA receptors are voltage-dependent and calcium-permeable, which allows them to act as a coincidence detector and regulate functional and synaptic plasticity. Autoradiography reveals that NMDA and kainate receptors are upregulated in the MZ of the FL and that AMPA receptors are upregulated in the both the microgyrial zone (MZ) and surrounding cortical tissue (Zilles et al., 1998). These results suggest an enhancement of glutamatergic signaling and in particular, the fast excitatory responses mediated by AMPA receptors. FL also blunts the normal developmental switch from NR2B to NR2A containing NMDA receptors. NR2B containing NMDA receptors have longer opening times, higher glutamate affinity and tend to be extrasynaptic in the adult brain (Yashiro and Philpot, 2008). FL cortex maintains a more immature state with a larger contribution coming from NR2B at adult ages compared to sham-injured cortex (DeFazio

and Hablitz, 2000; Takase et al., 2008). Due to higher expression of NR2B, there may be more calcium influx during NMDA receptor activation in the FL cortex. This could lead to long term changes in downstream gene expression, synaptic plasticity, and morphological development.

Receptor specific antagonists have been used to parse apart which channels are responsible for different component of the epileptiform activity in FL cortex. NMDA antagonist can block the late recurrent activity, but not the initial epileptiform response (Luhmann et al., 1998). NR2B-specific antagonists reveal that the NR2B subunit containing NMDA receptors contribute significantly to the spread of epileptiform activity (Bandyopadhyay and Hablitz, 2006), which is in agreement with the high expression level of this NMDA subtype. The early epileptiform activity can be blocked with AMPA receptor antagonists (Luhmann et al., 1998), illustrating the critical role of AMAP receptors to drive the excitatory response. Taken together these results demonstrate that AMPA receptors initiate the epileptiform response following stimulation and that NMDA, and in particular NR2B-containing NMDA, receptors drive the late component of recurrent activity.

Glutamate Transporters

Glutamate signaling is also altered following FL through changes in transporters and glutamate handling. High-speed glutamate biosensor imaging reveals that evoked glutamate signals propagate over a larger cortical area and are skewed towards the MZ (Dulla et al., 2013). The same study reveals that removal of exogenous glutamate is enhanced in the MZ, but decreased in the PMZ (Dulla et al., 2013). A major regulator of

extracellular glutamate dynamics is active uptake by high-affinity glutamate transporters (excitatory amino acid transporters, EAATs). EAAT3/EAAC1 is expressed on neurons but the astrocytic glutamate transporters, GLAST and GLT-1, are responsible for the majority of glutamate reuptake from the extracellular space (Danbolt, 2001). Blocking all transport with TBOA or using the GLT-1-specific blocker DHK, enhanced evoked responses and increased spontaneous epileptiform discharges preferentially in the lesion cortex (Campbell and Hablitz, 2005; Campbell and Hablitz, 2004). Blocking glutamate transporters also increased the holding current of pyramidal cells, through the activation of a tonic NMDA current (Campbell and Hablitz, 2008).

Recent studies make use of transporter currents from astrocytes to further examine the role of glutamate uptake in the FL cortex. Glutamate uptake through EAATs is electrogenic and the decay kinetics of this transporter current reveal the clearance rate of glutamate (Diamond, 2005). Campbell et al. (2014) recently found that astrocytic transporter currents recorded from the hyperexcitable PMZ are smaller and shorter in duration, suggesting decreased transporter function. Other studies, however, find no differences in the transporter kinetics of FL versus sham astrocytes (Armbruster et al., 2014; Hanson et al., 2016), but rather report changes in the number of astrocytes in the cortex following FL and the abundance and function of different EAAT subtypes. Specifically, GLT-1 expression is increased in the PMZ at P7 (but decreased in the adult cortex), while GLAST expression is increased in the MZ and PMZ of the adult cortex (Hanson et al., 2016). These results indicate a shift in the typical balance of GLT-1 and GLAST, such that GLT-1 is favored in the P7 PMZ and GLAST in the mature PMZ.

Recordings of transport currents coupled with laser scanning glutamate photolysis also reveal that individual astrocytes have a larger domain from which they remove glutamate and that glutamate uptake in the mature FL cortex is more dependent on GLAST activity (Armbruster et al., 2014). Taken together, these results are consistent with the idea that FL prolongs immature cortical phenotypes into the adult brain.

GABAergic signaling

In addition to the abundant changes in glutamatergic signaling, alterations in the inhibitory γ-Aminobutyric acid (GABA) system are also apparent in the FL cortex. Deficits in GABAergic signaling can contribute to hyperexcitability and many anticonvulsant drugs act through enhancing GABAergic function. However, special consideration must be given to the role of GABA in the developing cortex, as it exerts depolarizing and potentially excitatory actions on immature neurons (Khazipov et al., 2015). Depolarizing actions of GABA are due to elevated intracellular chloride ($[Cl]_i$), which sets the reversal potential of currents through the $GABA_A$ channels (E_{GABA}) at values more positive than the resting membrane potential. The $[Cl]_i$ is set in part by the expression of cation-chloride co-transporters (CCCs) and as these shift through development, $[Cl]_i$ decreases and E_{GABA} becomes progressively more negative (Payne et al., 2003). GABA transporters (GAT) remove GABA from the extracellular space and modulation of GATs can reshape GABA signaling; however, unlike the EAATs, GAT alterations have not been reported in the FL cortex. In this section we review changes in GABA receptors, CCCs and interneuron number following FL and briefly speculate on the role of disinhibition in contributing to FL pathology.

GABA receptors

GABA receptors can be either metabotropic ($GABA_B$) or ionotropic ($GABA_A$), with the $GABA_A$ receptors mediating the majority of fast inhibitory neurotransmission in the central nervous system. In the FL cortex, both $GABA_A$ and $GABA_B$ receptors are decreased in the MZ, as demonstrated with autoradiography (Zilles et al., 1998). $GABA_A$ receptors are additionally decreased in the surrounding PMZ (Peters et al., 2004; Zilles et al., 1998). This would suggest a general decrease of inhibitory transmission in the FL cortex. The $GABA_A$ receptor exists predominantly as a heteropentamer, with the most common configuration being two α, two β and one γ or δ subunit. Immunohistochemistry reveals that the most abundant $GABA_A$ subunits α2 and γ2 are downregulated in the MZ (Redecker et al., 2000), which is in agreement with a general downregulation of $GABA_A$ receptors. Widespread decreases in α1, α2, α3, α5 and γ2 subunits are found in the medial PMZ, indicating changes in subunits that would likely alter the affinity of the receptor (Redecker et al., 2000). Interestingly, $GABA_A$ subunits are also decreased in the lateral PMZ and even in the hippocampus and areas of the contralateral cortex (Redecker et al., 2000). These results demonstrate that GABA receptor expression is robustly effected by FL, perhaps reflecting a high plasticity in the expression of these receptor types.

Cation-chloride co-transporters

Low intracellular Cl^- is necessary to maintain the hyperpolarizing actions of GABA and the CCCs play an important role in Cl^- homeostasis. NKCC1 promotes accumulation of Cl^- in the cell and KCC2 promotes extrusion (Ben-Ari et al., 2012; Kahle et al., 2008;

Watanabe and Fukuda, 2015). Typically the ratio of NKCC1 to KCC2 is higher early in development. Following FL, NKCC1 mRNA is increased and KCC2 mRNA is decreased transiently at P4 (Fukuda and Wang, 2013; Shimizu-Okabe et al., 2007; Wang et al., 2014). These changes occur in both GABAergic and principal neurons (Wang et al., 2014) and would presumably drive depolarizing actions of GABA. This alteration in CCC expression may contribute to the formation of the lesion and potential drive hyperconnectivity. At the same P4 time point, $GABA_A$ receptor activation appears to contribute to calcium (Ca^{2+}) oscillations in cells located in the MZ, as these oscillations can be blocked by application of bicuculline (Wang et al., 2014). Ca^{2+} transients can control migration of immature neurons and disruptions in activity patterns are known to alter long-term network connectivity (Heck et al., 2007). These results suggest that depolarizing actions of $GABA_A$ (due to downregulation of KCC2) drive the observed Ca^{2+} oscillations and may facilitate the migration of neurons into the MZ.

Interneuron loss

In contrast to the robust and widespread changes in GABA receptors, defining the loss of interneurons in the FL cortex has been less clear. Rosen et al. (1998) report that immunoreactivity for parvalbumin interneurons is transiently decreased in the MZ and PMZ from P13-15 but recovers to normal levels by P21. A separate report shows no change in immunoreactivity for GABA or parvalbumin in the adult FL cortex, but a selective loss of calbindin-positive cells in the PMZ (Schwarz et al., 2000) or MZ (Kharazia et al., 2003). Loss of parvalbumin, calretinin and calbindin immunoreactivity has also been demonstrated in the MZ at P21-P24 by Hablitz and DeFazio (1998). Lastly,

immunoreactivity for somatostatin-positive cells reveals a loss of this population of interneurons at adult (P30), but not juvenile (P14) ages in the PMZ (Patrick et al., 2006). Taken together, these results suggest a mild loss of interneurons following freeze lesion, which could contribute to a loss of inhibitory transmission. As populations of interneurons appear to have different vulnerabilities after FL, additional studies will be necessary to reach a clear consensus on the extent of interneuron loss in this model.

Does disinhibition contribute to hyperexcitability?

More importantly, it is not understood how changes in GABA receptors, chloride homeostasis, or the loss of interneurons contributes to hyperexcitability in the FL cortex. Polysynaptic IPSPs are reduced or absent in the FL cortex and interneurons appear to receive weaker excitatory input (Luhmann et al., 1998), suggesting a loss of functional inhibition. However, IPSC amplitude on layer V pyramidal cells is increased in a glutamatergic-dependent manner (Brill and Huguenard, 2010; Jacobs and Prince, 2005), which suggests that inhibitory transmission is actually enhanced despite the loss in interneurons and GABA receptors. Whole-cell patch clamp of fast spiking (FS) interneurons, combined with laser-scanning photostimulation of caged glutamate, further revealed that EPSC hotspots are increased on FS-interneurons in the FL cortex, while IPSC hotspots are decreased (Jin et al., 2014). Taken together these results suggest that increased excitatory drive onto interneurons may compensate for losses at the cellular and molecular level. FS-interneurons also receive less inhibition, revealed by a decreased sIPSCs frequency (Jin et al., 2014), which would further contribute to overall increased inhibitory drive in the network. These results suggest that while interneurons

and GABAergic systems are certainly altered by FL, disinhibition is unlikely to play as important of a role as glutamate-mediated excitation in generating epileptiform activity in this model.

Ion channel/intrinsic properties

As neurotransmitter systems eventually carry out their actions via the neurons that they activate, it is crucial to consider changes in neuronal membrane properties and how neurons and astrocytes together control ionic homeostasis. Small changes in how neuronal properties shape electrical activity can lead to widespread alterations in network activity. The most relevant neuronal intrinsic property which appears to be altered in the FL model is the function of HCN channels. Additionally, astrocytic control of potassium levels also may be disrupted in the FL model, which would have far reaching effects on neuronal excitability.

HCN channels

Hyperpolarization-activated non-selective cation (HCN) channels are principally located in pyramidal cell dendrites and contribute to depolarizing the resting membrane potential, as well as regulating membrane resistance, and generally constrain synaptic excitability (Shah, 2014). Immunohistochemistry staining for HCN1 is decreased in the PMZ of FL animals and this is accompanied by abnormal dendritic arborization (Hablitz and Yang, 2010). Whole-cell patch clamp recording of pyramidal neurons in the PMZ reveals a hyperpolarized resting membrane potential and increased input resistance that could be reversed by blocking the HCN-dependent current I(h) (Albertson et al., 2011). Despite the membrane hyperpolarization, depolarizing currents in these cells

results in more spikes (Albertson et al., 2011). HCN-dependent currents also appear to be reduced in fast-spiking and accommodating interneurons in the FL cortex (Albertson et al., 2017). Decreased levels of HCN channels and the I(h) current may therefore contribute to cellular and network hyperexcitability in the FL cortex.

Potassium Buffering

Astrocytes play an important role in redistributing elevated potassium (K^+) from areas of high neuronal activity, which is dependent on K^+ channels and astrocyte coupling through gap junction (Steinhauser et al., 2012). Reactive astrocytes surrounding the MZ show increased intercellular coupling (Bordey et al., 2001) and expression of inwardly rectifying potassium (K(IR)) channels. However astrocytes in layer i of the MZ and proliferating astrocytes from the base of the malformation show reduced K(IR) (Bordey et al., 2001) and presumably would have a lower K+ buffering capacity. These results suggest that while the core of the lesion may have reduced K^+ buffering, the hyperexcitable PMZ has an increased ability to remove K^+—perhaps as a compensatory mechanism in response to the increase activity. Future studies will be necessary to link these changes in astrocytic properties to alterations in network activity.

Potential therapeutic strategies

Despite decades of research on the FL model, very few studies have focused on therapeutic approaches to decrease the pathologies associated with FL. Epileptiform activity persists in the PMZ, even after separation from the MZ with a transcortical cut (Jacobs et al., 1999), which highlights the potential difficultly of surgical resection as a treatment option, as the epileptogeneic zone extends beyond the cortical malformation.

Acute application of AMPA or NMDA antagonists can constrain components of the epileptiform activity (Bandyopadhyay and Hablitz, 2006; DeFazio and Hablitz, 2000; Jacobs et al., 1999; Luhmann et al., 1998); however similar *in vivo* applications remain limited. A single-dose of nerve growth factor (NGF) injected intraparenchymally, immediately after FL near the site of lesion, upregulated TrkA and doublecortin expression and decreased p75 expression 7 days later (Chiaretti et al., 2011). These results suggest that NGF may decrease apoptosis after FL. *In vivo* treatment with the NMDA antagonist MK-801 on the day of FL decreased the volume of the cortical malformation (Rosen et al., 1995); however this treatment was also associated with a high mortality rate and the effects on hyperexcitability were not examined. More work is therefore needed to identify potential therapeutic targets that could attenuate pathological changes following FL.

Critical Analysis of the FL Model

Like all models of human disease, the FL model has strengths and weaknesses. First, we will consider the weaknesses of the FL model. The most obvious and overarching weakness is that the model itself is etiologically unrealistic. No one has ever acquired a DCM or epilepsy from a neonatal freezing insult. This calls into question the relevance of the mechanisms identified in the FL to human epilepsy. This criticism, however, can be made for many, many models of epilepsy include chemoconvulsant and kindling models. There are a number of acquired models of epilepsy, however, including multiple models of traumatic brain injury and models of febrile seizures that are relatively etiologically realistic. Focal PMG is often due to hypoxic insult (Squier and Jansen, 2014), however

this approach has not been used experimentally to induce a PMG-like cortical malformation. Obviously, genetic models have the potential to be etiologically realistic, but even they come with their own caveats.

The next significant weakness of the FL model is that FL only replicates focal DCMs. A great number of DCMs encompass large areas of cortex. The FL model, by its nature, evokes changes only in a small area. Additionally, the FL model likely only replicates DCMs caused by neonatal brain insult, such as PMG and FCD type IIId. However, DCMs are a heterogeneous population of disorders resulting from a variety causes, including several genetic mutations, in addition to environmental causes such as hypoxia, viral infection and traumatic injury. It is therefore unlikely that single animal model would encompass all of these DCM sub-types.

Finally, the FL model only results in non-convulsive, spike wave seizures, which differs from the diversity of seizures types associated with DCMs. Generalized tonic-clonic seizure was the most common seizure type associated with FCD in a cohort of patients who were referred for resective surgery (Fauser et al., 2006). PMG is most often associated with focal, dyscognitive seizures and only a minority of patients present with non-convulsive or absence seizures (Shain et al., 2013). Even though the FL model is imperfect, it has many strengths that make it a valuable tool.

One of the main benefits of the FL model is the opportunity to study the molecular and cellular changes that occur in the developing brain following an early life insult. As many epilepsies occur in the immature brain, identifying key molecular pathways that are affected by neonatal insult, and lead to network hyperexcitability, is crucial to

unravelling the complexities of injuries in the developing brain. The FL is an ideal model for these types of studies. It allows for precise focal and temporal delivery of a repeatable insult. Because there are so many dynamic processes occurring in the neonatal brain, and injury evokes its own diverse set of molecular and cellular changes, it is crucial to use models that allow the simple and repeatable delivery of a focal insult.

A further strength of the FL model is that it allows the study of a discreet temporal window between the delivery of a focal brain insult and the onset of a network level pathology. The time from FL (P0) to the onset of network hyperexcitability (P11-14) is extremely stereotypical, suggesting that there is a set time course of events that occur from the time of insult until the manifestation of hyperexcitability. These changes include cell death (Rosen et al., 1995), altered synaptic function (Jacobs and Prince, 2005; Jin et al., 2014; Luhmann et al., 1998), circuit reorganization (Jacobs et al., 1996; Jacobs et al., 1999), activation of inflammatory pathways (Ravizza et al., 2006), and alteration of blood brain barrier permeability (Marchi et al., 2006). In the FL models, these systems can be studied during the transformation of a developing network into a hyperexcitable network. This also highlights the multifaceted molecular and cellular changes that occur in the FL model. Unlike genetic models, which either delete or modify an individual gene, the FL and similar models evoke a myriad of changes evoked by acute insult. This mirrors the complexity of changes that occur in human acquired epilepsies.

Because of the unique and stereotyped timeline of the development of hyperexcitability, the FL also can be used as a tool for preclinical screening of

compounds which might be therapeutically useful following early life brain insult. There are, however, surprisingly few studies which have taken advantage of the FL in this way.

Next, the FL model does not rely on chemical or pharmacological manipulations to induce network abnormalities. This is a strength, as very few human epilepsies arise from any type of pharmacological insult. Utilizing models that evoke network abnormalities from acute physical or vascular insults more closely represent the human condition, and may produce more relevant and impactful preclinical findings. This is by no means a criticism of chemoconvulsant models, as many key molecular pathologies in epilepsy and epileptogenesis have been garnered from the kainite and pilocarpine models. The FL, and other similar models, simply offers an alternative that more closely replicates neonatal brain insults that may occur during gestation or perinatally.

The last, and perhaps most important, strength of the FL model is the striking similarities in morphological, molecular, and cellular pathologies between the model and human PMG and FCD. FL generates spontaneous seizures, which is a clinical finding in all DCMs. FL and polymicrogyria are both characterized by stereotyped 4 layered cortex (Crino, 2015; Humphreys et al., 1991). There are significant amounts of reactive astrocytosis in both the FL model and human DCMs (Bordey et al., 2001; Kakita et al., 2005). Both have components of altered cellular morphology and localization (Crino, 2015). Glutamate levels are increased in human DCMs (Cavus et al., 2005) and glutamate homeostasis is altered in both the FL and in human focal cortical dysplasia (Gonzalez-Martinez et al., 2011; Rakhade and Loeb, 2008; van Landeghem et al., 2006) Interneuron density is also altered in both the FL and in human focal cortical dysplasia

(Andre et al., 2010; Cossart et al., 2005; Fauser et al., 2013; Sakakibara et al., 2012). Lastly, the FL generates areas of hyperexcitability outside the region of malformation. This mimics some subtypes of human DCMs in which seizure foci are not directly in the area of malformation (Sisodiya, 2000). In summary, the FL is a reliable, consistent model of DCM and offers the ability to study epileptogenic processes in the developing cortex.

1.3: Thrombospondin and α2δ-1-driven synaptogenesis

The work of this thesis has identified thrombospondin and α2δ-1 signaling as a novel signaling pathway that is critical for driving several key pathological features of the neonatal FL. Our lab has a long-standing interest in the role of astrocytes in both normal development and disease. We became interested in thrombospondin/α2δ-1 signaling after it was implicated in astrocyte-mediated excitatory synaptogenesis (Christopherson et al., 2005; Eroglu, 2009) and we observed that both components of this pathway are upregulated in the FL cortex.

Thrombospondins

Thrombospondins (TSP) are a large family of highly conserved, secreted glycoproteins that function as part of the extracellular matrix. Thrombospondin-1 was first isolated from platelets that had been stimulated with thrombin (Baenziger et al., 1971). Since then five TSPs have been identified, which are divided into two subfamilies, A and B. Subfamily A consists of TSP-1 and TSP-2, which are formed as trimers; subfamily B consists of TSP-3, TSP-4 and TSP-5, which are assembled as pentamers (Adams, 2001). The TSPs are expressed throughout the body and perform a variety of functions through interactions with multiple binding partners. Each TSP has a unique expression pattern and are primarily expressed in non-overlapping cell populations (Adams, 2001). Mice that have genetic knock-out of TSP-1 have increased white blood cell counts and several lung abnormalities (Lawler et al., 1998). While knock-out of TSP-2 present with fragile skin and unusually flexible tails, resulting from disordered collagen fiber patterns

(Kyriakides et al., 1998). These different phenotypes further illustrate the distinct distribution and function of each TSP.

TSP1-4 are expressed in the brain (Iruela-Arispe et al., 1993; Lawler et al., 1993; O'Shea et al., 1990) and are predominately expressed by astrocytes (Cahoy et al., 2008; Eroglu, 2009). TSP1 and 4 have been shown to play a role in neurite outgrowth (Arber and Caroni, 1995; O'Shea et al., 1991) and TSP1 plays a role in postnatal neuronal migration (Blake et al., 2008). The most well-defined role of the TSPs in the CNS is promoting glutamatergic synaptogenesis. In a landmark study by Christopherson et al. (2005), they show that TSP is the astrocyte-secreted factor responsible for excitatory synaptogenesis. The addition of TSP alone to neuronal cultures was able to mimic the level of synapse formation seen when astrocytes and neurons are co-cultured. Furthermore, astrocyte-conditioned media that was immuno-depleted of TSP lost its synaptogenic properties. Finally, they showed that knock-out of TSP1/2 leads to fewer synapses *in vivo.* TSP promotes the formation of structural synapses in culture, which are post-synaptically silent, suggesting other factors are necessary *in vivo* to induce postsynaptic function. TSP action is specific to excitatory synaptogenesis and does not affect inhibitory synapse formation (Hughes et al., 2010).

<u>α2δ-1</u>

α2δ-1 has been identified as the neuronal receptor for TSP-driven synaptogenesis (Eroglu et al., 2009). α2δ-1 is an auxiliary subunit of voltage-gated calcium channels (VGCC) that plays a role in trafficking the VGCCs to the synapse and increases the release probability of the channels (Felix et al., 1997; Hoppa et al., 2012). There are 4

α2δ isoforms (α2δ-1, α2δ-2, α2δ-3 and α2δ-4), which are encoded by the genes *CACNA2D1*, *CACNA2D2*, *CACNA2D3* and *CACNA2D4*, respectively. In heterologous systems, each isoform is able to associate with all VGCC types; however, there may be greater selectivity *in vivo*. α2δ-1 (and presumably all the α2δ isoforms) is transcribed from the single gene, which is post-translationally cleaved into separate α2 and δ proteins linked by a disulfide bond (Davies et al., 2007; Jay et al., 1991). The majority of the protein is extracellular, with one transmembrane spanning portion (Davies et al., 2007; Jay et al., 1991).

The α2δs are found in various tissues of the body, including skeletal, cardiac and smooth muscle, endocrine tissue and the central (CNS) and peripheral nervous system (PNS) (Dolphin, 2012). α2δ-1, -2 and -3 are expressed in the brain (Barclay et al., 2001; Cole et al., 2005; Ellis et al., 1988), with α2δ-1 being the highest in cerebellum, hippocampus and the cortex (Cole et al., 2005; Klugbauer et al., 1999). The expression of α2δ-1 transcript is also correlated with excitatory neurons (Cole et al., 2005). Within the CNS, α2δ-1 is found primarily in the neuropil (Taylor and Garrido, 2008). Expression is high pre-synaptically, in line with its known association with VGCCs (Hoppa et al., 2012), but can also be found in the dendrites (Bauer et al., 2009; Eroglu, 2009). Compelling evidence for TSP/α2δ-1-driven synaptogenesis comes from a study by Eroglu et al. (2009). The use of recombinant, truncated TSP constructs identified the EGF-like repeats to be critical for TSP-mediated synaptogenesis. α2δ-1 binds to this domain through an interaction with the α2 VWF-A domain. *In vitro* α2δ-1 upregulation increased synaptogenesis and α2δ-1 knockdown blocked TSP-driven synaptogenesis. Finally, α2δ-

1 overexpression *in vivo* increased the number of Vglut2+ excitatory synapses in the adult cortex (Eroglu, 2009). The synaptogenic function of α2δ-1 appears to be independent from calcium channel association (Wang et al., 2012); however, the downstream signaling remains elusive.

α2δ-1 in disease

α2δ-1 dysfunction has been implicated in various disease states, including epilepsy, neuropathic pain, and cardiac abnormalities. α2δ-1 knockout in mice is associated with decreased calcium currents in cardiomyocytes (Fuller-Bicer et al., 2009) and human mutations have been linked to Brugada (Burashnikov et al., 2010) and short QT syndromes (Templin et al., 2011). These cardiac phenotypes are presumably due to α2δ-1-dependent effects on calcium channels.

α2δ-1 also plays a well-established role in peripheral injury and neuropathy. α2δ-1 is upregulated in several models of nerve injury and neuropathic pain (Bauer et al., 2009; Li et al., 2014; Luo et al., 2001; Newton et al., 2001). Overexpression of α2δ-1 is able to induce spinal hyperexcitability and a pain phenotype in the absence of injury (Li et al., 2006) and α2δ-1 knockout attenuates hypersensitivity following nerve ligation (Patel et al., 2013). Increased synaptogenesis is implicated in driving neuropathic pain following nerve injury (Li et al., 2014), suggesting that α2δ-1-mediated synaptogenesis is responsible for driving injury-induced neuropathy.

TSP and α2δ-1 are also upregulated in a model of cortical trauma that is associated with increased excitatory synapse formation and hyperexcitabity (Li et al., 2012). Furthermore, human mutations in the α2δ-1 gene, *CACNA2D1*, have recently been

reported in patients with epilepsy associated with polymicrogyria and West syndrome (Hino-Fukuyo et al., 2015; Vergult et al., 2015). Finally, overexpression of $\alpha 2\delta$-1 drives cortical synaptogenesis, increased excitatory connectivity, and epileptiform EEG activity (Faria et al., 2017). Taken together, we can see that $\alpha 2\delta$-1 plays varied roles in diseases by altering calcium channel function and both developmental and injury-induced synaptogenesis.

1.4: Gabapentin: α2δ-1 antagonist and neuroprotective agent

The anticonvulsant and antiallodynic drug gabapentin has been shown to block the interaction between TSP and α2δ-1, and we have therefore used gabapentin to investigate the role of α2δ-1 signaling in FL pathophysiology. However, GBP has several known targets in the CNS, which must be considered when using GBP treatments. We will also review the use of gabapentin clinically and in several disease models.

Development of gabapentin and discovery of targets

Gabapentin (GBP) was originally developed as a GABA analogue and selected based on anticonvulsant properties (Belliotti et al., 2005; Bryans and Wustrow, 1999; Satzinger, 1994). Subsequent observations in patient populations led to the discovery of its utility in pain management (Mellick and Mellick, 1997; Rosner et al., 1996; Segal and Rordorf, 1996). Despite structural similarities, GBP was found to have no action at GABA receptors (Jensen et al., 2002; Taylor et al., 2007). For many years the mechanism of action remained elusive, before the discovery of high affinity binding of GBP to α2δ-1 (Gee et al., 1996). The effects of GBP on calcium currents remain controversial, as studies report either no effect (Schumacher et al., 1998) or mild effects (Davies et al., 2006; Stefani et al., 1998), depending on neuronal type, drug concentration and experimental conditions. However, GBP does appear to disrupt calcium channel trafficking, as GBP treatment is able to reduce cell surface localization of calcium channel subunits (Bauer et al., 2009; Hendrich et al., 2008; Tran-Van-Minh and Dolphin, 2010). GBP also strongly inhibits TSP-induced synapse formation, without effecting

established synapses (Eroglu et al., 2009), presumably by disrupting TSP/α2δ-1 signaling.

GBP also has several secondary sites of action within the CNS, which may also play a role in its therapeutic effects. GBP binds α2δ-2, although with a lower affinity than α2δ-1 (Gong et al., 2001). Despite a lack of direct binding to GABA receptors, GBP has been shown to enhance promoted accumulation of GABA (Honmou et al., 1995; Loscher et al., 1991) and to inhibit calcium influx through voltage-gated channels in a $GABA_B$ dependent manner (Bertrand et al., 2001). At high concentrations, GBP can increase glutamic acid decarboxylase activity (Taylor et al., 1992). Taken together, these results suggest that GBP treatment could have minor actions on GABAerigic transmission. GBP has also been shown to inhibit protein kinase C activity (Maneuf and McKnight, 2001; Yeh et al., 2011), NMDA receptor-activated currents (Kim et al., 2009) and voltage-gated persistent sodium currents (Yang et al., 2009). However, these effects of GBP are mild, in comparison to the now well-established site of action at α2δ-1.

GBP in pain treatment

GBP is widely used to treat neuropathic pain, including diabetic neuropathy and post-herpetic neuralgia (Backonja and Glanzman, 2003; Stacey et al., 2008; Taylor et al., 2007; Wheeler, 2002). Animal studies have shown that GBP is effective in treating pain associated with inflammation and tissue injury (Hwang and Yaksh, 1997; Luo et al., 2002; Xiao et al., 2007), without effecting acute pain (Hunter et al., 1997; Stanfa et al., 1997). The binding of GBP to α2δ-1 is critical for its analgesic effects, as demonstrated by mice with a knockin point mutation in the GBP binding site on α2δ-1 (Field et al.,

2006). These animals develop neuropathic pain normally, but are insensitive to GBP treatment. $\alpha 2\delta$-1 is also upregulated in a model of gabapentin-sensitive nerve injury that is correlated with an increase in excitatory synapse number in the dorsal horn of the spinal cord (Li et al., 2014). Excitatory connectivity as assessed by mEPSC frequency is also increased in this model. GBP treatment blocked the rise in mEPSC frequency and attenuated pain-associated behaviors (Li et al., 2014), suggesting that GBP attenuates $\alpha 2\delta$-1-mediated synaptogenesis to reduce injury-induced neuropathic pain. Further evidence for this hypothesis comes from work showing that GBP also blocks the increased mEPSC frequency and pain state induced by direct injection of TSP into the spinal cord (Park et al., 2016). GBP may also act by attenuating trafficking of $\alpha 2\delta$-1 and calcium channels to the plasma membrane (Bauer et al., 2009), which would decrease neurotransmitter release and spinal sensitization.

GBP as an anticonvulsant and potential anti-epileptogenic treatment

GBP is also used as an add-on therapy to treat drug resistant epilepsy (Al-Bachari et al., 2013; Appleton et al., 1999; Goa and Sorkin, 1993). Presumably, GBP acts through $\alpha 2\delta$-1 for its anticonvulsant effects; however, this has not been directly demonstrated. GBP may also have utility as an anti-epileptogenic agent. In a study by Li et al. (2012), GBP was shown to decrease hyperexcitability in a model of post-traumatic epilepsy. $\alpha 2\delta$-1 and TSP are upregulated following partial cortical isolation ("undercut"). There is also increased excitatory synaptogenesis and network hyperexcitability in the undercut cortex. GBP treatment following the injury is able to attenuate synapse formation and

prevent the epileptiform activity (Li et al., 2012), which suggest that α2δ-1-mediated synaptogenesis may drive epileptogenesis following cortical injury.

GBP as a neuroprotective agent

GBP reduces cell death in models of stroke (Kim et al., 2010; Traa et al., 2008; Williams et al., 2006), cortical trauma (Li et al., 2012) and spinal cord injury (Emmez et al., 2010; Kale et al., 2011). TSP is upregulated following stroke (Lin et al., 2003) and cortical injury (Li et al., 2012). α2δ-1 is also upregulated following injury to both the peripheral and central nervous system (Boroujerdi et al., 2008; Li et al., 2012). These results suggest that injury leads to increases in both the receptor and ligand of TSP/α2δ-1-mediated synaptogenesis. Therefore, inhibition of TSP/α2δ-1 signaling may account for the neuroprotective effects of GBP. GBP may also act at α2δ-1 to reduce calcium currents and constrain excitability and subsequent excitotoxicity. GBP decreases infarct volume after ischemic injury and this neuroprotective effect is correlated with the reduction in seizure events (Williams et al., 2006), consistent with GBP attenuating excitotoxic cell death. GBP has been shown to reduce NMDA-induced excitotoxicity (Kim et al., 2009; Matsumoto et al., 2015), although it is unclear if this is due to an inhibition of calcium currents, direct effects on NMDA receptors or other potential mechanisms. α2δ-1 may also drive cell death through calcium-dependent caspase-mediated apoptosis (Kondratskyi et al., 2015). Additionally, GBP may act through α2δ-1-independent mechanisms.

1.5: Contributions of this thesis

The work of this thesis uses the neonatal freeze lesion, as a model of neonatal injury and developmental cortical malformation (DCM). The DCM sub-syndromes polymicrogyria (PMG) and focal cortical dysplasia (FCD) type IIId are associated with neonatal insult. FL recapitulates many of the key features of PMG and FCD type IIId, including etiology, cell death, astrocytosis, anatomical reorganization, and spontaneous seizures. Despite extensive research on the pathology of neonatal FL, very few studies have successfully identified therapeutic strategies for treating FL-induced cortical reorganization or epileptiform activity. This remains an important question as many patients with epilepsies associated with DCMs do not have good seizure control with currently available treatments. We have identified $\alpha 2\delta$-1 signaling as a novel pathway which contributes to FL-driven pathology. Antagonizing $\alpha 2\delta$-1 signaling via pharmacological or genetic manipulations can reduce several key pathologies associated with FL injury, including apoptotic cell death, anatomical reorganization, excitatory synaptogenesis, astrocytosis, and network hyperexcitability. Furthermore, we have addressed an important question regarding the specificity of gabapentin's (GBP) actions, as multiple targets, beyond $\alpha 2\delta$-1, have been identified. We show that GBP has dual effects on both cell death pathways and injury-induced synaptogenesis. For the first time, we demonstrate that the neuroprotective actions of GBP, as well as the majority of effects on cortical synapse formation and network function, are mediated by $\alpha 2\delta$-1. However, GBP can reduce FL-induced increases in excitatory synapse number in

α2δ-1 KO mice, indicating that GBP has α2δ-1-independent effects on synaptogenesis. This work will help to optimize treatment strategies using GBP and highlights the therapeutic potential of targeting α2δ-1 signaling in neonatal injury and developmental cortical malformations.

Chapter 2: Materials and Methods

2.1: Animals

All animal procedures were performed in accordance with the National Institutes of Health Guild for the Care and Use of Laboratory Animals and followed the guidelines of Tufts University's Institutional Animal Care and Use Committee. Mice had access to food and water ad libitum and were kept on a standard 14 hr/10 hr light-dark cycle. All experimental manipulations were performed during the light phase. $\alpha 2\delta$-1 knockout ($\alpha 2\delta\text{-}1^{-/-}$) animals were generated by crossing heterozygous ($\alpha 2\delta\text{-}1^{+/-}$) breeding pairs maintained on a C57BL6/J background. Both Wild-type ($\alpha 2\delta\text{-}1^{+/+}$) littermates and C57BL6/J mice (generated from wild-type C57BL6/J breeding pairs) were used. A single breeding pair was housed together continuously and pups were weaned and separated by sex at postnatal day 21 (P21).

$\alpha 2\delta$-1 Knockout Mice

$\alpha 2\delta\text{-}1^{-/-}$ mice were a generous gift of Guopeng Feng (Massachusettes Institute of Technology). The absence of the $\alpha 2\delta$-1 protein was confirmed by Western blot analysis of total cortical homogenate (Fig 2.1 F). These mice showed no obvious phenotype and developed normally with regard to size and weight. Behavioral analysis was performed and $\alpha 2\delta$-1 knockouts showed no change in open field activity or time spent in the center of the open field (Fig 2.1 C and D). They also performed normally on the rotarod (Fig 2.1 B) and alternating T-maze test (Fig 2.1 E), suggesting normal motor and cognitive function. Chronic 24/7 EEG recording was performed in $\alpha 2\delta$-1 knockouts and WT littermates. No obvious change in EEG signal was seen and we did not detect any spontaneous electrographic or behavioral seizures (Fig 2.1 A).

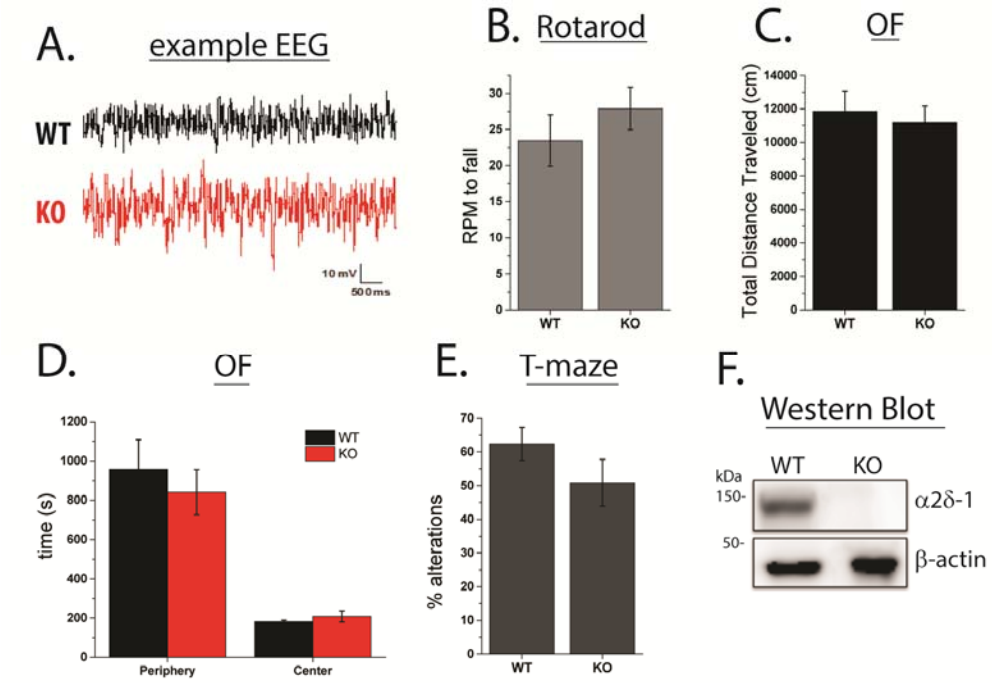

Figure 2.1: Behavioral characterization of α2δ-1 knockout mice

(A) Representative EEG traces from α2δ-1 knockout (KO) and wild-type (WT) naïve mice, recorded at 10 weeks of age. (B) Average rotations per minute (RPM) that WT and KO mice fell off an accelerating rotarod. (C) Average total distance traveled in 20 minute open field (OF) test. (D) Average time spent in the center versus periphery during the OF test. (E) Average percent spontaneous alterations in T-maze test. (F) Western blot analysis of α2δ-1 protein expression in WT and KO animals compared to β-actin loading control.

Behavioral Tests

10-week old male mice were used for behavioral testing. Behavioral assays were performed in the Tufts Center for Neuroscience Research Animal Behavior Facility. Animals were tested on a battery of tests, starting with the least stressful test (Open

Field) and moving to more stressful tests (Spontaneous Alteration and Rotarod) on subsequent days. *Open Field Test.* Mice were individually placed into the center of a 40 cm × 40 cm open field apparatus with 16 × 16 equally spaced photocells (Hamilton-Kinder). The total distance traveled, and the amount of time spent in the center of the open field as well as the total number of beam breaks were measured during the 20 min test using MotorMonitor software (Hamilton-Kinder). *Spontaneous Alteration.* Mice were placed in a 3 arm T-maze. After being placed in the starting arm, the barrier was removed to allow the rodent free choice to enter either the left or right arm. After entering an arm, a barrier was placed to keep the animals in that arm for 30 seconds. The mouse was returned to the home cage for one minute between trails and a total of 10 trials were performed. Generally, rodents will engage in exploratory behavior in the maze and alternate between the arms. The percent of trial in which the animal spontaneously alternated arms was reported. *Rotarod.* Motor coordination and balance was measured in the mice utilizing an acceleration paradigm on a 5 position Rotarod (ENV 577M, Med Associates). Mice were trained at a constant, slow speed of 14 rpm until they could successfully stay on the beam for 5 minutes. Testing was carried out utilizing a fast acceleration paradigm (4-40 rpm over 5 minutes). Mice were tested over the course of three trials (30 minutes apart) and latency to fall and the RPM at which mice fall was reported.

EEG Recording

Naïve, ten week old wild-type and $\alpha 2\delta$-1 littermates were implanted for electroencephalogram (EEG) recording based on a Tufts Institutional Animal Care and

Use Committee approved protocol. Briefly, animals were anesthetized (100 mg/kg ketamine and 10 mg/kg xylazine). An incision was made on the scalp, the surface of the skull was dried, and 4 burr holes will drilled with care to avoid puncturing the dura. Four 0.1" stainless steel screws (Pinnacle Technologies) were gently screwed into the drilled holes. A common reference electrode was placed anterior to the left side of the interparietal bone, and two EEG eletrodes were placed in the left front bone (for front/motor cortex) and in the right parietal bone (for somatosensory cortex). A separate ground electrode was also placed anterior to the right side of the interparietal bone. The screws were then attached to a headmount (Pinnacle Technology) which was fixed using dental cement. Following surgery, the animals were given 7 days to recover. Chronic 24-hr EEG recordings were acquired using a 100× gain preamplifier high-pass filtered at 1.0 Hz (Pinnacle Technology) with video monitoring for 2 weeks. LabChart Pro software (ADInstruments) was used for data acquisition and analysis.

Freeze lesion

Experimental microgyri in primary somatosensory cortex (right hemisphere) were induced in P0 wild-type or $\alpha 2\delta$-1 knockout mouse pups by freeze lesioning as described previously in rats (Dulla et al., 2013; Jacobs and Prince, 2005), with some modifications. Animals were anesthetized by hypothermia. An incision into the scalp was made of approximately 3 mm, over the right somatosensory cortex. A copper probe (1 mm x 1.5 mm) cooled with dry ice to − 50 to − 60 °C was placed onto the exposed skull for 5 secs. Sham operated littermates were generated by leaving the probe at room temperature.

After freeze-lesioning, the incision was closed using surgical glue, and pups were warmed and returned to the dam.

Drug Treatments

For drug treatment experiments, mice were treated with once daily intraperitoneal (I.P.) injections of either gabapentin (200 mg/kg) or vehicle (sterile injection saline) from P1 to P7.

2.2: Electrophysiology

Preparation of Acute Brain Slices

Cortical brain slices containing sensorimotor cortex (400 µM) were prepared from mice of either sex. Briefly, mice were anesthetized with isoflurane, decapitated, and the brains were rapidly removed and placed in chilled (4°C) low-Ca, low-Na slicing solution consisting of (in mM): 234 sucrose, 11 glucose, 24 NaHC02, 2.5 KCl, 1.25 NaH2PO4, 10 MgSO4 and 0.5 CaCl2, equilibrated with a mixture of 95% O2:5% CO2. The brain was glued to the slicing stage of a Vibratome 3000 sectioning system and slices were cut in a coronal orientation. The slices were then incubated in 32°C oxygenated aCSF (in mM: NaCl, 126, KCl, 2.5, NaH2PO4, 1.25, MgSO4, 1, CaCl2, 2, glucose, 10, NaHCO2, 26) for 1 hour, and then allowed to cool to room temperature and subsequently used for recording.

Field Recordings

Slices were placed in an interface chamber maintained at 34°C, superfused with oxygenated aCSF at 2 ml/min and cortical projections were stimulated with a tungsten concentric bipolar electrode at the layer VI –white matter boundary. Electrical stimulation consisted of 10–50 µA, 100 µs pulses at 30 s intervals delivered by a stimulus isolator (World Precision Instruments). Glass micropipettes (resistance ≅ 1 MΩ) were filled with aCSF and placed in layer V of the cortex directly above the stimulation electrode. Electrophysiological data were recorded with an Axon Multiclamp 700A amplifier and Digidata 1322A digitizer (sampling rate = 20kHz) with Lab Chart software (AD Instruments). Threshold stimulation intensity was identified as the minimum

amount of current required to elicit a detectable cortical field potential response (≥ 0.05 mV).

Patch Clamp Recordings

Slices were placed in the recording chamber of an Olympus Bx51 microscope with continual superfusion of oxygenated aCSF maintained at 32°C (2mL/min). Layer V pyramidal neurons were visually identified with infrared differential interference contrast (DIC) microscopy and whole cell patch-clamp recordings were made with a borosilicate glass electrode (3–5 MΩ) filled with (in mM): 140 CsMs, 10 HEPES, 5 NaCl, 0.2 EGTA, 5 Q×314, 1.8 MgATP, 0.3 NaGTP and pH 7.25. The recording electrode was placed approximately 200 μm from the site of injury in the PMZ of FL animals or comparable cortical area in sham injured animals. Data was collected using an axon Multiclamp 700B amplifier, Digidata 1440A digitizer and pClamp software. Miniature excitatory post-synaptic potentials (EPSCs) were recorded at a holding potential of -70mV (the Cl^- reversal potential) in the presence of 1μM TTX. Miniature inhibitory post-synaptic potentials (IPSCs) were recorded at a holding potential of 0mV (the reversal potential for excitatory currents) in the presence of 1μM TTX. Only recordings with an access resistance that varied <20% were accepted for analysis.

Acute Slice Electrophysiological Data Analysis

Field recordings were analyzed using Lab Chart (AD Instruments), pClamp (Axon Instruments) and MATLAB software. Traces were recorded at threshold stimulation, the minimum stimulation required to elicit a detectable response, and at 2× and 10× threshold stimulation. Each sweep was analyzed for epileptiform activity to calculate the

percent of epileptiform activity per slice. The area under the curve was used to determine the integrated network activity and was calculated by integrating the extracellular field potential during the first 1000 ms following initial stimulation. Frequency power was calculated with custom MATLAB scripts and was normalized to pre-stimulus levels. Spontaneous and miniature EPSC recordings were analyzed using Clampfit (Axon Instruments Inc.) and Mini Analysis (Synaptosoft). Recordings of 60–120 seconds were analyzed for average amplitude and inter-event frequency.

Kainic Acid-induced Epileptiform Activity and EGG Recordings

Six week old freeze lesion and sham control littermates were implanted for electroencephalogram (EEG) recording based on a Tufts Institutional Animal Care and Use Committee approved protocol. Briefly, animals were anesthetized (100 mg/kg ketamine and 10 mg/kg xylazine). An incision was made on the scalp and a headmount (Pinnacle Technology) was fixed to the skull using four screws and dental cement. The locations of the EEG screws were as follows: two screws were placed in each hemisphere anterior to bregma, and two screws were placed in each hemisphere posterior to bregma. Signals from these screws were used to generate differential EEG recordings. Following surgery, the animals were given 5–7 days to recover. EEG recordings were acquired using a 100× gain preamplifier high-pass filtered at 1.0 Hz (Pinnacle Technology). A baseline EEG was recorded for one hour and then animals were given an intraperitoneal injection of 20 mg/kg kainic acid (KA; Sigma).

Epileptiform activity was measured posthoc as previously described (Klaassen et al., 2006; Lee and Maguire, 2013; Maguire and Mody, 2009; Maguire et al., 2005). KA-

induced seizures were defined by rapid onset of high-amplitude activity (2.5X the standard deviation of the baseline) and were only counted if they lasted longer than 5 s. Quantification of seizure activity was also based on the changes in power of the fast-Fourier transform of the EEG. EEG activity that was abnormal, but that did not meet the criteria to be included as a seizure, was also included in the analysis of epileptiform activity. This included periods of rhythmic spiking lasting longer than 30 s. This set of criteria is similar to published reports from other groups (Castro et al., 2012). Seizure latency was defined as the time from KA injection to the onset of the first electrographic seizure. Total time exhibiting epileptiform activity (% epileptiform activity) was computed as the integrated time of all epileptiform and ictal activity during the 2 hour recording period divided by 120 min. Seizure duration was defined as the time from the initiation of an individual episode for the epileptiform EEG pattern until the return to baseline. These values were averaged across all recorded seizures on an animal by animal basis. LabChart Pro software (ADInstruments) was used for data acquisition and analysis. Spectral analysis was performed using Fast Fourier Transforms in MATLAB. 6 second non-overlapping windows were used to generate average power spectra for both the pre-KA treatment and the 2 hour EEG recording following KA injection. Mean power spectra were then normalized to the average power from 18-80 Hz and binned in 0.25 Hz bins. Mean spectra for each animal was then averaged together for each treatment condition for control and KA EEG. KA mean EEG was then normalized frequency bin by frequency bin to pre-KA EEG and t-tests were performed on individual frequency bins.

2.3: Glutamate Biosensor Imaging

Production of Glutamate FRET Biosensor

BL21(DE3) bacteria were transformed with pRSET-FLII^{81}E-1μ plasmids and streaked on an LB plate with ampicillin (100 μg/ml) (Dulla et al., 2008). After overnight incubation at 37°C, a single colony was picked and grown in 1L LB with ampicillin (100μg/ml) for 3 days at 25°C in the dark with rapid shaking (300 rpm). Cells were harvested by centrifugation, resuspended in extraction buffer (50 mM Sodium Phosphate, 300 mM NaCl, pH7.2), and lysed with CelLytic B reagent (Sigma). The Forster resonance energy transfer (FRET) sensor was purified by Talon His-affinity chromatography (Clontech). Binding to the resin was performed in batch at 4°C, washed in a column with extraction buffer, and then eluted with extraction buffer containing 150 mM imidazole.

Loading of FRET-Based Glutamate Sensor Protein

Loading of glutamate biosensor was done as previously described (Dulla et al., 2008). A 35 mm tissue culture dish was filled with ≈ 2 mL aCSF and a 0.4 μm Millicell (Millipore) culture plate was inserted. Care was taken to ensure that no bubbles were present under the plate insert and that no aCSF spilled onto its top surface. A single brain slice, prepared as above, was transferred from the incubation chamber onto the plate insert and excess aCSF was removed. The dish containing the slice was then placed in a humidified and warmed (32 °C) chamber equilibrated with 95% O_2:5% CO_2. 50 μL of concentrated glutamate FRET sensor protein (≈ 50 ng/μL) was then carefully applied to the top surface of the slice. After 5-10 minutes of incubation, slices were removed from the loading chamber and placed into the recording chamber.

Biosensor Imaging

Collection of glutamate biosensor data was done as previously described (Dulla et al., 2008). Slices were placed into the recording chamber of an Olympus BX51WI microscope with continual superfusion of aCSF for simultaneous imaging with an Olympus 4X objective. Excitation with 440 nm wavelength light was used. A Neuro-CCD camera (RedShirt Imaging) was used to collect 40 x 80 pixel imaging data at 1000 Hz. Each imaging experiment consisted of collecting five movies each containing 1500 frames with 30 s between movies. Each captured 1500 ms movie contained a 90 ms period of dark noise (camera signal before shutter opening) captured before fluorescence was turned on. Fluorescence was turned on for 1210 ms, and then turned off for 200 ms. Slices were stimulated 250 ms after fluorescence was turned on. Emission signals first passed through a 455 nm DCLP dichroic mirror to eliminate excitation fluorescence and were then separated into two channels using a Photometrics Dual-View or Optosplit two channel imaging system to isolate cyan fluorescent protein (CFP) and Venus, a variant of yellow fluorescent protein (YFP) signals. Ratiometric images of CFP/Venus signals were created and analyzed as described below.

Glutamate Imaging Data Analysis

Imaging data was analyzed using customized MATLAB software. Raw imaging data was first split into CFP and Venus and the ratio of the two fluorophores was computed. An average pre-stimulation ratio image was then made by averaging the 40 ms of imaging data prior to the stimulus. The pre-stimulation image was then subtracted from all

images resulting in a ΔFRET image. Processed ΔFRET images were then converted into $\Delta FRET_{signal}/\Delta FRET_{noise}$ data, pixel-by-pixel, by dividing all time-points by the standard deviation of ΔFRET during the pre-stimulus time period. Imaging data was then analyzed to determine the peak amplitude of the signal.

2.4: Western blot

Expression of α2δ-1 was analyzed via western blot. Cortex from adult α2δ-1 KO and wild-type littermates was dissected and homogenized using lysis buffer (0.2% SDS, 50mM NaF, 1mM EDTA). Buffer (10mM Tris pH8, 150mM NaCl, 5mM EDTA, 1% triton, 10mM NaF, 2mM Na_3VO_4 and 10mM $Na_4P_2O_7$) with 100X Halt protease inhibitor cocktail was added and samples were spun down for 15 minutes at 4°C. Loading buffer (10 μL 2-Mercaptoethanol and 190 μL Laemmli Buffer) was added to samples 1:1 and samples were heated to 70°C for 10 minutes. 25 μg of protein was loaded onto a 10% SDS-PAGE gel and analyzed via electrophoresis. Protein was detected using antibodies for α2δ-1 (1:500, Abcam), and anti-β-actin (1:1000, Abcam) was used to confirm equal loading. Protein bands were visualized using enhanced chemiluminescence and imaged with a LAS-3000 imaging system.

2.5: Tissue Preparation and Immunohistochemistry

Immunohistochemistry

Fixed mouse brains were prepared by either submersion fixation (P3) or transcardial perfusing (P7-P60) with PBS followed by overnight fixation with 4% paraformaldehyde. Fixed brains were sectioned at 40 µm using a Thermo Fisher Microm HM 525 cryostat. All rinses and incubations were done in free floating brain sections, with gentle agitation. Brain sections were blocked using blocking buffer (5% normal goat serum, 1% bovine serum albumin, in PBS) for 1 hour at room temperature. Thrombospondin1/2 (1:250, Abcam), α2δ-1 (1:500, Abcam), GFAP (1:500, Abcam), NeuN (1:1000, Millipore), CUX1 (1:100, Santa Cruz), CTIP2 (1:500, Abcam) and activated Caspase-3 (1:500, Abcam) antibodies were diluted in PBS with 2% Triton-X 100 and 5% blocking buffer. Cortical sections were incubated with diluted primary antibodies overnight at 4°C. Following 3 rinses in PBS for 10 minutes, appropriate secondary antibodies (Jackson Labs) were diluted in PBS with 5% blocking buffer and added to cortical sections for 2 hours at room temperature while being protected from the light. Sections were then rinsed 3 times in PBS, for 10 minutes each before mounting. Slices were mounted using Vectashield (Vector Labs) and were stored at 4°C and protected from light until imaging. Slices were imaged on a Keyence BZ-X700 fluorescence microscope or Nikon A1R confocal microscope, taking care to use consistent imaging settings across groups. All staining was analyzed with ImageJ.

Synapse Counting

Tissue preparation, staining and analysis was adapted from the protocol from Ippolito and Eroglu (2010). Brains were fixed as above and sectioned at 14 µm. Brain sections were blocked using 20% normal goat serum in PBS for 1 hour at room temperature. Vglut1 (1:2500, Millipore), PSD95 (1:500, Invitrogen) and GFAP (1:1000, Abcam) were diluted in PBS with 0.3% Triton-X 100 and 10% normal goat serum. Cortical sections were incubated with diluted primary antibodies for 42 hours at 4°C. Sections were rinsed 3 times, for 10 minutesin PBS and then appropriate secondary antibodies (Jackson Labs) were diluted in PBS with 0.3% Triton-X 100 and 10% normal goat serum and added to cortical sections for 2 hours at room temperature, while being protected from the light. Following 3 rinses of 10 minutes in PBS, slices were mounted using fluoromount-G (Southern Biotech) and imaged with a Nikon A1R confocal microscope. Images were collected with a 100X oil immersion objective and Maximum Intensity Projections (MIP), of 3 serial optical sections at 0.175um steps, were generated. 5 MIPs were generated and analyzed per section. These were averaged to give one value per brain section. Synapses were quantified in ImageJ using the Puncta Analyzer plug in.

TUNEL assay

Brains were prepared by transcardial perfusion with PBS followed by overnight fixation with 4% paraformaldehyde. Fixed brains were sectioned at 40 µm using a Thermo Fisher Microm HM 525 cryostat. Terminal deoxynucleotidyl transferase dUTP nick end labeling (TUNEL) was detected using an ApopTag peroxidase *in situ* apoptosis detection kit (Millipore). Briefly, endogenous peroxidase activity was blocked by incubation of the

sections with 3% H_2O_2 for 5 minutes. TdT enzyme provided by the kit was used to label dUTP nick ends with DAB as the substrate. Nuclei were counterstained with methyl green and slices were mounted using Permount (Fisher Scientific). Tissue sections were evaluated by conventional bright-field microscopy and analyzed in ImageJ.

2.6: Statistical Analysis

For all studies, control experiments were performed including sham injury and vehicle treatment. All experiments used animals of the same age between groups. Additionally, WT littermates were used as controls in experiments testing the effect of genetic deletion of $\alpha 2\delta$-1. Gabapentin versus vehicle and sham versus FL was randomized by litter, ensuring a mix of treatments and genotypes throughout all studies. The distribution of genotypes followed a Mendelian distribution. The sex of the mice was approximately 50% male and 50% female except in behavioral and EEG studies in which only male mice were used. Sample size has been calculated to ensure power >0.8 for α=0.05. Power was calculated using G*Power Software.

For comparison between two experimental groups, a student's t-test was used when data was normally distributed or a Mann-Whitney U-test when data was not normally distributed. For comparisons between three or more groups, a one-way ANOVA was used. For comparison of cumulative probabilities, a Kolmogorov-Smirnov test was used. For all experiments using $\alpha 2\delta$-1 KOs, we first verified that there is a significant effect of FL compared to sham. We then compared WT FL to WT FL+GBP, WT FL to KO FL, and KO FL to KO FL+GBP. To control for multiple comparisons, a Holm-Bonferroni correction was used. All data is presented as either means ± SEM or as a box-whisker plots ± SEM, with mean values indicated by X on the plots. Values of $p < 0.05$ or more were considered statistically significant. OriginLab and MATLAB software was used to perform the statistical analyses.

Chapter 3:

Antagonizing α2δ-1 is Neuroprotective Following Neonatal Freeze Lesion

3.1: Thrombospondin and α2δ-1 immunoreactivity is increased after FL

Astrocyte-secreted thrombospondins regulate excitatory synapse formation in the developing CNS, (Christopherson et al., 2005; Eroglu et al., 2009) and they have been shown to be upregulated following injury correlated with an increase in reactive astrocytosis (Lin et al., 2003). To establish if thrombospondin levels are altered in our model, freeze lesion and sham lesion brains were probed for thrombospondin 1 and 2 (TSP1/2) immunoreactivity. We found significant increases in TSP1/2 immuno-fluorescence in FL cortex 3 (Fig. 3.1 A and B; 2.21 ± 0.056 fold increase compared to sham, n=3; $p<.001$) and 7 days following FL (1.81 ± 0.173 fold increase compared to sham, n=9; $p<.05$). Diffuse TSP1/2 staining was observed in the injured area, nearby GFAP immunoreactivity (Fig. 3.1 C).

The immunoreactivity of TSP's neuronal receptor, the α2δ-1 subunit of voltage gated calcium channels, was also significantly increased 3 (Fig 3.1 E and F; 1.88 ± 0.135 fold increase compared to sham, n=6; $p<.001$) and 7 days following FL (1.57 ± 0.246 fold increase compared to sham, n=4; $p<.05$). By P14, there were no longer any significant differences in TSP1/2 or α2δ-1 immunoreactivity. These results indicate that both TSP1/2 and α2δ-1 immunoreactivity are transiently increased in the neocortex following FL at the site of injury. Therefore, TSP/α2δ-1 signaling is well poised to play a role in the pathological processes associated with FL. To address this question, we designed a treatment paradigm to block the interaction of TSP with α2δ-1, using the α2δ-1 antagonist gabapentin.

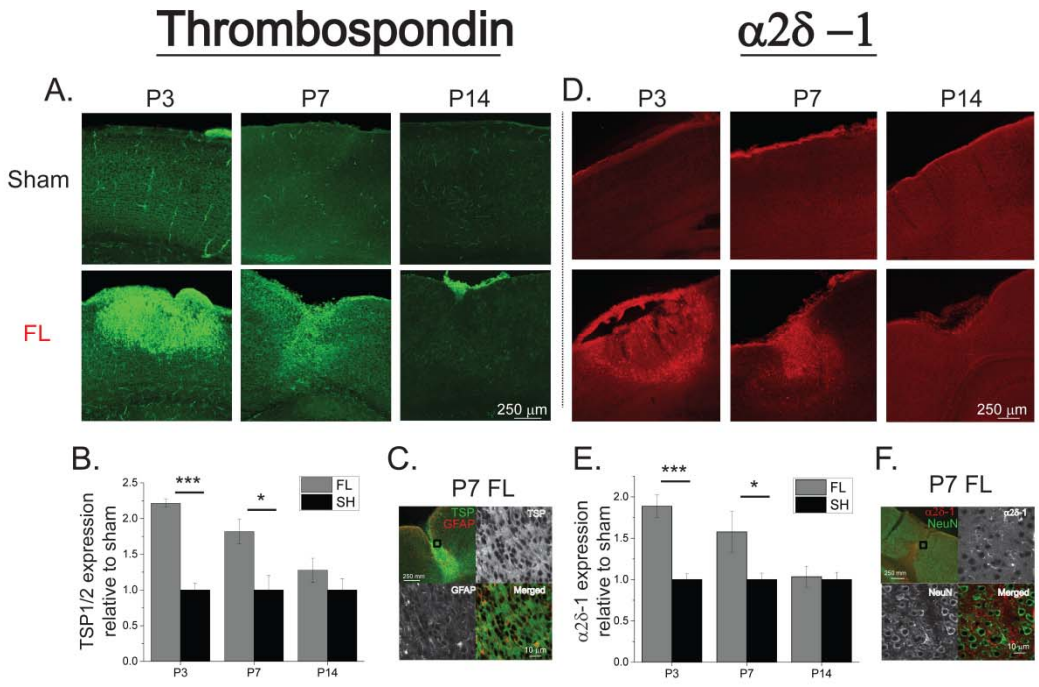

Figure 3.1: Thrombospondin and α2δ-1 immunoreactivity is increased after FL

(A) TSP1/2 staining in sham injured and FL cortex at P3, P7 and P14 (B) Average TSP1/2 fluorescence relative to sham (C) TSP1/2 (green) and GFAP (red) co-stain of a P7 FL animal and 60× magnification of the area in the black box for TSP1/2, GFAP and merged TSP1/2 (green) and GFAP (red) (D) α2δ-1 staining in sham injured and FL cortex at P3, P7 and P14 (E) Average α2δ-1 fluorescence relative to sham (F) α2δ-1 (red) and NeuN (green) co-stain of a P7 FL animal and 60× magnification of the area in the black box for α2δ-1, NeuN and merged α2δ-1 (red) and NeuN (green), *** $P < 0.001$ and *$P < 0.05$. Reproduced with permission from (Andresen et al., 2014). TSP staining was performed by Amaro Taylor.

3.2: Pharmacological attenuation of α2δ-1 signaling decreases cell death following FL

GBP treatment has been shown to reduce cell death in models of post-traumatic epilepsy (Li et al., 2012) and stroke (Traa et al., 2008), suggesting that α2δ-1 signaling may contribute to insult-induced cortical cell death. Here, we tested whether attenuating α2δ-1 signaling via *in vivo* GBP treatment was neuroprotective in the FL model. To identify dead and dying cells in the neonatal cortex, we used Tdt-mediated dUTP-biotin nick end labeling (TUNEL) labeling and activated caspase-3 immunolabeling (Watanabe et al., 2002). We found that FL induced significant cell death in the cortex at P7 (Fig 3.2; *Capspase-3 immunoreactivity*: Sham, 4.1 ± 1.0 cells per 0.1 mm^2, n=11; FL, 61.5 ± 4.4 cells per 0.1 mm^2, n = 10; $p < 0.001$; *TUNEL*: Sham, 0.5 ± 0.2 cells per 0.1 mm^2, n = 7; FL, 59.1 ± 16.6, n = 8; $p < 0.001$). The majority of cell death was seen at the site of FL and in the surrounding cortical tissue. Other developmental time points were examined and the peak expression of cell death markers was seen at approximately P5-7 (data not shown). Therefore the effects of α2δ-1 signaling on cell death were quantified at P7. To determine the role of α2δ-1 signaling in FL-induced cell death, we treated animals systemically with GBP after FL. Sham and FL animals were treated with 200 mg/kg GBP or vehicle (daily intraperitoneal, I.P., injection) daily from P1-7. We found that GBP treatment significantly reduced cell death following FL, as measured using both assays (*Caspase-3 immunoreactivity*: 26.1 ± 6.2 cells per 0.1 mm^2, n = 14; $p < 0.01$; *TUNEL*: 19.9 ± 7.7, n = 13 and 14.6 ± 3.8 cells per 0.1 mm^2, n = 7; $p < 0.01$). Very few cells expressed either marker of cell death in sham animals (*Caspase-3*

immunoreactivity: 2.3 ± 0.4 cells per 0.1 mm^2, n = 10; *TUNEL*: 0.1 ± 0.04, n = 8) and there was no effect of GBP treatment on cell death in sham animals.

3.3: Genetic deletion of α2δ-1 attenuates FL-induced cell death

Next, we examined whether genetic deletion of α2δ-1 recapitulated GBP's neuroprotective effects after FL. Mice with a global, germ-line knockout of the α2δ-1 gene (*CACNA2D1*) were generated and the absence of the α2δ-1 protein was confirmed by Western blot analysis of total cortical homogenate. We found that mice lacking α2δ-1 (α2δ-1 KO) had reduced cell death at P7 following FL (Fig 3.2; *Caspase-3 immunoreactivity:* 38.8 ± 9.7, n = 10; $p < 0.001$ as compared to WT FL; TUNEL: 14.6 ± 3.8 cells per 0.1 mm^2, n = 7; $p < 0.05$), consistent with α2δ-1 signaling contributing to FL-induced cell death. Previously, it has been unknown whether GBP's effects on cell death act via α2δ-1 signaling or via another pathway. To test this, we treated α2δ-1 knockout animals with GBP after FL. Interestingly, GBP treatment did not further reduce cell death in α2δ-1 KO animals (*Caspase-3 immunoreactivity:* 22.3 ± 9.9, n = 6; *TUNEL*: 19.7 ± 3.4 cells per 0.1 mm^2, n = 8). This indicates that GBP likely acts via α2δ-1 to reduce cell death, as α2δ-1 deletion eliminates GBP's neuroprotective effects. Genetic deletion of α2δ-1 did not affect expression of cell death markers in sham animals (*Caspase-3 immunoreactivity:* 5.8 ± 2.2, n = 4; *TUNEL*: 0.6 ± 0.2 cells per 0.1 mm^2, n =8), nor did GBP treatment affect cell death in sham α2δ-1 knockout mice (*Caspase-3 immunoreactivity:* 5.2 ± 1.8, n = 6; *TUNEL*: 0.7 ± 0.3 cells per 0.1 mm^2, n = 8).

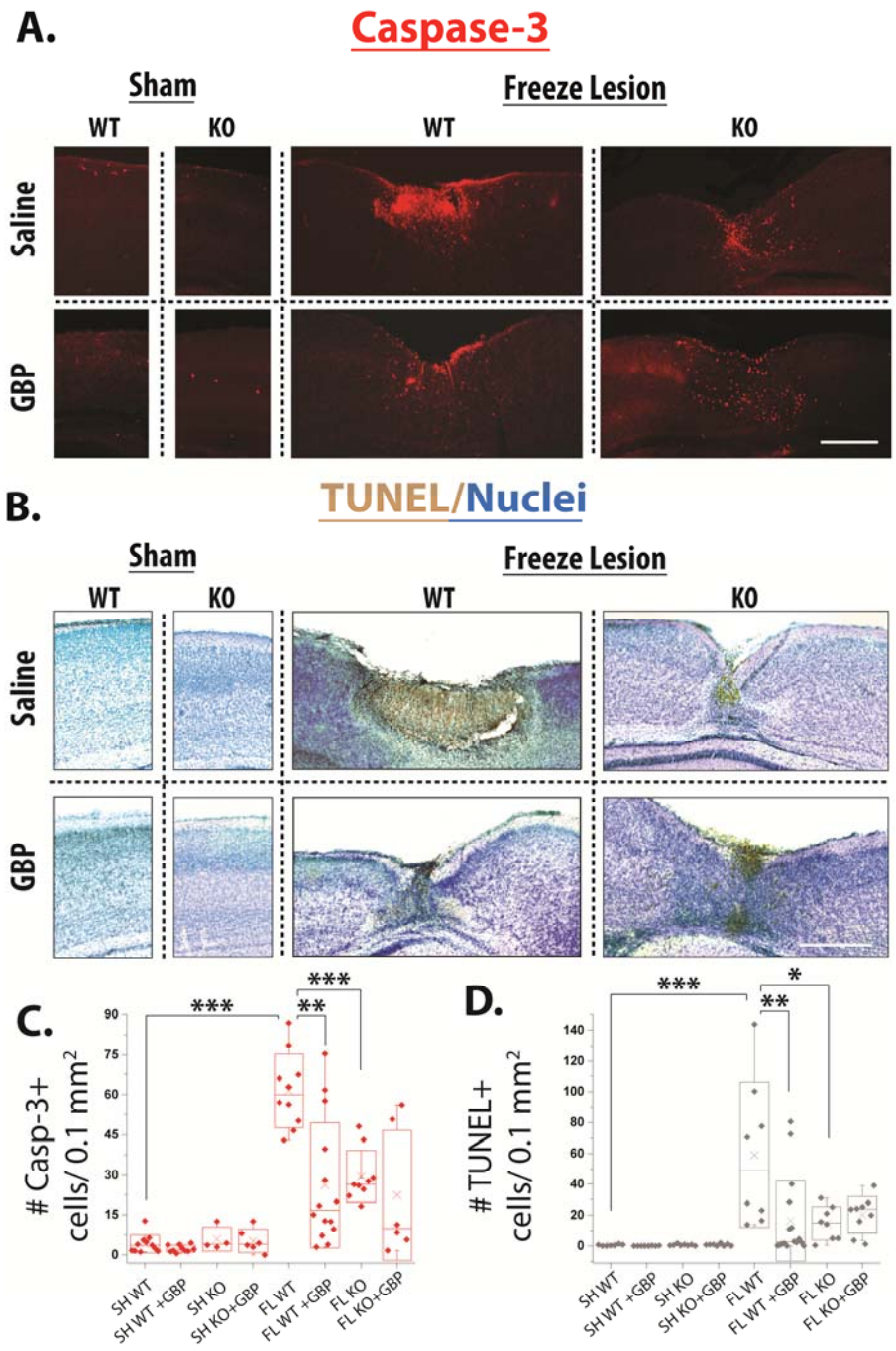

Figure 3.2: Gabapentin treatment or α2δ-1 deletion decreases cell death following FL

(A) Representative images of cleaved caspase-3 (casp-3) staining in P7 WT and $\alpha2\delta\text{-}1^{-/-}$ sham ±GBP and WT and $\alpha2\delta\text{-}1^{-/-}$ FL ±GBP. Scale bar = 500 µm. (B) Representative bright-field images of TUNEL assay (TUNEL+ cells stained brown by DAB), nuclei counterstained by methyl green in P7 WT and $\alpha2\delta\text{-}1^{-/-}$ sham ±GBP and WT and $\alpha2\delta\text{-}1^{-/-}$ FL ±GBP. Scale bar = 500 µm. (C) Box-Whisker plot of casp-3+ cells per 0.1 mm^2, ** $p < 0.01$ and ***$p < 0.001$ (D) Box-Whisker plot of TUNEL+ cells per section, * $p < 0.05$, ** $p < 0.01$ and *** $p < 0.001$.

3.4: Attenuating α2δ-1 signaling reduces FL-induced cortical malformation

Because genetic and pharmacological inhibition of α2δ-1 signaling reduced cell death, we hypothesized that similar manipulations would decrease FL-induced cortical reorganization. To test this hypothesis, we examined anatomical changes induced by FL in GBP-treated and α2δ-1 knockout animals. Because FL creates a 3-dimensional cortical malformation, we prepared serial cortical brain sections from P28 FL animals that encompassed the entire FL, and equivalent isotopic brain regions in shams. We identified areas of malformation by examining NeuN (marker of neurons) immunolabeled sections. The area of malformed, or missing, cortex was quantified throughout the reconstructed cortex. When FL resulted in loss of cortical tissue, this loss was quantified by drawing a line continuous with the adjacent pial surface and calculating the area of predicted tissue loss. The area of missing cortex was added to the area of malformed cortex, characterized by large-scale cortical disorganization, to calculate lesion area per slice (Fig. 3.3 A). The area was calculated in serial sections through the volume of the lesion and used to estimate the total lesion volume. Consistent with our cell death data, the volume of the lesion was decreased in FL animals treated with GBP (Fig. 3.3 B; 1.65 ± 0.13 mm^3, n = 3 animals versus 1.25 ± 0.03, n = 3 animals; $p < 0.05$). α2δ-1 KO mice also showed reduced lesion size compared to WT FL (1.08 ± 0.13, n = 4 and 1.64 ± 0.06 mm^3, n = 4 for vehicle and GBP-treated animals, respectively; $p < 0.01$). These results demonstrate that reducing α2δ-1 signaling with either GBP treatment or α2δ-1 KO reduces the areas of cortical malformation following FL. Similar to cell death data, treating α2δ-1 KO animals with GBP did not

result in additional reductions in cortical malformation. This again suggests that GBP's neuroprotective effects are mediated by $\alpha 2\delta$-1.

3.5: Attenuating α2δ-1 signaling decreases GFAP immunoreactivity following FL

In parallel to measuring lesion volume, we also examined immunoreactivity for glial fibrillary acid protein (GFAP), a protein that is strongly upregulated by reactive astrocytes in the cerebral cortex. Our previous work, and the work of others, shows that FL causes significant reactive astrocytosis (Armbruster et al., 2014; Bordey et al., 2001; Campbell et al., 2014; Dulla et al., 2013; Hanson et al., 2016). To quantify GFAP labeling in the cortex, we examined immunolabeled serial sections through the entire FL volume at P28. GBP treatment significantly reduced FL-induced increases in GFAP immunolabeling (Figs. 3.3 A and D; 9.47% ± 1.24, n = 5 animals) compared to vehicle treated FL animals (26.23% ± 6.97, n = 5 animals; $p < 0.05$). Similarly, genetic deletion of α2δ-1 KO also reduced GFAP immunolabeling after FL (2.92% ± 0.74, n = 4; $p < 0.01$) without any additive effects of GBP treatment (6.77% ± 2.36, n = 4). Consistent with previous findings, these results show that GBP treatment reduces astrocyte reactivity, as measured by GFAP immunolabeling in the cortex.

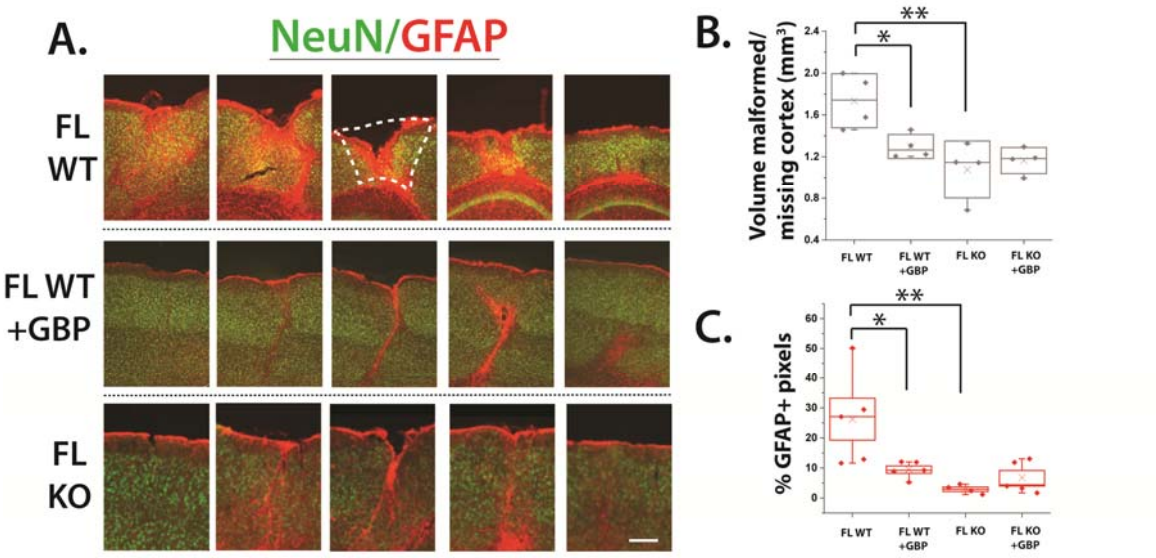

Figure 3.3: Gabapentin treatment or α2δ-1 knockout decreases malformation volume and astrocyte reactivity after FL

(A) GFAP (red) and NeuN (green) staining in P28 WT FL, WT GBP-treated FL and $\alpha 2\delta\text{-}1^{-/-}$ FL cortex. Serial sections taken at 480 µm intervals, spanning the total length of the microgyrus (MZ). Scale bar = 100 µm. Dotted white line showing area of both missing and malformed cortical tissue. (B) Volume of missing or malformed cortex (mm^3), estimated from area calculated in serial sections, * $p < 0.05$. (C) Percent of GFAP positive pixels in ~600 μm^2 ROI from white matter to the pial surface, centered around the MZ, * $p < 0.05$. Staining in WT FL and WT FL+GBP was performed by David Hampton.

3.6: FL induces α2δ-1-dependent laminar reorganization of the cortex

In order to better understand FL-induced anatomical changes, we examined the expression of layer specific markers in the cortex at P28. CUX1 and CTIP2 are transcription factors that preferentially label superficial (LII/III) and deep (LIV/VI) cortical layers, respectively (Insolera et al., 2014). Consistent with published data, CTIP2+ cells are abundant in deep cortical layers (588 ± 52 per mm^2, n = 11), and found sporadically in outer layers (Fig. 3.4; 26 ± 5 per mm^2, n = 11) in the sham injured cortex. Conversely, CUX1+ cells are more abundant in the outer layers and are sparser in deep layers (743 ± 31 versus 119 ± 26 per mm^2). In contrast to the normal 6-layered cortex, FL creates a 4-layered microgyrial zone (MZ). Layer i is continuous with cortical layer I. Layer ii is neuron-rich and makes up the bulk of the MZ (Dvorak and Feit, 1977). Layer iii is a neuron-free area and layer iv is a small layer comprised of presumed deep layer neurons. Studies postulate that neurons in MZ layer iii are similar to layer II/III neurons and that layer IV-VI cortical neurons are lost, but the expression of layer-specific markers following FL has not been examined. We found that layer ii of the MZ is predominately composed of CUX1+ cells and layer iv of CTIP2+ cells, in line with previous predictions. Interestingly, the density of CUX1+ cells in MZ layer ii (285 ± 34 per mm^2, n = 7, $p < 0.001$, compared to sham-injured layer II/III) and CTIP2+ cells in MZ layer iv (240 ± 31 per mm^2; $p < 0.001$, compared to layer V-VI) was decreased compared to equivalent layers in sham cortex. Additionally, the ratio of superficial layer (layer ii or II/III) to deep layer (iv or V-VI) is significantly higher in FL MZ cortex (7.26 ± 1.87, n = 7)

compared to sham-injured cortex (1.12 ± 0.06, n = 11; $p < 0.001$) reflecting the loss of deep layer cells and concurrent expansion of the outer layer in FL cortex.

Based on these findings, we next examined how attenuating $\alpha 2\delta$-1 signaling affects layer-specific changes in the microgyral zone. Sham and FL animals were treated with GBP, as described above, and CTIP2+ and CUX1+ cells were identified at P28. GBP treatment restored the density of CUX1+ cells in the outer layers to sham-injured levels (668 ± 32 per mm^2, n = 21; $p < 0.001$, compared to vehicle-treated FL) and significantly increased the density of deep layer CTIP2+ cells (111 ± 14 per mm^2; $p < 0.001$, compared to vehicle-treated FL). Consistent with a significant rescue of deep layer cortical neurons, FL animals treated with GBP have a significantly smaller superficial/deep layer ratio of 2.93 ± 0.37 (n = 21; $p < 0.001$) and the MZ more closely resembles the normal 6-layered cortex. GBP treatment did not affect CUX1+ (659 ± 31 per mm^2, n = 15) or CTIP2+ cell (495 ± 42 per mm^2) density in sham injured animals.

We next examined how genetic deletion of $\alpha 2\delta$-1 affected laminar reorganization in the microgyral zone. $\alpha 2\delta$-1 knockout attenuated FL-induced decreases in CUX1+ and CTIP2+ cell density (723 ± 59, $p < 0.001$ and 646 ± 84 cells per mm^2, n = 5, $p < 0.01$, compared to WT FL). FL-induced changes in the ratio of superficial/deep layers were also significantly attenuated in $\alpha 2\delta$-1 knockout animals. (1.52 ± 0.13, n = 8; $p < 0.01$). Genetic deletion of $\alpha 2\delta$-1 did not affect CUX1+ (762 ± 42 cells per mm^2, n = 7) or CTIP2+ (564 ± 87 cells per mm^2) cell density in sham animals. GBP-treatment also did not affect CUX1+ and CTIP2+ cell density in $\alpha 2\delta$ knockout mice (692 ± 81 and 676 ± 103 cells per mm^2, n = 7).

We next examined the cellular density of CUX1 and CTIP2 in the paramicrogyrial zone (PMZ), the area immediately adjacent to the MZ responsible for generating epileptiform network activity. Interestingly, the PMZ has long been considered an area of normal cortical lamination. While gross cortical lamination is normal, we find that FL alters the density of CUX1+ and CTIP2+ cells in the PMZ. The density of CUX1+ cells in superficial layers (380 ± 37 cells per mm^2; $p < 0.001$) and density of CTIP2+ cells in deep layers (240 ± 31 cells per mm^2; $p < 0.001$) are significantly reduced in the PMZ as compared to sham injured cortex. GBP treatment prevents the layer-specific decreases in CUX1+ and CTIP2+ cells in the PMZ (671 ± 28 and 560 ± 29 cells per mm^2, respectively; $p < 0.001$), as does $\alpha 2\delta$-1 KO (672 ± 48 and 579 ± 86 cells per mm^2; $p < 0.001$ and $p < 0.05$). GBP treatment does not provide further protection against anatomical reorganization, again suggesting GBP mediates it protective effects via $\alpha 2\delta$-1. These results demonstrate that FL disrupts cortical lamination, as assayed by the expression of layer-specific markers, via $\alpha 2\delta$-1 signaling.

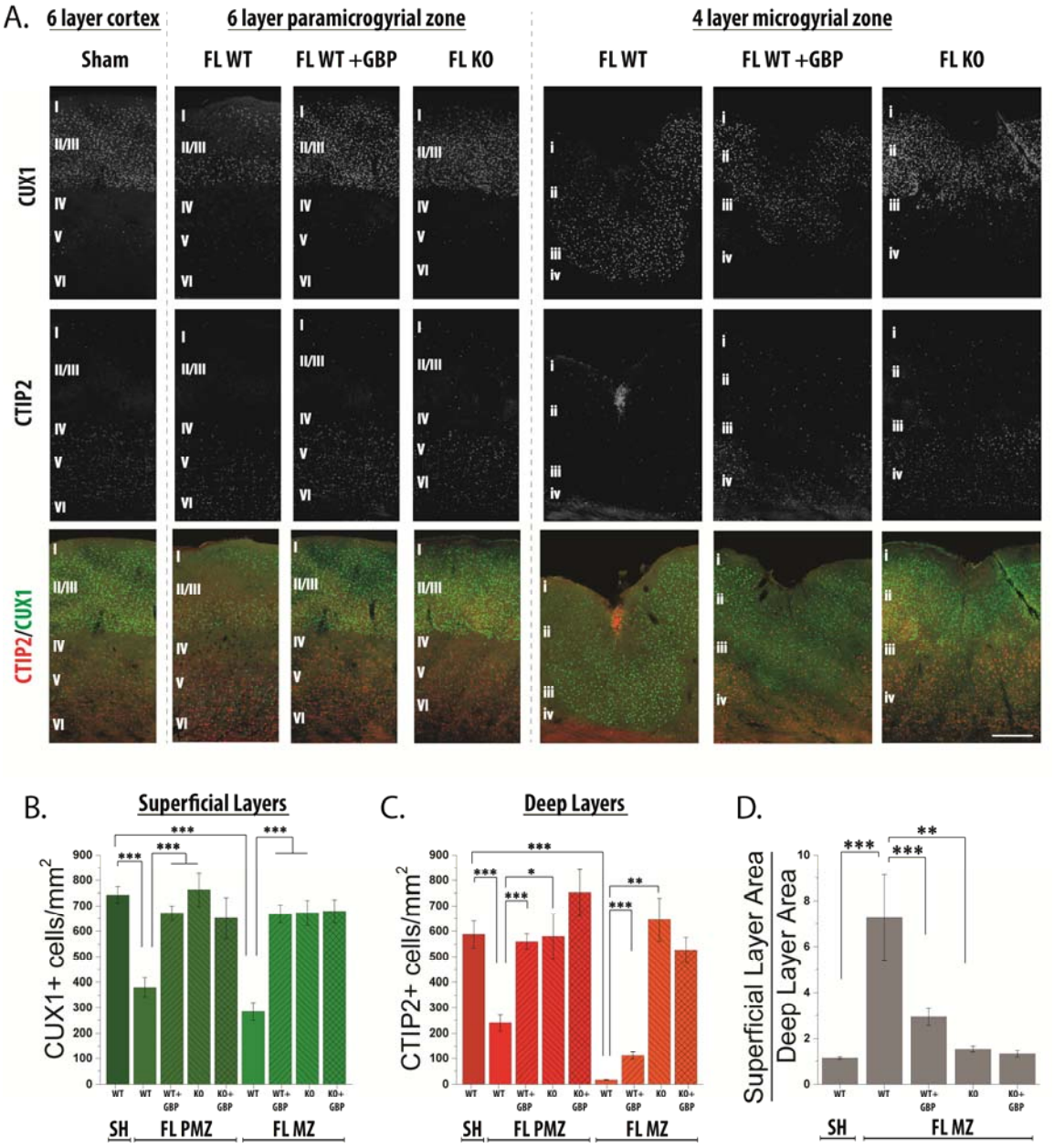

Figure 3.4: Gabapentin treatment or α2δ-1 knockout attenuates the loss of layer-specific markers in the FL cortex

(A) Representative images of CUX1 (green) and CTIP2 (red) staining in P28 WT sham cortex and the PMZ and MZ of WT FL, WT FL+GBP and $\alpha2\delta\text{-}1^{-/-}$ FL cortex. Scale bar = 250 µm. (B) Average CUX1+ cells per mm^2 in the outer layers, *** $p < 0.001$. (C) Average CTIP2+ cells per mm^2 in the deep layers, *** $p < 0.001$. (D) Ratio of area of outer layer (layer II/III in sham and layer ii in FL) to area of inner layer (layer V and VI in sham and layer iv in FL) in sham, FL, FL+GBP and α2δ-1 KO FL cortex, *** $p < 0.001$, ** $p < 0.01$ and * $p < 0.05$.

3.7: Total neuron number is normal in the FL cortex

Because the expression of CUX1 and CTIP2 was altered by FL, we wondered whether neuronal density was also affected. To test this, we next performed NeuN staining and counted the total number of neurons in the cortex. Confocal images of the outer and deep cortical layer were used to determine neuronal density. In comparison to the dramatic changes found in CUX1 and CTIP2 staining following FL, no significant reduction in total neuron number was observed (Fig. 3.5). These results suggest that overall neuronal density is normal in the FL cortex at P28, and changes in CUX1+ and CTIP2+ cell density reflect changes in marker expression.

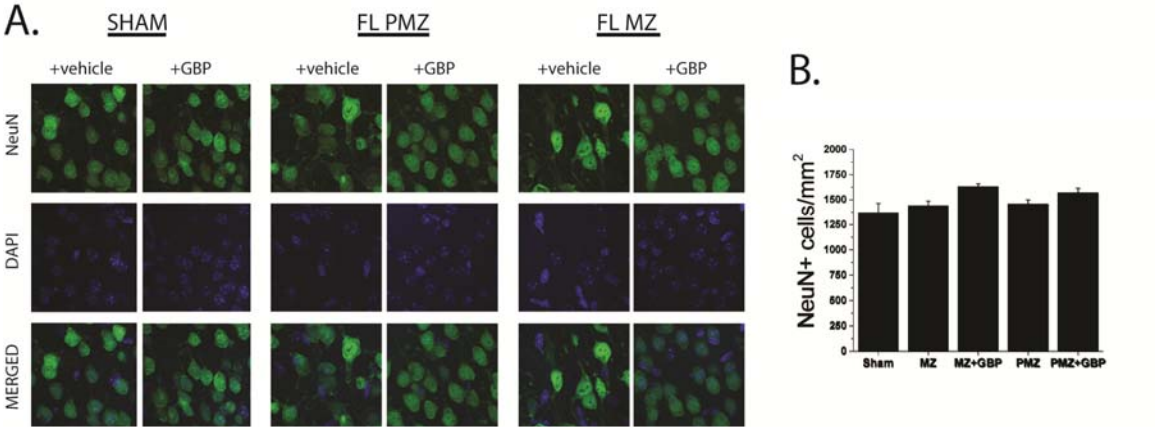

Figure 3.5: Total neuronal density is normal in the FL cortex

(A) Representative images of NeuN+ cells and DAPI in P28 WT sham cortex and the PMZ and MZ of WT FL and WT FL+GBP (B) Average NeuN+ cells per mm^2

3.8: Conclusions

In conclusion, we have shown in this chapter that $\alpha 2\delta$-1 signaling drives cell death and cortical reorganization following FL. The initial freezing insult begins a cascade of events that drives caspase-mediated cell death, which peaks several days after injury. Antagonizing $\alpha 2\delta$-1 signaling with either GBP treatment or genetic deletion is neuroprotective. Furthermore, GBP has no additive effects in the $\alpha 2\delta$-1 KO animals, suggesting that $\alpha 2\delta$-1 is the receptor responsible for the neuroprotective effects of GBP. In addition to attenuating cell death following injury, antagonizing $\alpha 2\delta$-1 signaling also has long-lasting effects on reducing laminar disruptions, lesion formation and astrocyte reactivity.

Chapter 4:

α2δ-1 Signaling Drives Excitatory Synaptogenesis and Network Hyperexcitability following Neonatal Freeze Lesion

4.1: Decreasing α2δ-1 signaling attenuates FL-driven increases in synaptogenesis

TSP/α2δ-1 signaling promotes excitatory synapse formation during development (Eroglu et al., 2009) and we hypothesize that increased TSP and α2δ-1 drives exuberant synaptogenesis following FL. GBP has been shown to decreases excitatory synaptogenesis during development (Eroglu et al., 2009) and following injury (Li et al., 2012; Li et al., 2014). We therefore predict that antagonizing α2δ-1 signaling will attenuate aberrant excitatory synaptogenesis in the FL cortex. We examined excitatory synapse number by immunolabeling with the pre and postsynaptic markers, VGLUT1 and PSD95. Synapse counting was performed at P28, in layer V of the paramicrogyrial zone (PMZ) as this is the region that was previously shown to be hyperexcitable following FL and have increased excitatory synaptic activity. Co-localization of VGLUT1 and PSD95 puncta were quantified (Ippolito and Eroglu, 2010) to determine the density of putative excitatory synaptic contacts. We found that sham-injured WT animals had a synaptic density of 488 ± 70 per mm^2 (n = 8) (Fig 4.1). There was no difference among sham-injured animals with GBP treatment and/or genetic deletion of α2δ-1 (WT+GBP: 484 ± 72, n = 8; KO: 421 ± 61, n = 8; KO+GBP: 381 ± 20, n = 7). FL induced a marked increase in the density of putative excitatory synapses in WT mice (Fig 4.1 A and B; 758 ± 68 per mm^2, n = 7; $p < 0.001$). Both GBP treatment and genetic deletion of α2δ-1 attenuated FL-induced increase in colocalized VGLUT1/PSD95 puncta (567 ± 41, n = 7 and 556 ± 60, n = 9; $p < 0.01$). These results demonstrate that FL induces α2δ-1-mediated synaptogenesis and that inhibition of α2δ-1 signaling can attenuate this aberrant synaptogenesis. In contrast to our other assays, we found that GBP treatment

in α2δ-1 KO mice further reduced excitatory synapse number (368 ± 45 per mm^2, n = 8) compared to vehicle-treated α2δ-1 KO FL mice ($p < 0.01$). This additive effect indicates that GBP can have α2δ-1-indepenent effects on synaptogenesis.

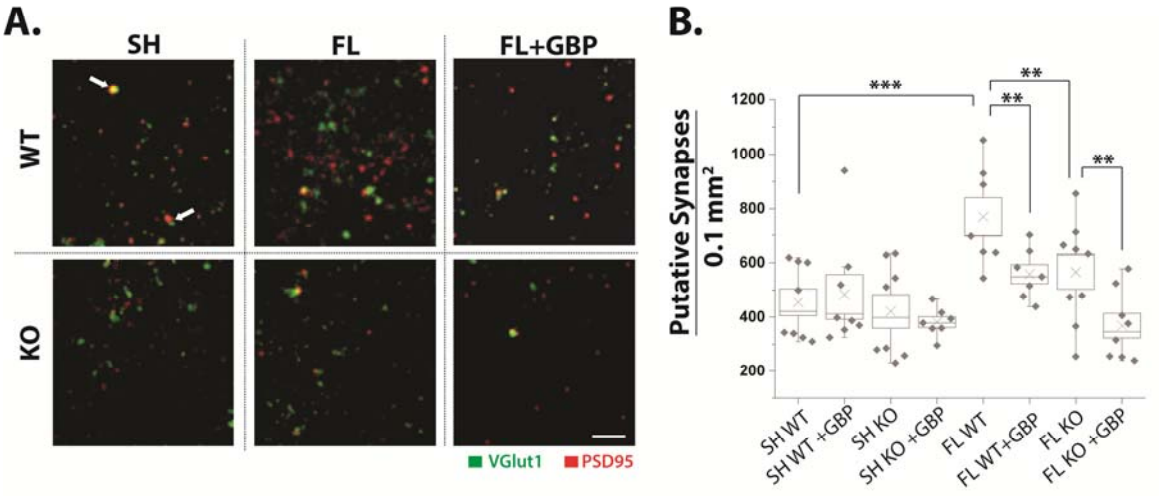

Figure 4.1: Gabapentin treatment or α2δ-1 deletion decreases FL-driven synaptogenesis

(A) Maximum intensity projections (MIP) from of 3 optical sections of confocal images of VGlut1 (green) and PSD95 (red) collected at 100X from layer V of WT and 2-1 KO FL and Sham-injured animals, with vehicle or GBP treatment. White arrow indicates co-localization of VGLUT1 and PSD95, representing a site of synaptic contact. Scale bar = 500 nm. (B) Box-Whisker plot of number of synapses (co-localization of VGlut1/PSD95) per 1.00 mm^3 per MIP, ** $p < 0.01$ and ** $p < 0.001$.

4.2: Decreasing α2δ-1 signaling attenuates FL-driven rise in the frequency of miniature excitatory postsynaptic currents

Given the changes in excitatory synapse number, we next wanted to assess the role of α2δ-1 signaling on functional synaptic connectivity by examining miniature excitatory postsynaptic currents (mEPSCs) in the FL cortex. mEPSCs were recorded from layer V pyramidal neurons in acute cortical slices held at -70 mV and perfused with normal aCSF containing 1 μm TTX. We found no significant differences in resting membrane potential, rise or decay kinetics, or the amplitude of the mEPSC events between groups (Fig 4.2 B). The frequency of mEPSCs was used to determine differences in the number of functional excitatory synapses. We found that FL induced a rise in mEPSC frequency (Fig 4.2 A and B; 0.79 ± 0.19 Hz, n = 14; $p < 0.01$) compared to sham-injured animals (0.23 ± 0.05 Hz, n = 14). GBP treatment significantly reduced the mEPSC frequency (0.29 ± 0.09 Hz, n = 13; $p < 0.05$); α2δ-1 deletion non-significantly reduced mEPSC frequency (0.30 ± 0.04 Hz, n = 9; $p = 0.056$) following FL. The cumulative probability distribution of the inter-event interval (IEI) was calculated to further assess changes in mEPSC frequency. The leftward shift in the IEI cumulative probability in WT FL cortex (Fig 4.2 D; $p < 0.001$), compared to WT sham, again demonstrates the increased number of functional excitatory synapse following FL. The IEI cumulative probability is shifted rightward in both GBP treated WT FL and α2δ-1 KO FL animals ($p < 0.001$), consistent with the ability of GBP treatment or α2δ-1 deletion to attenuate FL-driven synaptogenesis.

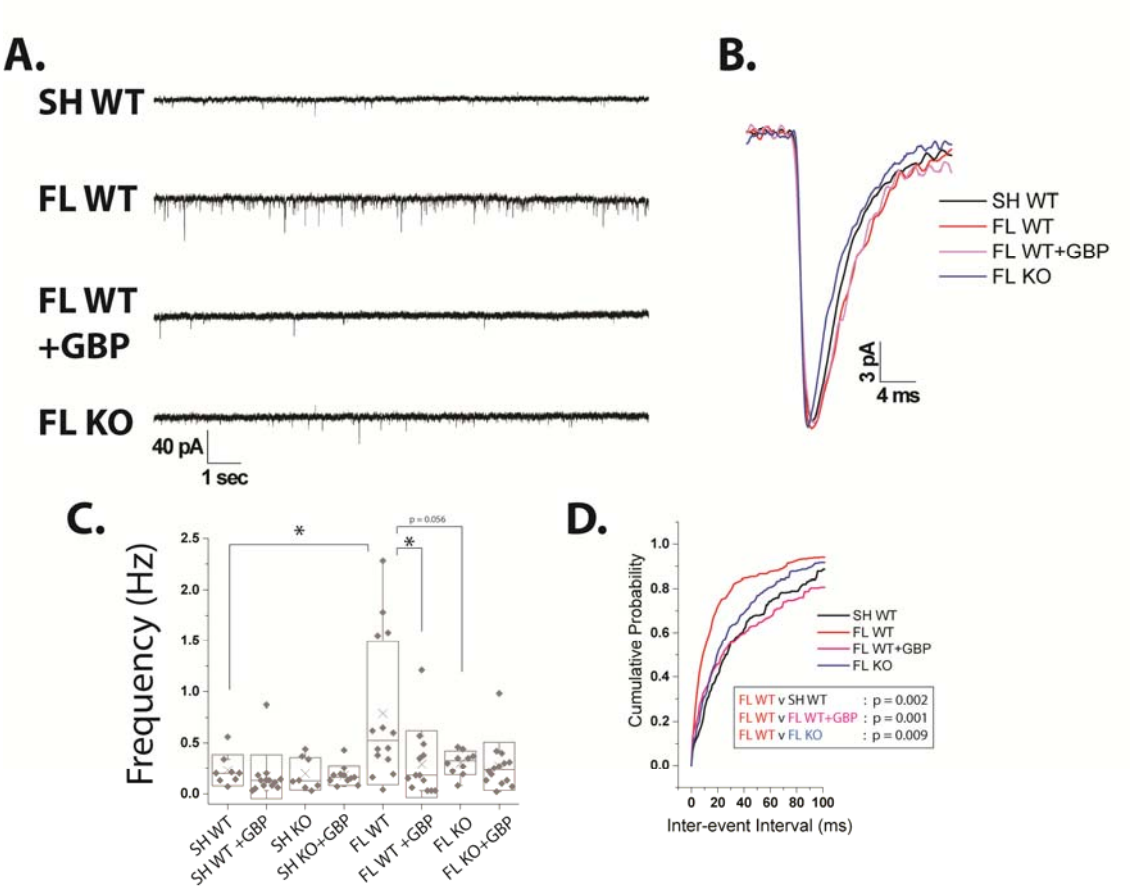

Figure 4.2: Gabapentin treatment or α2δ-1 knockout attenuates the rise in mEPSC frequency in the FL cortex

(A) Representative miniature excitatory postsynaptic current recording of layer V pyramidal neuron recorded from the PMZ of acute cortical slices prepared from P21-P28 WT sham, WT FL, WT FL+GBP and $\alpha 2\delta\text{-}1^{-/-}$ FL. (B) Example mEPSC from WT sham (black), WT FL (red), WT FL+GBP (pink) and $\alpha 2\delta\text{-}1^{-/-}$ FL (blue). (C) Box-Whisker plot of frequency of mEPSC events, *$p < 0.05$. (D) Cumulative probability of inter-event intervals of WT sham (black), WT FL (red), WT FL+GBP (pink) and $\alpha 2\delta\text{-}1^{-/-}$ FL (blue). WT FL has a significant rightward shift compared to WT sham, WT FL+GBP and $\alpha 2\delta\text{-}1^{-/-}$ FL, $p < 0.001$.

4.3: Gabapentin treatment does not affect FL-driven rise in the frequency of miniature inhibitory postsynaptic currents

Previous work has shown that TSP/$\alpha 2\delta$-1-mediated synaptogenesis does not increase inhibitory synapse number (Hughes et al., 2010). Here we assessed the role of $\alpha 2\delta$-1 signaling on inhibitory connectivity by examining miniature inhibitory postsynaptic currents (mIPSCs) in the FL cortex. mIPSCs were recorded from layer V pyramidal neurons in acute cortical slices held at 0 mV and perfused with normal aCSF containing 1 μm TTX. We found no significant differences in resting membrane potential, rise or decay kinetics, or the amplitude of the mIPSC events between groups (Fig 4.3 B). The frequency of mIPSCs was used to determine differences in the number of functional inhibitory synapses. Consistent with previous results (Jacobs and Prince, 2005), we found that FL induced a rise in mIPSC frequency compared to sham-injured animals, as demonstrated by the leftward shift in the IEI cumulative probability (Fig 4.3 C; $p < 0.001$). GBP treatment had no effect on the IEI following FL (Fig 4.3 C). These results suggest that GBP treatment specifically acts to disrupt excitatory synaptogenesis.

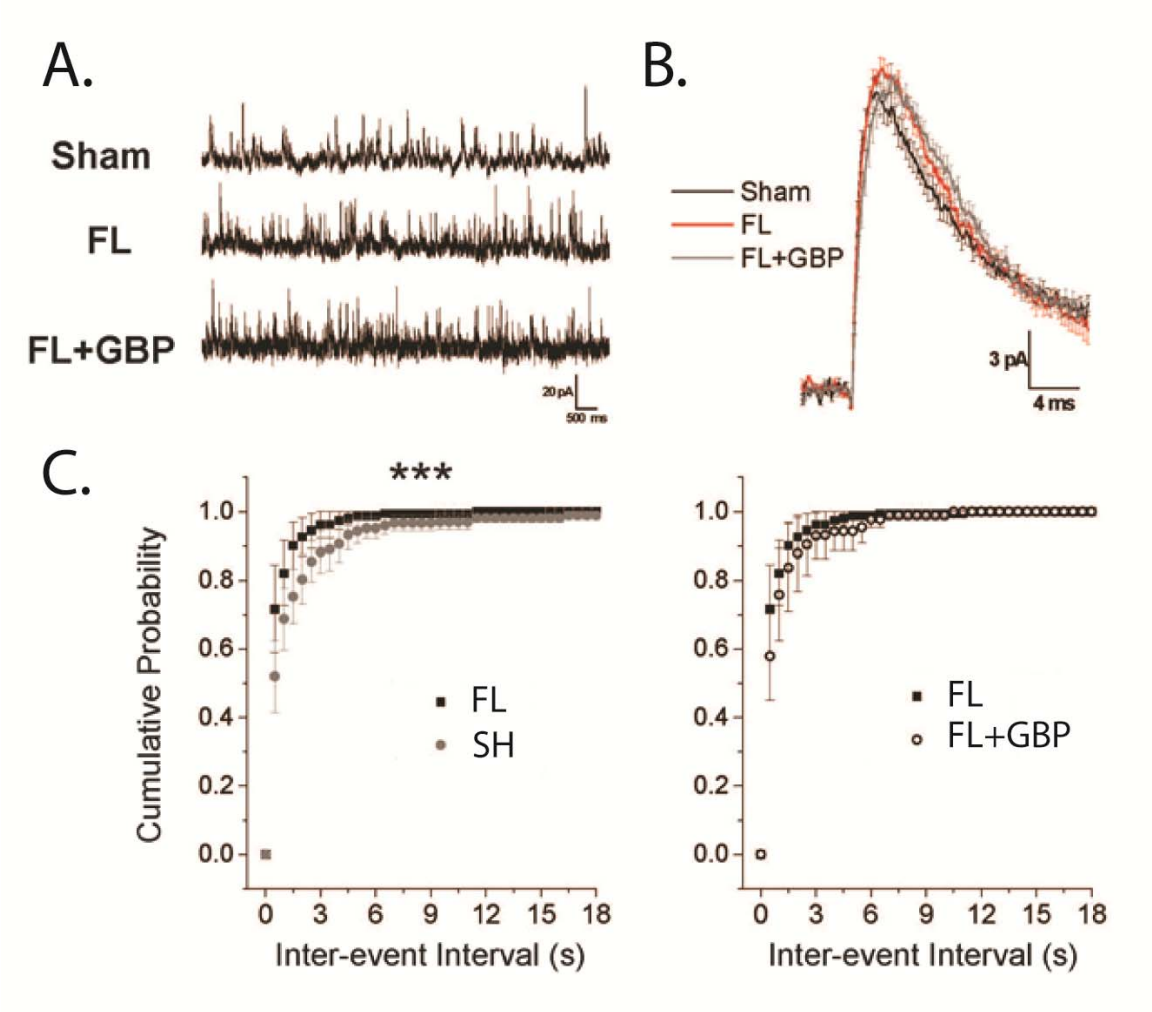

Figure 4.3: Gabapentin treatment does not attenuate the rise in mIPSC frequency in the FL cortex

(A) Representative miniature inhibitory postsynaptic current recording of layer V pyramidal neuron recorded from the PMZ of acute cortical slices prepared from P21-P28 sham, FL and FL+GBP. (B) Example mIPSC from sham (black), FL (red) and FL+GBP (grey). (C) Cumulative probability of inter-event intervals of FL (black squares), and SH (grey circles) and of FL (black squares) and FL+GBP (open circles). FL has a significant leftward shift compared to SH ($p < 0.001$).

4.4: Gabapentin treatment decreases network hyperexcitability following FL

Given the effects on excitatory synapses, we next aimed to investigate the effect of antagonizing $\alpha 2\delta$-1 on network hyperexcitability. We first examined evoked field excitatory post-synaptic potentials (fEPSPs) in acute brain slices from FL animals between P14 and P28. Stimulation intensity was set based on the minimum stimulation required to evoke a detectable fEPSP (threshold (TH) stimulation). TH stimulation intensity was not significantly different across experimental conditions. Epileptiform activity was defined as fEPSPs which contained high frequency activity, as well as increased peak amplitude and duration (Fig 4.4 A). The frequency of epileptiform activity was calculated as the percentage of fEPSPs that were epileptiform per slice. Brain slices from freeze lesion animals exhibited a significantly higher percentage of epileptiform fEPSPs (Fig 4.4 B; 54.83 ± 8.44%, n=25) compared to slices from sham injured animals (12.02 ± 6.12%, n=18; p<.001). Strikingly, slices from GBP-treated FL animals had a significantly decreased amount of epileptiform activity compared to slices from vehicle-treated FL animals (13.62 ± 5.24%, n=19; $p < 0.01$). There was no significant difference in the percentage of epileptiform activity in slices from GBP treated FL animals and sham injured animals. As a more quantitative measure of epileptiform activity, the areas of the fEPSPs were also calculated. fEPSPs from vehicle treated FL animals were significantly larger in area (Fig 4.4 C; 22.91 ± 4.38 mV*ms) compared to sham (9.56 ± 1.21 mV*ms; $p < 0.05$) and GBP treated FL animals (9.94 ± 1.45 mV*ms; $p < 0.05$). No significant differences in fEPSP areas were observed between sham and GBP

treated FL animals. Taken together, these results indicate that GBP treatment is able to reduce *in vitro* cortical hyperexcitability following FL.

We next examined the input-output relationship after FL by recording evoked fEPSPs at threshold and 2X threshold stimulus intensities. An increase in stimulation will normally elicit a correspondingly larger fEPSP. In sham-lesioned animals, acute cortical slices had normal input output relationships. 2X threshold stimulation evoked a significantly larger fEPSP (17.98±2.17 mV*ms) as compared to threshold stimulation (Fig 4.4 D). In FL animals, however fEPSP area at 2X stimulation (29.45±4.79 mV*ms) was not significantly different from threshold stimulation. These results suggest that the ability of the FL cortex to generate controlled, scaled responses to input is lost and that epileptiform activity is evoked in an all-or-none manner. The typical input-output relationship was restored in GBP treated FL animals, suggesting that GBP treatment after FL protects against pathological changes in cortical network function.

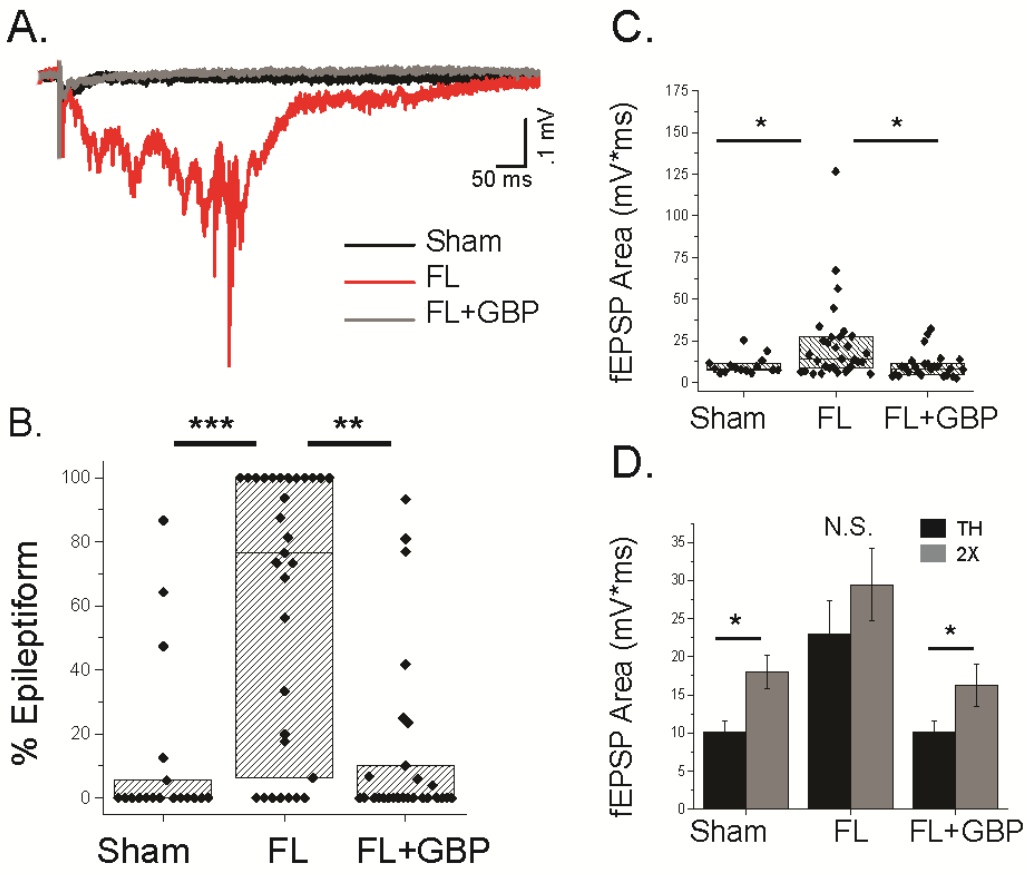

4.4: Gabapentin treatment decreases network hyperexcitability following FL

(A) Representative evoked field excitatory post-synaptic potentials (fEPSPs) recorded in the neocortex from sham injured (black), FL (red) and GBP treated FL animals (gray). (B) Box-Whisker plot of percent of stimulus-evoked fEPSPs which had epileptiform activity in acute brain slices at threshold stimulation, ** $P < 0.01$, *** $P < 0.001$. (C) Box-Whisker plot of fEPSP area (integrated area under the curve 1s post-stimulation) at threshold stimulation, *$P < 0.05$ (D) Average fEPSP area at threshold and 2× threshold stimulation for sham, FL and GBP treated FL animals, *$P < 0.05$. Reproduced with permission from (Andresen et al., 2014).

4.5: Gabapentin treatment decreases evoked extracellular glutamate signaling as measured using FRET based biosensor imaging

Previous studies utilizing high-speed glutamate biosensor imaging have shown an increase in stimulus evoked changes in extracellular glutamate levels in FL cortex compared to sham lesioned cortex (Dulla et al., 2013). The glutamate biosensor is a FRET-based fluorophore which allows us to monitor changes in extracellular glutamate signaling. Using this approach, we loaded acute cortical brain slices from GBP and vehicle treated FL mice with glutamate biosensor protein and performed glutamate imaging with simultaneously evoked extracellular field potential recordings. Glutamate signaling was analyzed by generating images of the ΔFRET (CFP/Venus ratio) signal divided by the ΔFRET noise on a pixel-by-pixel basis (Fig 4.5 A). Traces were then generated by plotting the $\Delta FRET_{signal}/\Delta FRET_{noise}$ over time and differences in the peak glutamate signal were quantified by calculating the maximum amplitude of each glutamate transient (Fig 4.5 B and D). The peak glutamate signal from slices of vehicle treated FL animals (4.46±1.35 $\Delta FRET_{signal}/\Delta FRET_{noise}$, n=6) was significantly increased when compared to sham injured (0.56±0.33, n=4; $p < 0.001$) and GBP treated FL animals (1.09±0.08, n=12; $p < 0.01$). These differences in glutamate signal complement the paired electrophysiological field data (Fig 4.5 C). Large changes in extracellular glutamate signal are associated with high amplitude and polyphasic field potentials, while small changes in the glutamate signal coincide with field potentials that are small in amplitude and duration. The reduced levels of stimulus evoked extracellular glutamate in GBP versus vehicle treated animals suggest that GBP treatment has

decreased the glutamatergic neurotransmission associated with epileptiform field activity following FL.

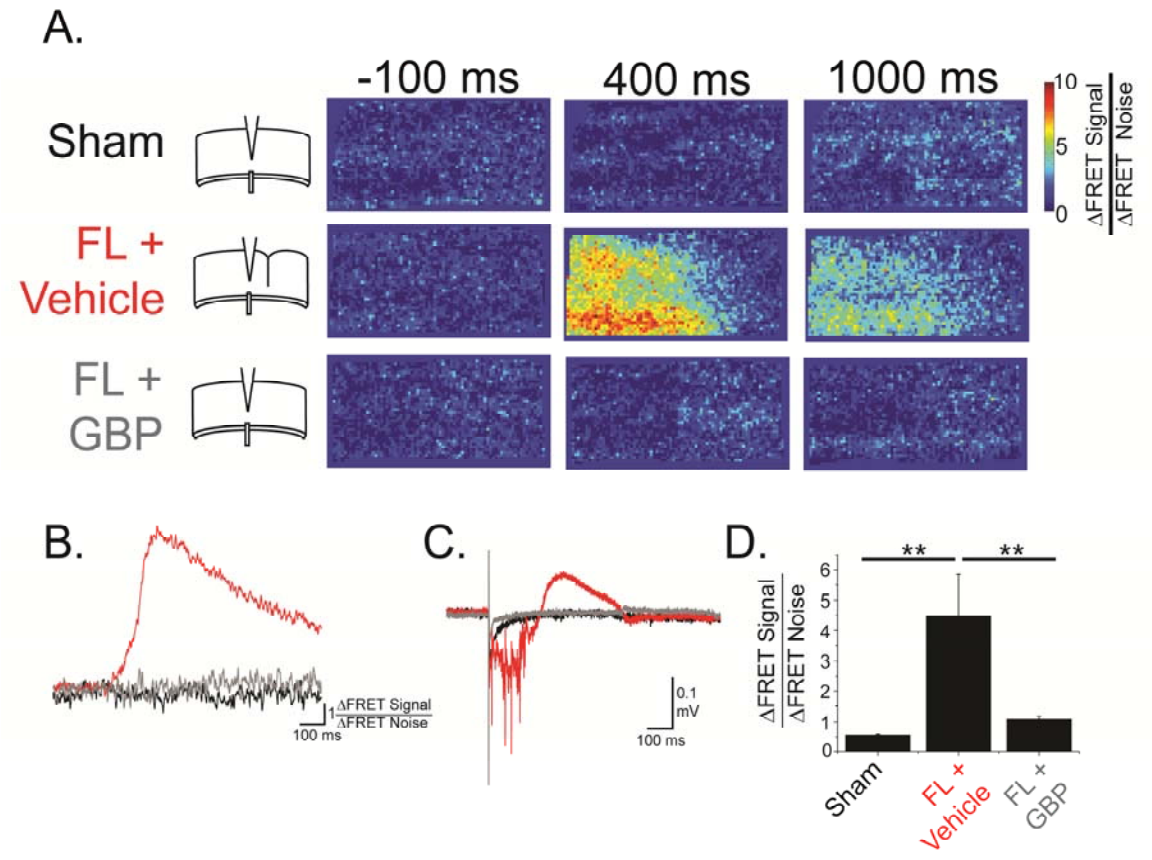

Figure 4.5: Gabapentin treatment decreases evoked extracellular glutamate signaling as measured using FRET based biosensor imaging

(A) Glutamate images of ΔFRET (CFP/Venus ratio) signal/ ΔFRET noise on a pixel-by-pixel basis at 100ms pre-stimulation, 400 ms post-stimulation and 1000 ms post-stimulation in sham, vehicle and GBP treated animals. Diagram illustrates cortical area being imaged with placement of recording electrode in cortical layer IV/V and stimulating electrode in the underlying white matter. (B) Individual ΔFRET signal/noise traces from sham (black), FL+Veh (red) and FL+GBP (gray) slices (C) and simultaneously recorded evoked fEPSPs. (D) Average peak amplitude of ΔFRET signal/noise, ** $P < 0.01$. Reproduced with permission from (Andresen et al., 2014).

4.6: Anticonvulsants with a different mechanism of action do not replicate the effects of gabapentin

Since gabapentin has anticonvulsant properties, we wanted to address the specificity of the observed decrease in hyperexcitability following FL by treating animals with an anticonvulsant that does not affect the TSP and α2δ-1 signaling pathway. Phenobarbital is a widely used antiepileptic drug, which acts by potentiating inhibition mediated by $GABA_A$ receptors and thus inhibiting excitation mediated by AMPA receptors (Macdonald and Barker, 1978). Phenobarbital has not been shown to effect α2δ-1 signaling. Freeze lesion and sham injured animals were given daily i.p injections of phenobarbital (20 mg/kg) or saline, from P1 to P7 to establish if anticonvulsant treatment following FL is sufficient to prevent the formation of a hyperexcitable network. Hyperexcitability was assessed by recording evoked cortical field potentials at P28 (Fig 4.6). We found that there was no significant decrease in the percentage of epileptiform activity in the phenobarbital treated FL animals (Fig 4.6 B; 53.52 ± 11.31%, n=4) as compared to the vehicle treated FL animals (64.28 ± 12.61%, n=3). fEPSPs from phenobarbital treated FL animals were also significantly larger in area (Fig 4.6 C; 17.48 ± 3.32 mV*ms) compared to sham injured animals (6.61 ± 0.45 mV*ms; $p < 0.01$) and had no significant differences compared to vehicle treated FL animals (20.03 ± 4.35 mV*ms). These results suggest that the effects of gabapentin on decreasing network hyperexcitability are not due to a general anticonvulsant mechanism.

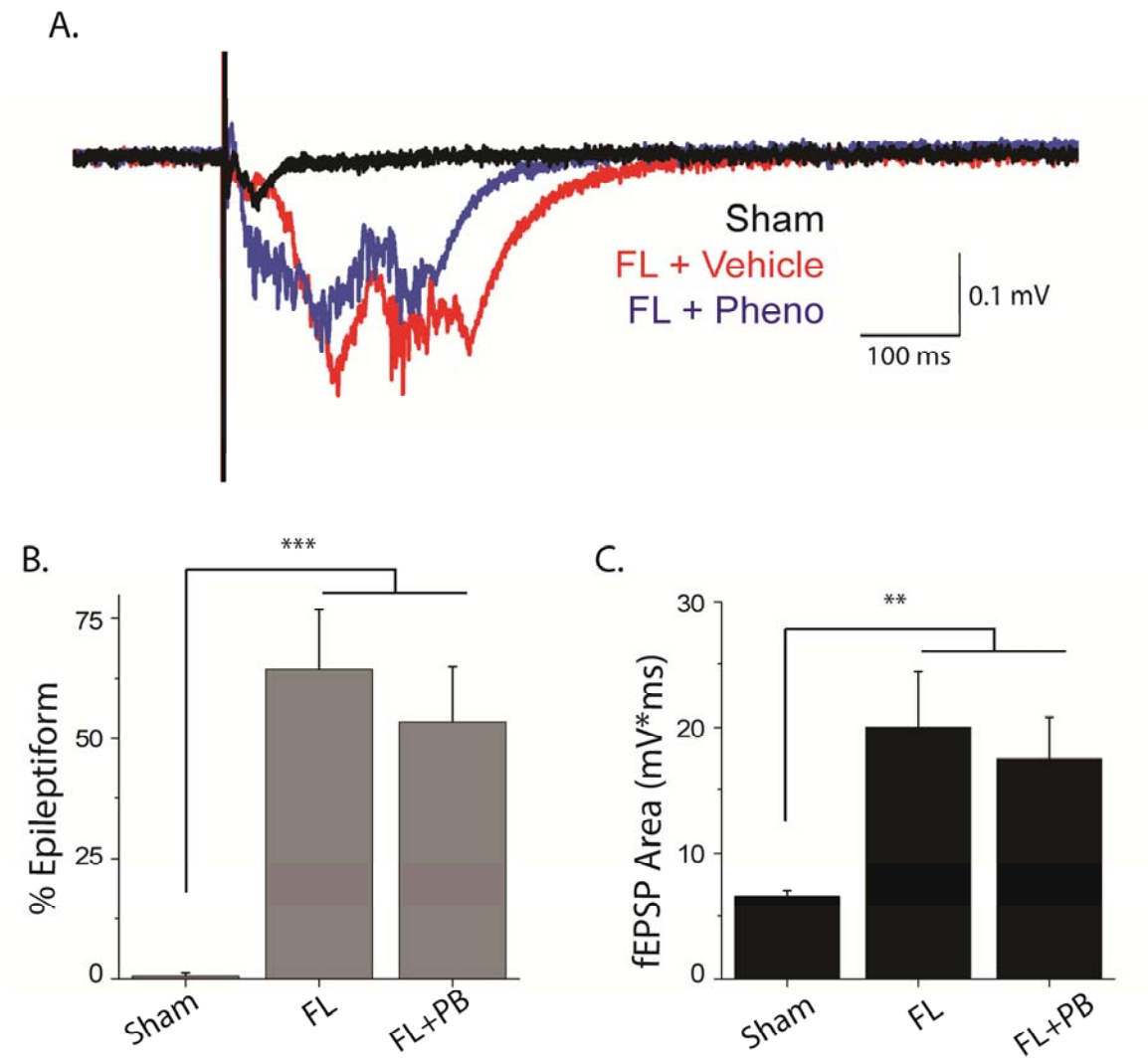

Figure 4.6: An anticonvulsant with a different mechanism of action does not replicate the effects of gabapentin

(A) Example evoked cortical field potential from sham (black), FL (red) and phenobarbital treated FL (blue). (B) Epileptiform activity (%) in acute brain slices, ***P < 0.001 (C) fEPSP area, ** P < 0.01. Reproduced with permission from (Andresen et al., 2014).

4.7: Gabapentin treatment decreases *in vivo* kainic acid-induced seizure activity

One limitation of the neonatal FL model is that despite showing reliable *in vitro* hyperexcitability, these animals do not readily demonstrate spontaneous behavioral seizures, (Kellinghaus et al., 2007, but see Kamada et al., 2013; Sun et at., 2016). Therefore, to assess *in vivo* hyperexcitability, EEG recordings were performed before and after acute i.p. kainic acid (KA) injection (20 mg/kg) to examine chemically-induced seizure activity in adult FL and sham injured animals. Briefly, FL and sham surgeries were performed at P0, GBP treatment occurred from P1-P7. EEG electrodes were implanted at 6 weeks of age and KA injections were given at 7 weeks of age. Power spectra were calculated from the 2 hour time window following KA injection (Fig 4.7 A-C). FL animals spent significantly more time seizing (Fig 4.7 D; 71.01 ± 5.64%, n=7) compared to sham injured animals (35.69 ± 8.29, n=7; $p < 0.01$) and on average had seizures that were longer in duration (Fig 4.7 E; 399.09 ±72.72 s vs. 146.81 ± 27.96 s, $p < 0.01$), demonstrating that FL animals have an increased seizure phenotype in response to acute KA injection. This increase in KA induced seizure activity was completely precluded in the GBP treated FL animals. Animals treated with GBP spent significantly less time seizing (17.87 ± 4.51%; $p < 0.001$) and displayed shorter average seizure durations (81.07 ± 11.42 s, n=7; $p < 0.001$) in comparison to the vehicle treated FL animals. Interestingly, spectral analysis of the EEG signals showed that GBP specifically suppressed theta activity (4-8 Hz) during KA-induced seizures (Fig. 4.7 F). These results suggest that GBP treatment after FL is able to block the formation of pathological

circuitry which leads to increased *in vivo* hyperexcitability caused by cortical malformation.

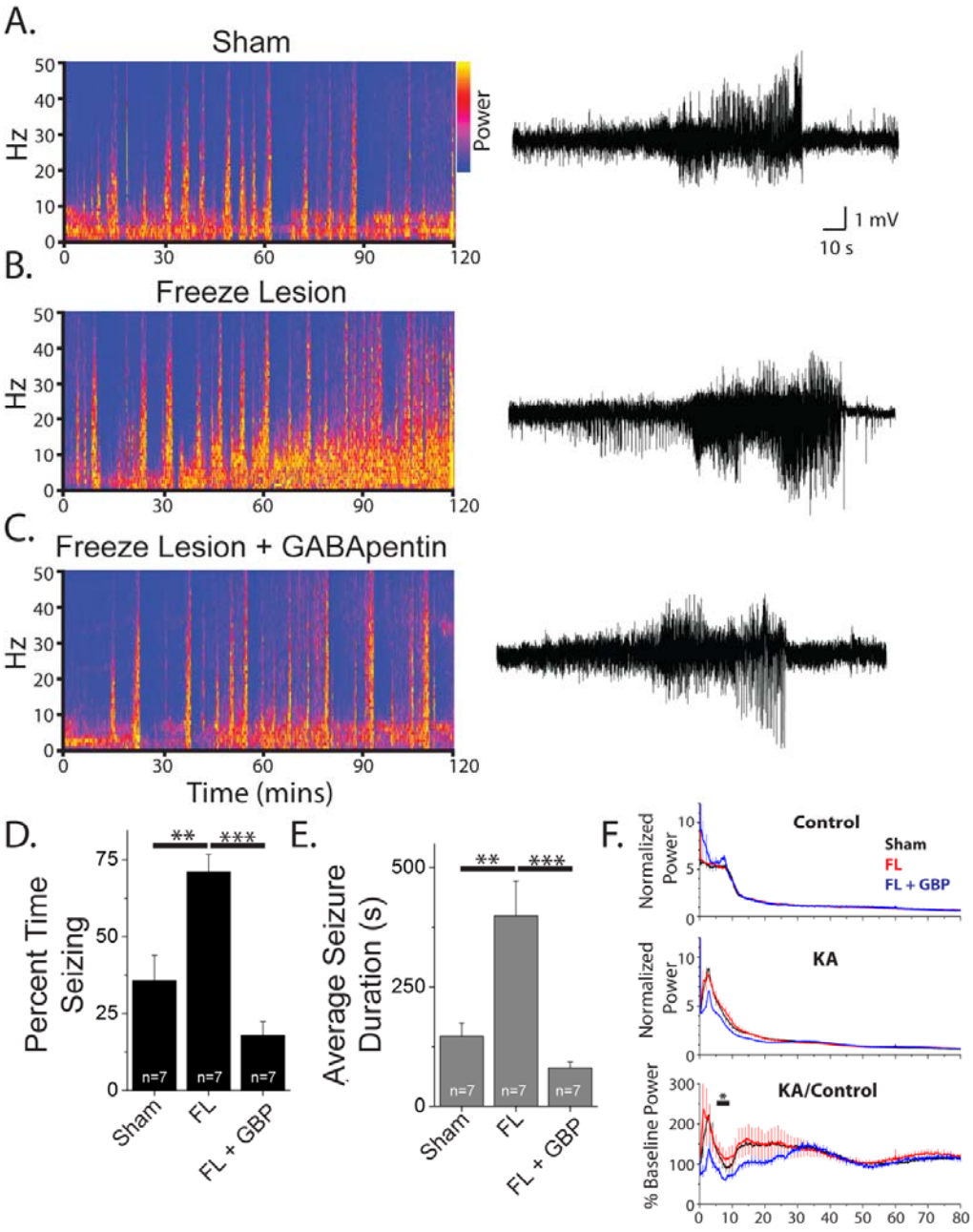

Figure 4.7: Gabapentin treatment decreases in vivo kainic acid-induced seizure activity

Representative power spectrum from 2 hour EEG recording of (A) sham injured, (B) FL and (C) GBP treated FL animals following acute kainic acid injection. (D) Percent time seizing and (E) average seizure duration, ** $P < 0.01$, *** $P < 0.001$. (F) Spectral analysis of EEG from sham (black), FL (red) and GBP treated FL animals (blue). Top, pre-kainic acid EEG, middle, kainic acid EEG, bottom, % baseline power normalized to pre-kainic acid EEG, * $P < 0.05$. Reproduced with permission from (Andresen et al., 2014). EEG and analysis performed by Jamie Maguire; spectral analysis was performed by Chris Dulla.

4.8: Genetic deletion of α2δ-1 partially attenuates FL-driven network hyperexcitability

We have shown that GBP treatment prevents the development of epileptiform evoked field excitatory post-synaptic potentials (fEPSP) recordings from acute cortical slices. Given that α2δ-1 deletion prevents FL-induced excitatory synaptogenesis, we hypothesized that α2δ-1 KO would also decrease network hyperexcitability. To test this hypothesis, fEPSPs were evoked as before by stimulating the white matter beneath the cortex and recording from layer V of the PMZ. Stimulation intensity was set as the minimum stimulation required to elicit a detectable response, and did not differ significantly between groups. We quantified the number of sweeps per slice with epileptiform activity (defined by high frequency activity, as well as increased amplitude and duration) and the integrated area under the curve of the fEPSP response. Normalized power in both the 10-100 Hz and 200-500 Hz range was also quantified. Slices from wild-type sham-injured animals show almost no epileptiform activity (Fig 4.8; 1%, n = 16 sections from 4 animals), a small fEPSP area (14.48 ± 1.75 mV*ms) and low power in both the low and high frequency range (1.91 ± 0.28 and 1.00 ± 0.01). Similar to previous studies, we found that FL animals have robust epileptiform activity (Fig 4.8 A and B; 76.6 ± 9%, n = 18 sections from 4 animals; $p < 0.001$), corresponding to a significantly larger fEPSP area (Fig 4.8 D; 47.35 ± 7.33 mV*ms; $p < 0.001$) and increased power in both frequency ranges (Fig 4.8 C and E; 12.91 ± 3.71, $p < 0.001$ and 1.54 ± 0.22; $p < 0.01$) compared to sham-injured animals. GBP treatment significantly decreased the percent epileptiform activity (Fig 4.8 A and B; 16.6 ± 7%, n = 12 section from 3 animals; $p < 0.001$), fEPSP area (Fig 4.8D; 13.02 ± 3.59 mV*ms; $p < 0.01$) and low frequency power

(Fig 4.8 E; 2.45 ± 0.68; $p < 0.05$) following FL. High frequency power is not effected by GBP treatment (1.11 ± 0.05), demonstrating that GBP treatment does not rescue all aspects of FL-driven network dysfunction. Genetic deletion of $\alpha 2\delta$-1 also attenuated epileptiform activity following FL (Fig 4.8 A and B; 47.1 ± 10%, n = 20 sections from 3 animals; $p = .06$), and significantly decreased fEPSP area (Fig 4.8 D; 26.92 ± 4.14 mV*ms; $p < 0.05$) and low frequency power (Fig 4.8 E; 3.66 ± 1.1; $p < 0.05$) compared to wild-type FL. $\alpha 2\delta$-1 KO also did not rescues FL-driven increase in high power frequency (1.12 ± 0.09) Interestingly, $\alpha 2\delta$-1 KO was not as effective as GBP treatment at preventing epileptiform activity, and reducing fEPSP area and low power frequency after FL. GBP treatment had no additive effect in $\alpha 2\delta$-1 KO animals after FL on percent epileptiform activity (Fig 4.8; 40.0 ± 14.3%, n = 12 sections from 3 animals), fEPSP area (26.95 ± 5.95 mV*ms) or frequency power (3.01 ± 0.68 and 1.15 ± 0.10) compared to vehicle-treated FL $\alpha 2\delta$-1 KOs, suggesting that the actions of GBP on network hyperexcitability are specific to antagonizing $\alpha 2\delta$-1 signaling. No differences were observed in epileptiform activity, fEPSP area, or frequency power in the sham-injured cortex with GBP treatment (12.2 ± 6%; 21.74 ± 1.99 mV*ms; 26.5 ± 0.54; 1.08 ± 0.03, n = 20 sections from 4 animals), $\alpha 2\delta$-1 deletion (14.0 ± 21%; 17.03 ± 1.36 mV*ms; 1.85 ± 0.24; 1.01 ± 0.05, n = 21 sections from 4 animals) or $\alpha 2\delta$-1 KO and GBP treatment (4.9 ± 3%; 21.39 ± 4.11 mV*ms; 2.93 ± 0.78; 1.12 ± 0.04 n = 11 sections from 3 animals). These results suggest an intermediate effect of $\alpha 2\delta$-1 deletion compared to acute pharmacological attenuation of $\alpha 2\delta$-1 on network hyperexcitability.

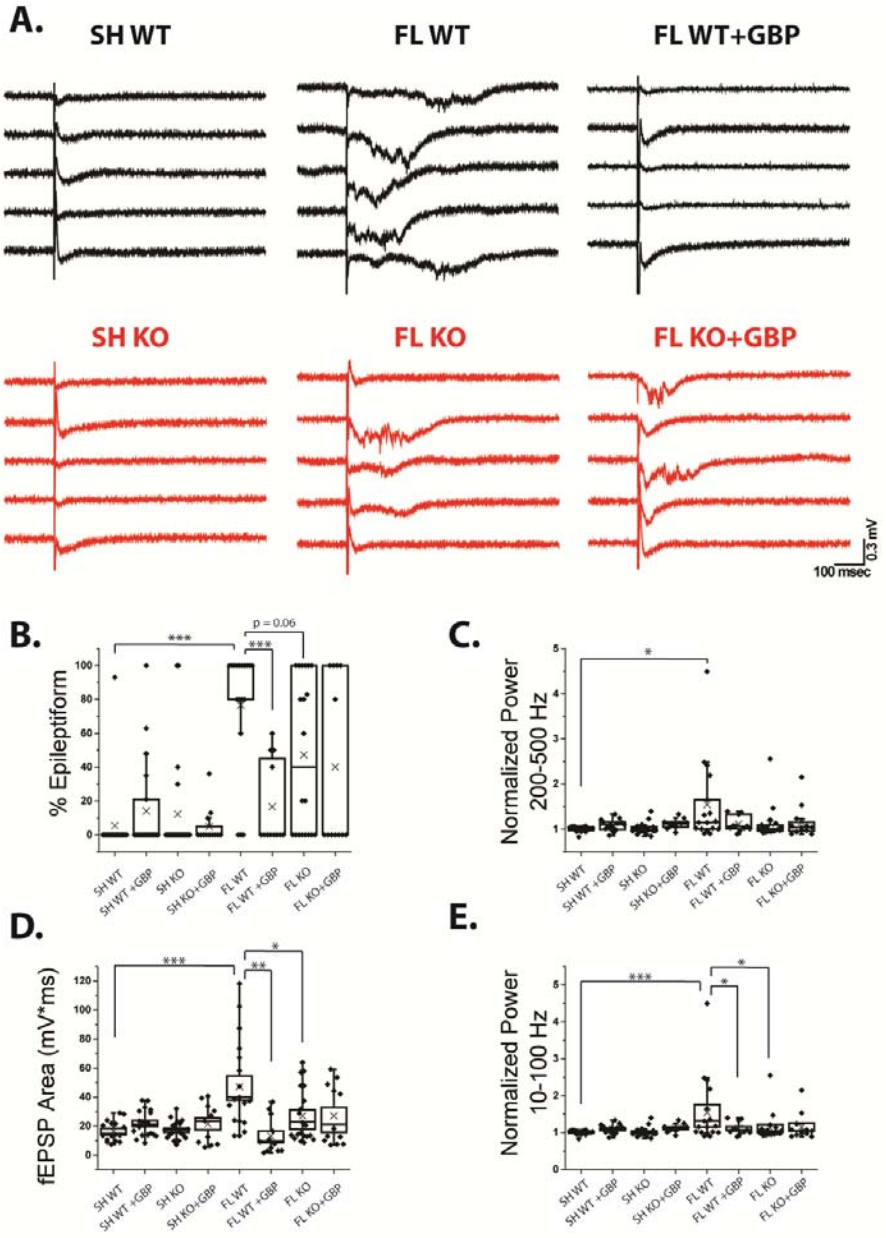

Figure 4.8: α2δ-1 knockout partially rescues network hyperexcitability following FL and is insensitive to gabapentin treatment

(A) Representative evoked cortical field EPSP traces recorded from the PMZ of acute cortical slices prepared from P21-P28 WT sham, $\alpha2\delta\text{-}1^{-/-}$ sham, WT FL, $\alpha2\delta\text{-}1^{-/-}$ FL , WT FL+GBP and $\alpha2\delta\text{-}1^{-/-}$ FL+GBP animals. (B) Box-Whisker plot of percent epileptiform sweeps per slice, *** $p < 0.001$. (C) Box-Whisker plot of normalized power in the 200-500 Hz range, * $p < 0.05$ (D) Box-Whisker plot of integrated area under the curve per slice, * $p < 0.05$, ** $p < 0.01$ and * $p < 0.05$. (E) Box-Whisker plot of normalized power in the 10-100 Hz range, * $p < 0.05$ and *** $p < 0.001$.

4.9: Conclusions

In conclusion, we have shown in this chapter that antagonizing $\alpha 2\delta$-1 signaling decreases injury-induced synaptogenesis and the formation of a hyperexcitable network, as assessed by *in vitro* glutamate biosensor imaging and evoked cortical field potentials and *in vivo* KA-induced seizure activity. We have also shown that, while the vast majority of GBP's effects in the FL cortex require $\alpha 2\delta$-1, GBP is able to decrease injury-induced synapse number in the $\alpha 2\delta$-1 KO cortex. This was specific to structural synapses as the frequency of miniature EPSCs, a proxy for functional synapses, was not affected by GBP in the KOs. Finally, we have shown that, in contrast to GBP treatment, genetic deletion of $\alpha 2\delta$-1 is only partially protective against epileptiform activity, as assessed by fEPSP. GBP is unable to further reduce epileptiform activity in the KO FL cortex, suggesting that compensatory changes in the KO most likely mediate this intermediate effect on field activity.

Chapter 5: Discussion

5.1: Overview

The work of this thesis has focused on the role of α2δ-1 in driving pathologies associated with the neonatal freeze lesion model of developmental cortical malformation. FL recapitulates many of the key features of insult-induced DCMs, such as polymicrogyria, schizencephaly, and focal cortical dysplasia type IIId, including etiology, cell death, astrocytosis, anatomical reorganization, and spontaneous seizures (Sun et al., 2016; Williams et al., 2016). The FL model allows for the study of changes that occur between insult and network dysfunction in a stereotyped model, as the cortical malformation develops over the first week post-injury and epileptiform activity emerges by the second week. We have found that the pro-synaptogenic proteins TSP and α2δ-1 are transiently upregulated following FL, and are therefore well-poised to play a role in driving anatomical reorganization and the formation of a hyperexcitable network. Using a combination of pharmacological and genetic manipulations, we found that α2δ-1 does indeed drive exuberant excitatory synaptogenesis following FL. Furthermore, we found that α2δ-1 also drives gabapentin-sensitive cell death. This was the first demonstration that GBP acts through α2δ-1 for its neuroprotective effects. Attenuating α2δ-1 signaling helped to restore normal cortical structure following FL, reduced astrocyte reactivity, and attenuated FL-induced increases in excitatory synapse number and glutamatergic synaptic transmission. Interestingly, GBP also had α2δ-1-independent effects on synaptogenesis. GBP treatment prevented the onset of epileptiform activity; however, genetic deletion of α2δ-1 was only partially protective against FL-driven hyperexcitability. GBP treatment was unable to reduce network activity in the α2δ-1

knockouts, which suggests that GBP acts through $\alpha 2\delta$-1 to effect injury-induced epileptiform activity. Taken together, we have shown that $\alpha 2\delta$-1 is the receptor responsible for GBP-mediated neuroprotection and the attenuation of aberrant synaptogenesis and excitatory connectivity. We have also identified $\alpha 2\delta$-1 signaling as a novel therapeutic target for epilepsy associated with neonatal insult and cortical malformations.

5.2: α2δ-1-mediated cell death and neuroinflammation

Previous work has shown that GBP is neuroprotective in a variety of injury models (Kale et al., 2011; Kim et al., 2010; Li et al., 2012; Traa et al., 2008). However, no study has directly tested the site of action responsible for this effect. While α2δ-1 has been identified as the receptor responsible for GBP-sensitive synaptogenesis (Eroglu et al., 2009), GBP also has effects on other molecular targets (α2δ–2 (Gong et al., 2001), GABAergic transmission (Bertrand et al., 2001; Honmou et al., 1995) NMDA receptors (Kim et al., 2009), sodium channels (Yang et al., 2009), and protein kinase C (Yeh et al., 2011)). Using the α2δ-1 knockout (KO) mouse, we have shown here that deletion of α2δ-1 mimics the neuroprotective effects of GBP treatment following FL. α2δ-1 KO mice are also insensitive to GBP treatment; it is therefore likely that GBP decreases cell death by inhibiting TSP/α2δ-1 signaling.

TSP and α2δ-1 are further implicated in cell death signaling as their protein expression is altered in multiple injury types. Human studies show elevated thrombospondin-1 in plasma after head trauma (Wang et al., 2016), and human endothelial cells upregulate thrombospondin-1 after oxidative stress (Ning et al., 2011). TSP1 and TSP2 are also increased in rodent models of stroke (Lin et al., 2003). α2δ-1 expression is likewise upregulated in injury models in both the central and peripheral nervous system (Boroujerdi et al., 2008; Li et al., 2012). We have shown here that TSP and α2δ-1 are upregulated in the FL cortex, leading to an overabundance of both ligand and receptor. Beyond changes in expression, α2δ-1's sub-cellular localization is altered in areas of neuronal death following chemoconvulsive seizures (Nieto-Rostro et al., 2014), which

suggests that subtle changes in α2δ-1 signaling may be relevant to cell death and epileptogenesis.

How α2δ-1 signaling leads to cell death is not clear, but calcium-dependent caspase-mediated apoptosis, appears to be involved. Loss of α2δ-1 decreases the duration of calcium channel currents in cardiac myocytes (Fuller-Bicer et al., 2009) and calcium channel density (Patel et al., 2013) in sensory neurons. Conversely, over expression of α2δ-1 increases neurotransmitter release following action potential firing in the hippocampus (Hoppa et al., 2012), which could lead to greater excitation. We see two ways in which α2δ-1 might contribute to injury-induced cell death. First, by increasing excitatory synapse formation and enhancing excitation, α2δ-1 activity likely potentiates glutamate-induced excitotoxicity. Second, by enhancing calcium currents and intracellular calcium levels, α2δ-1 may promote caspase activation. Both aspects of α2δ-1 may contribute to lesion-induced cell death, and undoubtedly occur in parallel with other forms of cell death that do not involve α2δ-1. Future studies will be required to identify which aspects of α2δ-1 function lead to injury-induced cell death. Finally, the anticonvulsant properties of GBP may underlie some of its neuroprotective effects. Treatment with an anticonvulsant that acts by a different mechanism of action could be used to address this possibility.

In addition to driving cell death, FL also induces robust astrocytosis (Armbruster et al., 2014; Bordey et al., 2001; Campbell and Hablitz, 2008; Dulla et al., 2013). Throughout this study, we have assumed that astrocytes are the source of thrombospondin (TSP) in the FL brain. Gene expression profiling in different brain cell types has shown that

mRNAs for TSPs are mostly enriched in glia, in particular by postnatal astrocytes (Eroglu et al., 2009). TSP immunostaining was generally seen isotopically with GFAP positive reactive astrocytes and in the area of lesion. This is consistent with the hypothesis that astrocytes are the source of TSP following lesion. However, TSP may also be secreted by microglia (Chamak et al., 1994) or could enter the neuropil from the circulatory system after breach of the blood brain barrier.

Here, we show that $\alpha 2\delta$-1 signaling plays an important role in driving reactive astrocytosis. GFAP immunoreactivity was greatly reduced by attenuating $\alpha 2\delta$-1 signaling, and no additional effect of GBP was seen in $\alpha 2\delta$-1 KO animals. Although astrocytes express $\alpha 2\delta$-1 at a low-level, it is more abundantly expressed by neurons (Zhang et al., 2014). This suggests that decreased astrocyte reactivity may be a secondary effect of reduced neuronal cell death and subsequent neuroinflammation, rather than a direct effect on $\alpha 2\delta$-1 expressed by astrocytes. If astrocytes themselves are the source of TSP, this would also suggest a feed-forward pathway, such that TSP/$\alpha 2\delta$-1 signaling may lead to prolonged astrocyte reactivity and TSP release. How TSP/$\alpha 2\delta$-1 signaling contributes more broadly to neuroinflammation and cell death signaling warrants future investigation.

Finally, we have shown that α2δ–1 activity following FL promotes lesion formation and disrupts the expression of laminar-specific markers (CUX1 and CTIP2) in both the microgyrus and paramicrogyrial zone (PMZ). Previous reports describe the neuronal architecture of the PMZ as normally laminated. Our results confirm that although gross level changes in cortical structure and total neuron number do not occur in the PMZ,

more subtle differences in neuronal identity exist. How loss of CTIP2 or CUX1 might contribute to altered neuronal function is unknown, but both act as transcription factors to control the expression of multiple downstream genes (Molyneaux et al., 2007; Sansregret and Nepveu, 2008). CUX1 and CTIP2 are hypothesized to contribute to neuron morphological development (Arlotta et al., 2005; Cubelos et al., 2010; Li et al., 2010), enabling the establishment of proper connectivity. Therefore, $\alpha 2\delta$-1-dependent loss of these markers may lead to structural and functional changes resulting in an abnormal neuronal phenotype in the PMZ. Overall we have shown that $\alpha 2\delta$-1 drives acute cell death following injury, which results in long-lasting changes in cortical structure and organization.

5.3: α2δ-1-mediated synaptogenesis and network hyperexcitability

In addition to the established role of TSP/α2δ-1 signaling in developmental synaptogenesis, our work also supports a role for α2δ-1 in pathological synaptogenesis. α2δ-1 KO and *in vivo* treatment with GBP attenuated injury-induced increases in both anatomical and functional synapses, in agreement with previous studies. We also found that GBP treatment was able to reduce the number of structural synapses in the injured α2δ-1 KO cortex. Other α2δ subunits may mediate this effect. α2δ–1, α2δ–2 and α2δ–3 are all widely expressed in the CNS, with each isoform having a distinct distribution (Cole et al., 2005). Genetic deletion of α2δ–1 does not grossly alter the expression of other α2δ isoforms (Fuller-Bicer et al., 2009); however, regional compensation or injury-specific alterations may still exist. GBP can bind to α2δ–2 (Gee et al., 1996) and α2δ–3 has been shown to play a synaptogenic role in drosophila (Kurshan et al., 2009). Taken together, these results suggest that other α2δ isoforms may account for the GBP effect on synapse number in the α2δ-1-KO FL cortex. Also important to note, only vGlut1+ synapses, the predominant vGlut in the cortex, were quantified here. TSP/α2δ-1 signaling drives the formation of vGlut2 containing synapses during normal development (Eroglu et al., 2009). Conversely, GBP treatment reduces injury-induced increases in vGlut1-containing excitatory synapses (Li et al., 2012). Our studies further support a role of α2δ–1 in driving vGlut1-containing synapse formation after injury, in addition to its role in driving vGlut2-containing synapses during development. This suggests that injury increases intracortical excitation, mediated by vGlut1-containing synapses (Fremeau et al., 2004). Changes in vGlut2-containing synapses, calcium

channel trafficking (Hendrich et al., 2008), and homeostatic plasticity may underlie the discrepancy in the effects of GBP in α2δ–1 KOs on functional versus structural synapses.

Finally, inhibiting α2δ-1 signaling reduced cortical network hyperexcitability after FL. GBP treatment was able to rescue the percent epileptiform activity, as well as the fEPSP area and low frequency (10-100 Hz) power. However, there was no effect on the FL-induced increase in high frequency (200-500 Hz) power. This shows that GBP specifically alters the slow component of hyperexcitable field activity, but does not prevent all types of network dysfunction. GBP treatment also did not reduce the FL-driven rise in miniature IPSC frequency. Interneuron activity has been linked to high frequency epileptiform activity (Jiruska et al., 2010; Morris et al., 2016) and may therefore underlie the high frequency component of epileptiform network activity in the FL cortex.

Additionally, we have shown that genetic deletion of α2δ-1 was only partially protective against changes in epileptiform activity. Despite attenuating FL-driven synaptogenesis in a manner similar to GBP treatment, α2δ-1 KO had an intermediate effect on reducing percent epileptiform activity, fEPSP area, and low frequency (10-100 Hz) power. Furthermore, GBP treatment had no effect on the residual epileptiform activity in the α2δ-1 KO animals, despite decreasing excitatory synapse number. This suggests that constraining excitatory synaptogenesis is not sufficient to completely prevent hyperexcitability in the α2δ-1 KO cortex, and that deletion of α2δ-1 may cause compensatory changes that predispose the cortex to injury-induced network pathology. Genetic deletion of α2δ-1 did not alter the amplitude or kinetics of excitatory currents, which argues against changes in post-synaptic receptors. Therefore, pre-synaptic

changes, via altered voltage-gated calcium channel function, or changes in the neuroinflammatory response may promote hyperexcitability in the $\alpha 2\delta$-1 KO cortex.

5.4: Does cell death contribute to epileptogenesis?

In general, the link between cell death and epileptogenesis remains controversial. Neuronal loss is evident in the hippocampus of patients with medial temporal lobe epilepsy (mTLE) (Chang and Lowenstein, 2003) and in many animal models of mTLE (Hofmann et al., 2016; Kienzler et al., 2009; Mouri et al., 2008; Zhang et al., 2009). However it remains unclear if neuronal loss is a result of recurrent seizure activity or a part of the etiology. Cell death may drive epileptogenesis by the selective loss of inhibitory interneurons or by promoting axonal sprouting and circuit reorganization. Some studies have found that neuroprotective treatment following status epilepticus can decrease spontaneous seizure frequency (Engel et al., 2010a; Jimenez-Mateos et al., 2010), suggesting that cell death does contribute to epileptogenesis. On the other hand, reducing cell death does not always lead to later seizure improvement (Engel et al., 2010b; Narkilahti et al., 2003) and in a model of early-life status epilepticus, many animals will develop spontaneous seizure without apparent cell loss (Raol et al., 2003). Furthermore, the role of cell death in epilepsy associated with developmental cortical malformations has not been well-studied. Interneuron loss is unlikely to underlie epileptiform activity in the FL cortex, as we have shown that inhibitory currents are actually increased; however, circuit reorganization induced by cell death may drive hyperexcitability. We have shown here that $\alpha 2\delta$-1 drives both cell death and network hyperexcitability following FL; however, it remains unknown if these are related or independent processes. Future studies will attempt to parse apart the two aspects of $\alpha 2\delta$-1 function, which will help to address the role of cell death in epileptogenesis.

5.5: Future Directions

We have shown here that α2δ-1 is an important mediator of injury-induced cell death. However, it is unknown how α2δ-1 activity drives cell death. Preliminary studies have begun to address this important question by performing qRT-PCR to identify changes in RNA levels of key cell death and inflammatory factors. GBP treatment after freeze lesion appears to selectively upregulate the cytokines CCL3, CCL4 and CCL7. These cytokines play an important role in the recruitment of peripheral monocytes and in macrophage activation (Bajetto et al., 2001). Future studies will assess myeloid infiltration and microglia activation following FL, using CD11b and Iba1 immunohistochemistry. We will then determine which aspects of these pathways are affected by GBP treatment and α2δ-1 knockout. These experiments will help to identify which neuroinflammatory events are activated by FL and how α2δ-1 signaling contributes to injury-induced cell death.

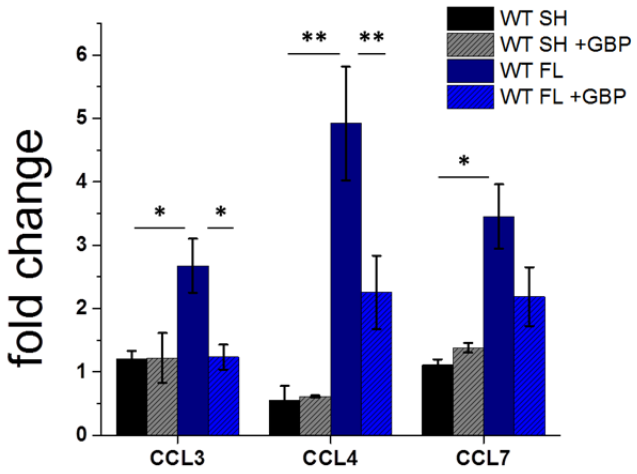

Figure 5.1: GBP treatment attenuates induction of CCL3/4/7

Fold change in mRNA levels of cortex from WT SH, SH+GBP, FL and FL+GBP animals (normalized to GAPDH and sham levels), ** $p < 0.01$ and * $p < 0.05$. PCR performed by Alexei Degterev.

We have also shown that α2δ-1 drives injury-induced synaptogenesis and epileptiform activity. However, we found several key differences with GBP treatment versus genetic deletion of α2δ-1. Most strikingly, α2δ-1 KO only partially reduced hyperexcitability as assessed by evoked cortical fEPSPs. This is despite the reduction in excitatory synapse number and mEPSC frequency. Future studies will address this discrepancy by assessing changes in calcium currents and pre-synaptic properties in the α2δ-1 KO, which may predispose the network to injury-induced dysfunction. We can also quantify Vglut2+ synapses to determine if other sub-types of excitatory synapses are altered by antagonizing α2δ-1 signaling.

Finally, understanding the contribution of cell death to network dysfunction will help shed light on the process of epileptogenesis. Since we have found that GBP treatment and genetic deletion of α2δ-1 can reduce cell death, cortical reorganization and epileptiform activity in the FL cortex, we want to parse apart the relationship between these events by directly inhibiting cell death. Using a combination of caspase- and necroptosis-inhibitors, we aim to achieve a similar reduction in total cell death following FL, as compared to GBP treatment or α2δ-1 knockout. We will then be able to assess network hyperexcitability and determine if attenuating cell death and neuroinflammation plays a role in inhibiting epileptiform activity. Conversely, we may find that hyperexcitability persists and this would illustrate that α2δ-1 drives changes in connectivity independent to changes in cell death pathways.

5.6: Final Conclusions

Taken together, our results highlight the dual roles of α2δ-1 signaling in driving both synaptogenesis and cell death in the FL cortex. A growing number of studies suggest that α2δ-1 signaling may contribute to the development of epilepsy in animal models and in humans. We have shown here that the FL model, which most closely mimics the DCMs polymicrogyria and focal cortical dysplasia Type IIId, has significant α2δ-1-mediated pathologies. Overexpression of α2δ-1 in control animals also leads to epileptiform EEG discharges and behavioral arrests, which are rescued by acute treatment with an anticonvulsant (Faria et al., 2017). Finally, human mutations in α2δ-1 have been linked to polymicrogyria (Vergult et al., 2015). This provides an important confirmation that abnormal α2δ-1 activity may be involved in epilepsy associated with human DCMs. Whether cell death plays a role in these cases is unknown. Furthermore, the functional consequences of these mutations are not known, but gain of function mutations could increase calcium currents, increase cell death, and drive pathological excitatory synaptogenesis. Also important to consider, although attenuating α2δ-1 signaling may reduce cell death and network hyperexcitability, it may compromise functional recovery. Reestablishing synaptic connectivity after injury is a critical aspect of rehabilitation and attenuating TSP1/2 signaling after stroke reduces behavioral recovery (Liauw et al., 2008). Care must be taken, therefore, in manipulating TSP/α2δ-1 signaling, as it plays a role in both the adaptive and pathological response to insult. Given this caveat, parsing apart the relationship between cell death, synaptogenesis,

and epileptiform activity will enable us to optimize treatment strategies that target $\alpha 2\delta$-1 signaling in neonatal injury and developmental cortical malformations.

Chapter 6: Bibliography

Adams, J.C. 2001. Thrombospondins: multifunctional regulators of cell interactions. *Annu Rev Cell Dev Biol* 17:25-51.

Al-Bachari, S., J. Pulman, J.L. Hutton, and A.G. Marson. 2013. Gabapentin add-on for drug-resistant partial epilepsy. *The Cochrane database of systematic reviews* CD001415.

Albertson, A.J., A.S. Bohannon, and J.J. Hablitz. 2017. HCN Channel Modulation of Synaptic Integration in GABAergic Interneurons in Malformed Rat Neocortex. *Frontiers in cellular neuroscience* 11:109.

Albertson, A.J., J. Yang, and J.J. Hablitz. 2011. Decreased hyperpolarization-activated currents in layer 5 pyramidal neurons enhances excitability in focal cortical dysplasia. *Journal of neurophysiology* 106:2189-2200.

Andre, V.M., C. Cepeda, H.V. Vinters, M. Huynh, G.W. Mathern, and M.S. Levine. 2010. Interneurons, GABAA currents, and subunit composition of the GABAA receptor in type I and type II cortical dysplasia. *Epilepsia* 51 Suppl 3:166-170.

Andresen, L., D. Hampton, A. Taylor-Weiner, L. Morel, Y. Yang, J. Maguire, and C.G. Dulla. 2014. Gabapentin attenuates hyperexcitability in the freeze-lesion model of developmental cortical malformation. *Neurobiology of disease* 71:305-316.

Angevine, J.B., Jr., and R.L. Sidman. 1961. Autoradiographic study of cell migration during histogenesis of cerebral cortex in the mouse. *Nature* 192:766-768.

Appleton, R., K. Fichtner, L. LaMoreaux, J. Alexander, G. Halsall, G. Murray, and E. Garofalo. 1999. Gabapentin as add-on therapy in children with refractory partial seizures: a 12-week, multicentre, double-blind, placebo-controlled study. Gabapentin Paediatric Study Group. *Epilepsia* 40:1147-1154.

Arber, S., and P. Caroni. 1995. Thrombospondin-4, an extracellular matrix protein expressed in the developing and adult nervous system promotes neurite outgrowth. *J Cell Biol* 131:1083-1094.

Arlotta, P., B.J. Molyneaux, J. Chen, J. Inoue, R. Kominami, and J.D. Macklis. 2005. Neuronal subtype-specific genes that control corticospinal motor neuron development in vivo. *Neuron* 45:207-221.

Armbruster, M., D. Hampton, Y. Yang, and C.G. Dulla. 2014. Laser-scanning astrocyte mapping reveals increased glutamate-responsive domain size and disrupted maturation of glutamate uptake following neonatal cortical freeze-lesion. *Frontiers in cellular neuroscience* 8:277.

Backonja, M., and R.L. Glanzman. 2003. Gabapentin dosing for neuropathic pain: evidence from randomized, placebo-controlled clinical trials. *Clin Ther* 25:81-104.

Baenziger, N.L., G.N. Brodie, and P.W. Majerus. 1971. A thrombin-sensitive protein of human platelet membranes. *Proceedings of the National Academy of Sciences of the United States of America* 68:240-243.

Bajetto, A., R. Bonavia, S. Barbero, T. Florio, and G. Schettini. 2001. Chemokines and their receptors in the central nervous system. *Front Neuroendocrinol* 22:147-184.

Baldassarre, M., Z. Razinia, C.F. Burande, I. Lamsoul, P.G. Lutz, and D.A. Calderwood. 2009. Filamins regulate cell spreading and initiation of cell migration. *PloS one* 4:e7830.

Bandyopadhyay, S., and J.J. Hablitz. 2006. NR2B antagonists restrict spatiotemporal spread of activity in a rat model of cortical dysplasia. *Epilepsy research* 72:127-139.

Barclay, J., N. Balaguero, M. Mione, S.L. Ackerman, V.A. Letts, J. Brodbeck, C. Canti, A. Meir, K.M. Page, K. Kusumi, E. Perez-Reyes, E.S. Lander, W.N. Frankel, R.M. Gardiner, A.C. Dolphin, and M. Rees. 2001. Ducky mouse phenotype of epilepsy and ataxia is associated with mutations in the Cacna2d2 gene and decreased calcium channel current in cerebellar Purkinje cells. *The Journal of neuroscience : the official journal of the Society for Neuroscience* 21:6095-6104.

Barkovich, A.J., R. Guerrini, R.I. Kuzniecky, G.D. Jackson, and W.B. Dobyns. 2012. A developmental and genetic classification for malformations of cortical development: update 2012. *Brain : a journal of neurology* 135:1348-1369.

Barkovich, A.J., and B.O. Kjos. 1992. Schizencephaly: correlation of clinical findings with MR characteristics. *AJNR. American journal of neuroradiology* 13:85-94.

Barkovich, A.J., and C.E. Lindan. 1994. Congenital cytomegalovirus infection of the brain: imaging analysis and embryologic considerations. *AJNR. American journal of neuroradiology* 15:703-715.

Barkovich, A.J., H. Rowley, and A. Bollen. 1995. Correlation of prenatal events with the development of polymicrogyria. *AJNR. American journal of neuroradiology* 16:822-827.

Barry, D.S., J.M. Pakan, and K.W. McDermott. 2014. Radial glial cells: key organisers in CNS development. *Int J Biochem Cell Biol* 46:76-79.

Barth, P.G. 1987. Disorders of neuronal migration. *The Canadian journal of neurological sciences. Le journal canadien des sciences neurologiques* 14:1-16.

Bauer, C.S., M. Nieto-Rostro, W. Rahman, A. Tran-Van-Minh, L. Ferron, L. Douglas, I. Kadurin, Y. Sri Ranjan, L. Fernandez-Alacid, N.S. Millar, A.H. Dickenson, R. Lujan, and A.C. Dolphin. 2009. The increased trafficking of the calcium channel subunit alpha2delta-1 to presynaptic terminals in neuropathic pain is inhibited by the alpha2delta ligand pregabalin. *The Journal of neuroscience : the official journal of the Society for Neuroscience* 29:4076-4088.

Bell, A., and K.M. Jacobs. 2014. Early susceptibility for epileptiform activity in malformed cortex. *Epilepsy research* 108:241-250.

Belliotti, T.R., T. Capiris, I.V. Ekhato, J.J. Kinsora, M.J. Field, T.G. Heffner, L.T. Meltzer, J.B. Schwarz, C.P. Taylor, A.J. Thorpe, M.G. Vartanian, L.D. Wise, T. Zhi-Su, M.L. Weber, and D.J. Wustrow. 2005. Structure-activity relationships of pregabalin and analogues that target the alpha(2)-delta protein. *J Med Chem* 48:2294-2307.

Ben-Ari, Y., I. Khalilov, K.T. Kahle, and E. Cherubini. 2012. The GABA excitatory/inhibitory shift in brain maturation and neurological disorders. *The Neuroscientist : a review journal bringing neurobiology, neurology and psychiatry* 18:467-486.

Benardete, E.A., and A.R. Kriegstein. 2002. Increased excitability and decreased sensitivity to GABA in an animal model of dysplastic cortex. *Epilepsia* 43:970-982.

Bertrand, S., G.Y. Ng, M.G. Purisai, S.E. Wolfe, M.W. Severidt, D. Nouel, R. Robitaille, M.J. Low, G.P. O'Neill, K. Metters, J.C. Lacaille, B.M. Chronwall, and S.J. Morris. 2001. The anticonvulsant, antihyperalgesic agent gabapentin is an agonist at

brain gamma-aminobutyric acid type B receptors negatively coupled to voltage-dependent calcium channels. *The Journal of pharmacology and experimental therapeutics* 298:15-24.

Blake, S.M., V. Strasser, N. Andrade, S. Duit, R. Hofbauer, W.J. Schneider, and J. Nimpf. 2008. Thrombospondin-1 binds to ApoER2 and VLDL receptor and functions in postnatal neuronal migration. *EMBO J* 27:3069-3080.

Bordey, A., S.A. Lyons, J.J. Hablitz, and H. Sontheimer. 2001. Electrophysiological characteristics of reactive astrocytes in experimental cortical dysplasia. *Journal of neurophysiology* 85:1719-1731.

Boroujerdi, A., H.K. Kim, Y.S. Lyu, D.S. Kim, K.W. Figueroa, J.M. Chung, and Z.D. Luo. 2008. Injury discharges regulate calcium channel alpha-2-delta-1 subunit upregulation in the dorsal horn that contributes to initiation of neuropathic pain. *Pain* 139:358-366.

Brill, J., and J.R. Huguenard. 2010. Enhanced infragranular and supragranular synaptic input onto layer 5 pyramidal neurons in a rat model of cortical dysplasia. *Cerebral cortex* 20:2926-2938.

Bryans, J.S., and D.J. Wustrow. 1999. 3-substituted GABA analogs with central nervous system activity: a review. *Med Res Rev* 19:149-177.

Burashnikov, E., R. Pfeiffer, H. Barajas-Martinez, E. Delpon, D. Hu, M. Desai, M. Borggrefe, M. Haissaguerre, R. Kanter, G.D. Pollevick, A. Guerchicoff, R. Laino, M. Marieb, K. Nademanee, G.B. Nam, R. Robles, R. Schimpf, D.D. Stapleton, S. Viskin, S. Winters, C. Wolpert, S. Zimmern, C. Veltmann, and C. Antzelevitch. 2010. Mutations in the cardiac L-type calcium channel associated with inherited J-wave syndromes and sudden cardiac death. *Heart Rhythm* 7:1872-1882.

Bystron, I., P. Rakic, Z. Molnar, and C. Blakemore. 2006. The first neurons of the human cerebral cortex. *Nature neuroscience* 9:880-886.

Cahoy, J.D., B. Emery, A. Kaushal, L.C. Foo, J.L. Zamanian, K.S. Christopherson, Y. Xing, J.L. Lubischer, P.A. Krieg, S.A. Krupenko, W.J. Thompson, and B.A. Barres. 2008. A transcriptome database for astrocytes, neurons, and oligodendrocytes: a new resource for understanding brain development and function. *The Journal of neuroscience : the official journal of the Society for Neuroscience* 28:264-278.

Campbell, S., and J.J. Hablitz. 2005. Modification of epileptiform discharges in neocortical neurons following glutamate uptake inhibition. *Epilepsia* 46 Suppl 5:129-133.

Campbell, S.L., and J.J. Hablitz. 2004. Glutamate transporters regulate excitability in local networks in rat neocortex. *Neuroscience* 127:625-635.

Campbell, S.L., and J.J. Hablitz. 2008. Decreased glutamate transport enhances excitability in a rat model of cortical dysplasia. *Neurobiology of disease* 32:254-261.

Campbell, S.L., J.J. Hablitz, and M.L. Olsen. 2014. Functional changes in glutamate transporters and astrocyte biophysical properties in a rodent model of focal cortical dysplasia. *Front Cell Neurosci* 8:425.

Carson, R.P., D.L. Van Nielen, P.A. Winzenburger, and K.C. Ess. 2012. Neuronal and glia abnormalities in Tsc1-deficient forebrain and partial rescue by rapamycin. *Neurobiology of disease* 45:369-380.

Castro, O.W., V.R. Santos, R.Y. Pun, J.M. McKlveen, M. Batie, K.D. Holland, M. Gardner, N. Garcia-Cairasco, J.P. Herman, and S.C. Danzer. 2012. Impact of corticosterone treatment on spontaneous seizure frequency and epileptiform activity in mice with chronic epilepsy. *PloS one* 7:e46044.

Cavus, I., W.S. Kasoff, M.P. Cassaday, R. Jacob, R. Gueorguieva, R.S. Sherwin, J.H. Krystal, D.D. Spencer, and W.M. Abi-Saab. 2005. Extracellular metabolites in the cortex and hippocampus of epileptic patients. *Annals of neurology* 57:226-235.

Chamak, B., V. Morandi, and M. Mallat. 1994. Brain macrophages stimulate neurite growth and regeneration by secreting thrombospondin. *Journal of neuroscience research* 38:221-233.

Chang, B.S., and D.H. Lowenstein. 2003. Epilepsy. *The New England journal of medicine* 349:1257-1266.

Chatrian, G.E., L. Bergamini, D.W. Klass, M. Lennox-Buchthall, and I. Peterson. 1974. A glossary of terms most commonly used by clinical electroencephalographers. *Electroencephalography & Clinical Neurophysiology* 37:538-548.

Chiaretti, A., A. Narducci, F. Novegno, A. Antonelli, F. Pierri, C. Fantacci, C. Di Rocco, and G. Tamburrini. 2011. Effects of nerve growth factor in experimental model of focal microgyria. *Child's nervous system : ChNS : official journal of the International Society for Pediatric Neurosurgery* 27:2117-2122.

Christopherson, K.S., E.M. Ullian, C.C. Stokes, C.E. Mullowney, J.W. Hell, A. Agah, J. Lawler, D.F. Mosher, P. Bornstein, and B.A. Barres. 2005. Thrombospondins are astrocyte-secreted proteins that promote CNS synaptogenesis. *Cell* 120:421-433.

Chu-Shore, C.J., P. Major, S. Camposano, D. Muzykewicz, and E.A. Thiele. 2010. The natural history of epilepsy in tuberous sclerosis complex. *Epilepsia* 51:1236-1241.

Cole, R.L., S.M. Lechner, M.E. Williams, P. Prodanovich, L. Bleicher, M.A. Varney, and G. Gu. 2005. Differential distribution of voltage-gated calcium channel alpha-2 delta (alpha2delta) subunit mRNA-containing cells in the rat central nervous system and the dorsal root ganglia. *The Journal of comparative neurology* 491:246-269.

Cossart, R., C. Bernard, and Y. Ben-Ari. 2005. Multiple facets of GABAergic neurons and synapses: multiple fates of GABA signalling in epilepsies. *Trends in neurosciences* 28:108-115.

Crino, P.B. 2015. Focal Cortical Dysplasia. *Seminars in neurology* 35:201-208.

Crino, P.B., K.L. Nathanson, and E.P. Henske. 2006. The tuberous sclerosis complex. *The New England journal of medicine* 355:1345-1356.

Crome, L. 1952. Microgyria. *The Journal of pathology and bacteriology* 64:479-495.

Cubelos, B., A. Sebastian-Serrano, L. Beccari, M.E. Calcagnotto, E. Cisneros, S. Kim, A. Dopazo, M. Alvarez-Dolado, J.M. Redondo, P. Bovolenta, C.A. Walsh, and M. Nieto. 2010. Cux1 and Cux2 regulate dendritic branching, spine morphology, and synapses of the upper layer neurons of the cortex. *Neuron* 66:523-535.

Cunningham, C.C., J.B. Gorlin, D.J. Kwiatkowski, J.H. Hartwig, P.A. Janmey, H.R. Byers, and T.P. Stossel. 1992. Actin-binding protein requirement for cortical stability and efficient locomotion. *Science* 255:325-327.

Dalic, L., and M.J. Cook. 2016. Managing drug-resistant epilepsy: challenges and solutions. *Neuropsychiatric disease and treatment* 12:2605-2616.

Danbolt, N.C. 2001. Glutamate uptake. *Progress in neurobiology* 65:1-105.

Davies, A., L. Douglas, J. Hendrich, J. Wratten, A. Tran Van Minh, I. Foucault, D. Koch, W.S. Pratt, H.R. Saibil, and A.C. Dolphin. 2006. The calcium channel alpha2delta-2 subunit partitions with CaV2.1 into lipid rafts in cerebellum: implications for localization and function. *The Journal of neuroscience : the official journal of the Society for Neuroscience* 26:8748-8757.

Davies, A., J. Hendrich, A.T. Van Minh, J. Wratten, L. Douglas, and A.C. Dolphin. 2007. Functional biology of the alpha(2)delta subunits of voltage-gated calcium channels. *Trends in pharmacological sciences* 28:220-228.

DeFazio, R.A., and J.J. Hablitz. 2000. Alterations in NMDA receptors in a rat model of cortical dysplasia. *Journal of neurophysiology* 83:315-321.

Diamond, J.S. 2005. Deriving the glutamate clearance time course from transporter currents in CA1 hippocampal astrocytes: transmitter uptake gets faster during development. *The Journal of neuroscience : the official journal of the Society for Neuroscience* 25:2906-2916.

Dobyns, W.B., O. Reiner, R. Carrozzo, and D.H. Ledbetter. 1993. Lissencephaly. A human brain malformation associated with deletion of the LIS1 gene located at chromosome 17p13. *JAMA* 270:2838-2842.

Dolphin, A.C. 2012. Calcium channel auxiliary alpha2delta and beta subunits: trafficking and one step beyond. *Nature reviews. Neuroscience* 13:542-555.

Dubeau, F., D. Tampieri, N. Lee, E. Andermann, S. Carpenter, R. Leblanc, A. Olivier, R. Radtke, J.G. Villemure, and F. Andermann. 1995. Periventricular and subcortical nodular heterotopia. A study of 33 patients. *Brain : a journal of neurology* 118 (Pt 5):1273-1287.

Dulla, C., H. Tani, S. Okumoto, W.B. Frommer, R.J. Reimer, and J.R. Huguenard. 2008. Imaging of glutamate in brain slices using FRET sensors. *Journal of neuroscience methods* 168:306-319.

Dulla, C.G., H. Tani, J. Brill, R.J. Reimer, and J.R. Huguenard. 2013. Glutamate biosensor imaging reveals dysregulation of glutamatergic pathways in a model of developmental cortical malformation. *Neurobiology of disease* 49:232-246.

Dvorak, K., and J. Feit. 1977. Migration of neuroblasts through partial necrosis of the cerebral cortex in newborn rats-contribution to the problems of morphological development and developmental period of cerebral microgyria. Histological and autoradiographical study. *Acta neuropathologica* 38:203-212.

Dvorak, K., J. Feit, and Z. Jurankova. 1978. Experimentally induced focal microgyria and status verrucosus deformis in rats--pathogenesis and interrelation. Histological and autoradiographical study. *Acta neuropathologica* 44:121-129.

Ellis, S.B., M.E. Williams, N.R. Ways, R. Brenner, A.H. Sharp, A.T. Leung, K.P. Campbell, E. McKenna, W.J. Koch, A. Hui, and et al. 1988. Sequence and expression of mRNAs

encoding the alpha 1 and alpha 2 subunits of a DHP-sensitive calcium channel. *Science* 241:1661-1664.

Emmez, H., A.O. Borcek, M. Kaymaz, F. Kaymaz, E. Durdag, S. Civi, O. Gulbahar, S. Aykol, and A. Pasaoglu. 2010. Neuroprotective effects of gabapentin in experimental spinal cord injury. *World neurosurgery* 73:729-734.

Engel, T., B.M. Murphy, S. Hatazaki, E.M. Jimenez-Mateos, C.G. Concannon, I. Woods, J.H. Prehn, and D.C. Henshall. 2010a. Reduced hippocampal damage and epileptic seizures after status epilepticus in mice lacking proapoptotic Puma. *FASEB journal : official publication of the Federation of American Societies for Experimental Biology* 24:853-861.

Engel, T., K. Tanaka, E.M. Jimenez-Mateos, A. Caballero-Caballero, J.H. Prehn, and D.C. Henshall. 2010b. Loss of p53 results in protracted electrographic seizures and development of an aggravated epileptic phenotype following status epilepticus. *Cell death & disease* 1:e79.

Eroglu, C. 2009. The role of astrocyte-secreted matricellular proteins in central nervous system development and function. *J Cell Commun Signal* 3:167-176.

Eroglu, C., N.J. Allen, M.W. Susman, N.A. O'Rourke, C.Y. Park, E. Ozkan, C. Chakraborty, S.B. Mulinyawe, D.S. Annis, A.D. Huberman, E.M. Green, J. Lawler, R. Dolmetsch, K.C. Garcia, S.J. Smith, Z.D. Luo, A. Rosenthal, D.F. Mosher, and B.A. Barres. 2009. Gabapentin receptor alpha2delta-1 is a neuronal thrombospondin receptor responsible for excitatory CNS synaptogenesis. *Cell* 139:380-392.

Faria, L.C., F. Gu, I. Parada, B. Barres, Z.D. Luo, and D.A. Prince. 2017. Epileptiform activity and behavioral arrests in mice overexpressing the calcium channel subunit alpha2delta-1. *Neurobiology of disease* 102:70-80.

Fauser, S., U. Haussler, C. Donkels, S. Huber, J. Nakagawa, M. Prinz, A. Schulze-Bonhage, J. Zentner, and C.A. Haas. 2013. Disorganization of neocortical lamination in focal cortical dysplasia is brain-region dependent: evidence from layer-specific marker expression. *Acta neuropathologica communications* 1:47.

Fauser, S., H.J. Huppertz, T. Bast, K. Strobl, G. Pantazis, D.M. Altenmueller, B. Feil, S. Rona, C. Kurth, D. Rating, R. Korinthenberg, B.J. Steinhoff, B. Volk, and A. Schulze-Bonhage. 2006. Clinical characteristics in focal cortical dysplasia: a retrospective evaluation in a series of 120 patients. *Brain : a journal of neurology* 129:1907-1916.

Felix, R., C.A. Gurnett, M. De Waard, and K.P. Campbell. 1997. Dissection of functional domains of the voltage-dependent Ca2+ channel alpha2delta subunit. *The Journal of neuroscience : the official journal of the Society for Neuroscience* 17:6884-6891.

Field, M.J., P.J. Cox, E. Stott, H. Melrose, J. Offord, T.Z. Su, S. Bramwell, L. Corradini, S. England, J. Winks, R.A. Kinloch, J. Hendrich, A.C. Dolphin, T. Webb, and D. Williams. 2006. Identification of the alpha2-delta-1 subunit of voltage-dependent calcium channels as a molecular target for pain mediating the analgesic actions of pregabalin. *Proceedings of the National Academy of Sciences of the United States of America* 103:17537-17542.

Fitch, R.H., P. Tallal, C.P. Brown, A.M. Galaburda, and G.D. Rosen. 1994. Induced microgyria and auditory temporal processing in rats: a model for language impairment? *Cerebral cortex* 4:260-270.

Fox, J.W., E.D. Lamperti, Y.Z. Eksioglu, S.E. Hong, Y. Feng, D.A. Graham, I.E. Scheffer, W.B. Dobyns, B.A. Hirsch, R.A. Radtke, S.F. Berkovic, P.R. Huttenlocher, and C.A. Walsh. 1998. Mutations in filamin 1 prevent migration of cerebral cortical neurons in human periventricular heterotopia. *Neuron* 21:1315-1325.

Fremeau, R.T., Jr., K. Kam, T. Qureshi, J. Johnson, D.R. Copenhagen, J. Storm-Mathisen, F.A. Chaudhry, R.A. Nicoll, and R.H. Edwards. 2004. Vesicular glutamate transporters 1 and 2 target to functionally distinct synaptic release sites. *Science* 304:1815-1819.

Fukuchi-Shimogori, T., and E.A. Grove. 2001. Neocortex patterning by the secreted signaling molecule FGF8. *Science* 294:1071-1074.

Fukuda, A., and T. Wang. 2013. A perturbation of multimodal GABA functions underlying the formation of focal cortical malformations: assessments by using animal models. *Neuropathology : official journal of the Japanese Society of Neuropathology* 33:480-486.

Fuller-Bicer, G.A., G. Varadi, S.E. Koch, M. Ishii, I. Bodi, N. Kadeer, J.N. Muth, G. Mikala, N.N. Petrashevskaya, M.A. Jordan, S.P. Zhang, N. Qin, C.M. Flores, I. Isaacsohn, M. Varadi, Y. Mori, W.K. Jones, and A. Schwartz. 2009. Targeted disruption of the voltage-dependent calcium channel alpha2/delta-1-subunit. *American journal of physiology. Heart and circulatory physiology* 297:H117-124.

Garcez, P.P., E.C. Loiola, R. Madeiro da Costa, L.M. Higa, P. Trindade, R. Delvecchio, J.M. Nascimento, R. Brindeiro, A. Tanuri, and S.K. Rehen. 2016. Zika virus impairs growth in human neurospheres and brain organoids. *Science* 352:816-818.

Garcia-Moreno, F., L. Lopez-Mascaraque, and J.A. De Carlos. 2007. Origins and migratory routes of murine Cajal-Retzius cells. *The Journal of comparative neurology* 500:419-432.

Gee, N.S., J.P. Brown, V.U. Dissanayake, J. Offord, R. Thurlow, and G.N. Woodruff. 1996. The novel anticonvulsant drug, gabapentin (Neurontin), binds to the alpha2delta subunit of a calcium channel. *The Journal of biological chemistry* 271:5768-5776.

Gleeson, J.G., R.F. Luo, P.E. Grant, R. Guerrini, P.R. Huttenlocher, M.J. Berg, S. Ricci, R. Cusmai, J.W. Wheless, S. Berkovic, I. Scheffer, W.B. Dobyns, and C.A. Walsh. 2000. Genetic and neuroradiological heterogeneity of double cortex syndrome. *Annals of neurology* 47:265-269.

Goa, K.L., and E.M. Sorkin. 1993. Gabapentin. A review of its pharmacological properties and clinical potential in epilepsy. *Drugs* 46:409-427.

Golyala, A., and P. Kwan. 2017. Drug development for refractory epilepsy: The past 25 years and beyond. *Seizure* 44:147-156.

Gong, H.C., J. Hang, W. Kohler, L. Li, and T.Z. Su. 2001. Tissue-specific expression and gabapentin-binding properties of calcium channel alpha2delta subunit subtypes. *The Journal of membrane biology* 184:35-43.

Gonzalez-Martinez, J.A., Z. Ying, R. Prayson, W. Bingaman, and I. Najm. 2011. Glutamate clearance mechanisms in resected cortical dysplasia. *Journal of neurosurgery* 114:1195-1202.

Gotz, M., and Y.A. Barde. 2005. Radial glial cells defined and major intermediates between embryonic stem cells and CNS neurons. *Neuron* 46:369-372.

Gotz, M., A. Stoykova, and P. Gruss. 1998. Pax6 controls radial glia differentiation in the cerebral cortex. *Neuron* 21:1031-1044.

Gressens, P. 2000. Mechanisms and disturbances of neuronal migration. *Pediatric research* 48:725-730.

Guerrini, R., and W.B. Dobyns. 2014. Malformations of cortical development: clinical features and genetic causes. *The Lancet. Neurology* 13:710-726.

Hablitz, J.J., and T. DeFazio. 1998. Excitability changes in freeze-induced neocortical microgyria. *Epilepsy research* 32:75-82.

Hablitz, J.J., and J. Yang. 2010. Abnormal pyramidal cell morphology and HCN channel expression in cortical dysplasia. *Epilepsia* 51 Suppl 3:52-55.

Hanna, G.R., and R.M. Stalmaster. 1973. Cortical epileptic lesions produced by freezing. *Neurology* 23:918-925.

Hanson, E., N.C. Danbolt, and C.G. Dulla. 2016. Astrocyte membrane properties are altered in a rat model of developmental cortical malformation but single-cell astrocytic glutamate uptake is robust. *Neurobiology of disease* 89:157-168.

Hauser, W.A., J.F. Annegers, and L.R. Elveback. 1980. Mortality in patients with epilepsy. *Epilepsia* 21:399-412.

Heck, N., W. Kilb, P. Reiprich, H. Kubota, T. Furukawa, A. Fukuda, and H.J. Luhmann. 2007. GABA-A receptors regulate neocortical neuronal migration in vitro and in vivo. *Cerebral cortex* 17:138-148.

Hendrich, J., A.T. Van Minh, F. Heblich, M. Nieto-Rostro, K. Watschinger, J. Striessnig, J. Wratten, A. Davies, and A.C. Dolphin. 2008. Pharmacological disruption of calcium channel trafficking by the alpha2delta ligand gabapentin. *Proceedings of the National Academy of Sciences of the United States of America* 105:3628-3633.

Hino-Fukuyo, N., A. Kikuchi, N. Arai-Ichinoi, T. Niihori, R. Sato, T. Suzuki, H. Kudo, Y. Sato, T. Nakayama, Y. Kakisaka, Y. Kubota, T. Kobayashi, R. Funayama, K. Nakayama, M. Uematsu, Y. Aoki, K. Haginoya, and S. Kure. 2015. Genomic analysis identifies candidate pathogenic variants in 9 of 18 patients with unexplained West syndrome. *Hum Genet* 134:649-658.

Hirotsune, S., M.W. Fleck, M.J. Gambello, G.J. Bix, A. Chen, G.D. Clark, D.H. Ledbetter, C.J. McBain, and A. Wynshaw-Boris. 1998. Graded reduction of Pafah1b1 (Lis1) activity results in neuronal migration defects and early embryonic lethality. *Nat Genet* 19:333-339.

Hirtz, D., D.J. Thurman, K. Gwinn-Hardy, M. Mohamed, A.R. Chaudhuri, and R. Zalutsky. 2007. How common are the "common" neurologic disorders? *Neurology* 68:326-337.

Hofmann, G., L. Balgooyen, J. Mattis, K. Deisseroth, and P.S. Buckmaster. 2016. Hilar somatostatin interneuron loss reduces dentate gyrus inhibition in a mouse model of temporal lobe epilepsy. *Epilepsia*

Honmou, O., A.A. Oyelese, and J.D. Kocsis. 1995. The anticonvulsant gabapentin enhances promoted release of GABA in hippocampus: a field potential analysis. *Brain research* 692:273-277.

Hoppa, M.B., B. Lana, W. Margas, A.C. Dolphin, and T.A. Ryan. 2012. alpha2delta expression sets presynaptic calcium channel abundance and release probability. *Nature* 486:122-125.

Hughes, E.G., S.B. Elmariah, and R.J. Balice-Gordon. 2010. Astrocyte secreted proteins selectively increase hippocampal GABAergic axon length, branching, and synaptogenesis. *Mol Cell Neurosci* 43:136-145.

Humphreys, P., G.D. Rosen, D.M. Press, G.F. Sherman, and A.M. Galaburda. 1991. Freezing lesions of the developing rat brain: a model for cerebrocortical microgyria. *Journal of neuropathology and experimental neurology* 50:145-160.

Hunter, J.C., K.R. Gogas, L.R. Hedley, L.O. Jacobson, L. Kassotakis, J. Thompson, and D.J. Fontana. 1997. The effect of novel anti-epileptic drugs in rat experimental models of acute and chronic pain. *Eur J Pharmacol* 324:153-160.

Hwang, J.H., and T.L. Yaksh. 1997. Effect of subarachnoid gabapentin on tactile-evoked allodynia in a surgically induced neuropathic pain model in the rat. *Reg Anesth* 22:249-256.

Iffland, P.H., 2nd, and P.B. Crino. 2017. Focal Cortical Dysplasia: Gene Mutations, Cell Signaling, and Therapeutic Implications. *Annu Rev Pathol* 12:547-571.

Ignacio, M.P., E.J. Kimm, G.H. Kageyama, J. Yu, and R.T. Robertson. 1995. Postnatal migration of neurons and formation of laminae in rat cerebral cortex. *Anat Embryol (Berl)* 191:89-100.

Insolera, R., H. Bazzi, W. Shao, K.V. Anderson, and S.H. Shi. 2014. Cortical neurogenesis in the absence of centrioles. *Nature neuroscience* 17:1528-1535.

Ippolito, D.M., and C. Eroglu. 2010. Quantifying synapses: an immunocytochemistry-based assay to quantify synapse number. *Journal of visualized experiments : JoVE*

Iruela-Arispe, M.L., D.J. Liska, E.H. Sage, and P. Bornstein. 1993. Differential expression of thrombospondin 1, 2, and 3 during murine development. *Dev Dyn* 197:40-56.

Jacobs, K.M., M.J. Gutnick, and D.A. Prince. 1996. Hyperexcitability in a model of cortical maldevelopment. *Cerebral cortex* 6:514-523.

Jacobs, K.M., M. Mogensen, E. Warren, and D.A. Prince. 1999. Experimental microgyri disrupt the barrel field pattern in rat somatosensory cortex. *Cerebral cortex* 9:733-744.

Jacobs, K.M., and D.A. Prince. 2005. Excitatory and inhibitory postsynaptic currents in a rat model of epileptogenic microgyria. *Journal of neurophysiology* 93:687-696.

Jacoby, A., and G.A. Baker. 2008. Quality-of-life trajectories in epilepsy: a review of the literature. *Epilepsy & behavior : E&B* 12:557-571.

Jansen, A., and E. Andermann. 2005. Genetics of the polymicrogyria syndromes. *Journal of medical genetics* 42:369-378.

Jay, S.D., A.H. Sharp, S.D. Kahl, T.S. Vedvick, M.M. Harpold, and K.P. Campbell. 1991. Structural characterization of the dihydropyridine-sensitive calcium channel alpha 2-subunit and the associated delta peptides. *The Journal of biological chemistry* 266:3287-3293.

Jensen, A.A., J. Mosbacher, S. Elg, K. Lingenhoehl, T. Lohmann, T.N. Johansen, B. Abrahamsen, J.P. Mattsson, A. Lehmann, B. Bettler, and H. Brauner-Osborne. 2002. The anticonvulsant gabapentin (neurontin) does not act through gamma-aminobutyric acid-B receptors. *Mol Pharmacol* 61:1377-1384.

Jimenez-Mateos, E.M., G. Mouri, R.M. Conroy, and D.C. Henshall. 2010. Epileptic tolerance is associated with enduring neuroprotection and uncoupling of the relationship between CA3 damage, neuropeptide Y rearrangement and spontaneous seizures following intra-amygdala kainic acid-induced status epilepticus in mice. *Neuroscience* 171:556-565.

Jin, X., K. Jiang, and D.A. Prince. 2014. Excitatory and inhibitory synaptic connectivity to layer V fast-spiking interneurons in the freeze lesion model of cortical microgyria. *Journal of neurophysiology* 112:1703-1713.

Jiruska, P., A.D. Powell, W.C. Chang, and J.G. Jefferys. 2010. Electrographic high-frequency activity and epilepsy. *Epilepsy research* 89:60-65.

Kahle, K.T., K.J. Staley, B.V. Nahed, G. Gamba, S.C. Hebert, R.P. Lifton, and D.B. Mount. 2008. Roles of the cation-chloride cotransporters in neurological disease. *Nature clinical practice. Neurology* 4:490-503.

Kakita, A., S. Kameyama, S. Hayashi, H. Masuda, and H. Takahashi. 2005. Pathologic features of dysplasia and accompanying alterations observed in surgical specimens from patients with intractable epilepsy. *Journal of child neurology* 20:341-350.

Kale, A., A.O. Borcek, H. Emmez, Z. Yildirim, E. Durdag, N. Lortlar, G. Kurt, F. Dogulu, and N. Kilic. 2011. Neuroprotective effects of gabapentin on spinal cord ischemia-reperfusion injury in rabbits. *Journal of neurosurgery. Spine* 15:228-237.

Kamada, T., W. Sun, K. Takase, H. Shigeto, S.O. Suzuki, Y. Ohyagi, and J. Kira. 2013. Spontaneous seizures in a rat model of multiple prenatal freeze lesioning. *Epilepsy research* 105:280-291.

Kellinghaus, C., G. Moddel, H. Shigeto, Z. Ying, B. Jacobsson, J. Gonzalez-Martinez, C. Burrier, D. Janigro, and I.M. Najm. 2007. Dissociation between in vitro and in vivo epileptogenicity in a rat model of cortical dysplasia. *Epileptic disorders : international epilepsy journal with videotape* 9:11-19.

Kharazia, V.N., K.M. Jacobs, and D.A. Prince. 2003. Light microscopic study of GluR1 and calbindin expression in interneurons of neocortical microgyral malformations. *Neuroscience* 120:207-218.

Khazipov, R., G. Valeeva, and I. Khalilov. 2015. Depolarizing GABA and developmental epilepsies. *CNS neuroscience & therapeutics* 21:83-91.

Kienzler, F., B.A. Norwood, and R.S. Sloviter. 2009. Hippocampal injury, atrophy, synaptic reorganization, and epileptogenesis after perforant pathway stimulation-induced status epilepticus in the mouse. *The Journal of comparative neurology* 515:181-196.

Kim, Y.K., J.G. Leem, J.Y. Sim, S.M. Jeong, and K.W. Joung. 2010. The effects of gabapentin pretreatment on brain injury induced by focal cerebral ischemia/reperfusion in the rat. *Korean journal of anesthesiology* 58:184-190.

Kim, Y.S., H.K. Chang, J.W. Lee, Y.H. Sung, S.E. Kim, M.S. Shin, J.W. Yi, J.H. Park, H. Kim, and C.J. Kim. 2009. Protective effect of gabapentin on N-methyl-D-aspartate-induced excitotoxicity in rat hippocampal CA1 neurons. *Journal of pharmacological sciences* 109:144-147.

Klaassen, A., J. Glykys, J. Maguire, C. Labarca, I. Mody, and J. Boulter. 2006. Seizures and enhanced cortical GABAergic inhibition in two mouse models of human autosomal dominant nocturnal frontal lobe epilepsy. *Proceedings of the National Academy of Sciences of the United States of America* 103:19152-19157.

Klugbauer, N., L. Lacinova, E. Marais, M. Hobom, and F. Hofmann. 1999. Molecular diversity of the calcium channel alpha2delta subunit. *The Journal of neuroscience : the official journal of the Society for Neuroscience* 19:684-691.

Kondratskyi, A., K. Kondratska, R. Skryma, and N. Prevarskaya. 2015. Ion channels in the regulation of apoptosis. *Biochimica et biophysica acta* 1848:2532-2546.

Krsek, P., A. Jahodova, B. Maton, P. Jayakar, P. Dean, B. Korman, G. Rey, C. Dunoyer, H.V. Vinters, T. Resnick, and M. Duchowny. 2010. Low-grade focal cortical dysplasia is associated with prenatal and perinatal brain injury. *Epilepsia* 51:2440-2448.

Krsek, P., B. Maton, B. Korman, E. Pacheco-Jacome, P. Jayakar, C. Dunoyer, G. Rey, G. Morrison, J. Ragheb, H.V. Vinters, T. Resnick, and M. Duchowny. 2008. Different features of histopathological subtypes of pediatric focal cortical dysplasia. *Annals of neurology* 63:758-769.

Krueger, D.A., A.A. Wilfong, K. Holland-Bouley, A.E. Anderson, K. Agricola, C. Tudor, M. Mays, C.M. Lopez, M.O. Kim, and D.N. Franz. 2013. Everolimus treatment of refractory epilepsy in tuberous sclerosis complex. *Annals of neurology* 74:679-687.

Kurshan, P.T., A. Oztan, and T.L. Schwarz. 2009. Presynaptic alpha2delta-3 is required for synaptic morphogenesis independent of its Ca2+-channel functions. *Nature neuroscience* 12:1415-1423.

Kuzniecky, R. 2015. Epilepsy and malformations of cortical development: new developments. *Current opinion in neurology* 28:151-157.

Kwan, P., and M.J. Brodie. 2000. Early identification of refractory epilepsy. *The New England journal of medicine* 342:314-319.

Kyriakides, T.R., Y.H. Zhu, L.T. Smith, S.D. Bain, Z. Yang, M.T. Lin, K.G. Danielson, R.V. Iozzo, M. LaMarca, C.E. McKinney, E.I. Ginns, and P. Bornstein. 1998. Mice that lack thrombospondin 2 display connective tissue abnormalities that are associated with disordered collagen fibrillogenesis, an increased vascular density, and a bleeding diathesis. *J Cell Biol* 140:419-430.

Lange, M., B. Kasper, A. Bohring, F. Rutsch, G. Kluger, S. Hoffjan, S. Spranger, A. Behnecke, A. Ferbert, A. Hahn, B. Oehl-Jaschkowitz, L. Graul-Neumann, K. Diepold, I. Schreyer, M.K. Bernhard, F. Mueller, U. Siebers-Renelt, A. Beleza-Meireles, G. Uyanik, S. Janssens, E. Boltshauser, J. Winkler, G. Schuierer, and U.

Hehr. 2015. 47 patients with FLNA associated periventricular nodular heterotopia. *Orphanet J Rare Dis* 10:134.

Lawler, J., M. Duquette, C.A. Whittaker, J.C. Adams, K. McHenry, and D.W. DeSimone. 1993. Identification and characterization of thrombospondin-4, a new member of the thrombospondin gene family. *J Cell Biol* 120:1059-1067.

Lawler, J., M. Sunday, V. Thibert, M. Duquette, E.L. George, H. Rayburn, and R.O. Hynes. 1998. Thrombospondin-1 is required for normal murine pulmonary homeostasis and its absence causes pneumonia. *J Clin Invest* 101:982-992.

Lee, J.H., M. Huynh, J.L. Silhavy, S. Kim, T. Dixon-Salazar, A. Heiberg, E. Scott, V. Bafna, K.J. Hill, A. Collazo, V. Funari, C. Russ, S.B. Gabriel, G.W. Mathern, and J.G. Gleeson. 2012. De novo somatic mutations in components of the PI3K-AKT3-mTOR pathway cause hemimegalencephaly. *Nat Genet* 44:941-945.

Lee, V., and J. Maguire. 2013. Impact of inhibitory constraint of interneurons on neuronal excitability. *Journal of neurophysiology* 110:2520-2535.

Leventer, R.J., R. Guerrini, and W.B. Dobyns. 2008. Malformations of cortical development and epilepsy. *Dialogues in clinical neuroscience* 10:47-62.

Li, C.Y., X.L. Zhang, E.A. Matthews, K.W. Li, A. Kurwa, A. Boroujerdi, J. Gross, M.S. Gold, A.H. Dickenson, G. Feng, and Z.D. Luo. 2006. Calcium channel alpha2delta1 subunit mediates spinal hyperexcitability in pain modulation. *Pain* 125:20-34.

Li, H., K.D. Graber, S. Jin, W. McDonald, B.A. Barres, and D.A. Prince. 2012. Gabapentin decreases epileptiform discharges in a chronic model of neocortical trauma. *Neurobiology of disease* 48:429-438.

Li, K.W., Y.P. Yu, C. Zhou, D.S. Kim, B. Lin, K. Sharp, O. Steward, and Z.D. Luo. 2014. Calcium channel alpha2delta1 proteins mediate trigeminal neuropathic pain states associated with aberrant excitatory synaptogenesis. *The Journal of biological chemistry* 289:7025-7037.

Li, N., C.T. Zhao, Y. Wang, and X.B. Yuan. 2010. The transcription factor Cux1 regulates dendritic morphology of cortical pyramidal neurons. *PloS one* 5:e10596.

Liauw, J., S. Hoang, M. Choi, C. Eroglu, M. Choi, G.H. Sun, M. Percy, B. Wildman-Tobriner, T. Bliss, R.G. Guzman, B.A. Barres, and G.K. Steinberg. 2008. Thrombospondins 1 and 2 are necessary for synaptic plasticity and functional recovery after stroke. *Journal of cerebral blood flow and metabolism : official journal of the International Society of Cerebral Blood Flow and Metabolism* 28:1722-1732.

Lin, T.N., G.M. Kim, J.J. Chen, W.M. Cheung, Y.Y. He, and C.Y. Hsu. 2003. Differential regulation of thrombospondin-1 and thrombospondin-2 after focal cerebral ischemia/reperfusion. *Stroke* 34:177-186.

Loscher, W., D. Honack, and C.P. Taylor. 1991. Gabapentin increases aminooxyacetic acid-induced GABA accumulation in several regions of rat brain. *Neuroscience letters* 128:150-154.

Luhmann, H.J. 2015. Models of cortical malformation-Chemical and physical. *Journal of neuroscience methods*

Luhmann, H.J., N. Karpuk, M. Qu, and K. Zilles. 1998. Characterization of neuronal migration disorders in neocortical structures. II. Intracellular in vitro recordings. *Journal of neurophysiology* 80:92-102.

Luhmann, H.J., T. Mittmann, R. Schmidt-Kastner, U.T. Eysel, L.A. Mudrick-Donnon, and U. Heinemann. 1996. Hyperexcitability after focal lesions and transient ischemia in rat neocortex. *Epilepsy research. Supplement* 12:119-128.

Luo, Z.D., N.A. Calcutt, E.S. Higuera, C.R. Valder, Y.H. Song, C.I. Svensson, and R.R. Myers. 2002. Injury type-specific calcium channel alpha 2 delta-1 subunit up-regulation in rat neuropathic pain models correlates with antiallodynic effects of gabapentin. *The Journal of pharmacology and experimental therapeutics* 303:1199-1205.

Luo, Z.D., S.R. Chaplan, E.S. Higuera, L.S. Sorkin, K.A. Stauderman, M.E. Williams, and T.L. Yaksh. 2001. Upregulation of dorsal root ganglion (alpha)2(delta) calcium channel subunit and its correlation with allodynia in spinal nerve-injured rats. *The Journal of neuroscience : the official journal of the Society for Neuroscience* 21:1868-1875.

Macdonald, R.L., and J.L. Barker. 1978. Different actions of anticonvulsant and anesthetic barbiturates revealed by use of cultured mammalian neurons. *Science* 200:775-777.

Maguire, J., and I. Mody. 2009. Steroid hormone fluctuations and GABA(A)R plasticity. *Psychoneuroendocrinology* 34 Suppl 1:S84-90.

Maguire, J.L., B.M. Stell, M. Rafizadeh, and I. Mody. 2005. Ovarian cycle-linked changes in GABA(A) receptors mediating tonic inhibition alter seizure susceptibility and anxiety. *Nature neuroscience* 8:797-804.

Maneuf, Y.P., and A.T. McKnight. 2001. Block by gabapentin of the facilitation of glutamate release from rat trigeminal nucleus following activation of protein kinase C or adenylyl cyclase. *British journal of pharmacology* 134:237-240.

Marchi, N., G. Guiso, S. Caccia, M. Rizzi, B. Gagliardi, F. Noe, T. Ravizza, S. Bassanini, S. Chimenti, G. Battaglia, and A. Vezzani. 2006. Determinants of drug brain uptake in a rat model of seizure-associated malformations of cortical development. *Neurobiology of disease* 24:429-442.

Matsumoto, A., H. Arisaka, Y. Hosokawa, S. Sakuraba, T. Sugita, N. Umezawa, Y. Kaku, K. Yoshida, and S. Kuwana. 2015. Effect of carbamazepine and gabapentin on excitability in the trigeminal subnucleus caudalis of neonatal rats using a voltage-sensitive dye imaging technique. *Biological research* 48:36.

Matsumoto, N., R.J. Leventer, J.A. Kuc, S.K. Mewborn, L.L. Dudlicek, M.B. Ramocki, D.T. Pilz, P.L. Mills, S. Das, M.E. Ross, D.H. Ledbetter, and W.B. Dobyns. 2001. Mutation analysis of the DCX gene and genotype/phenotype correlation in subcortical band heterotopia. *European journal of human genetics : EJHG* 9:5-12.

Mellick, G.A., and L.B. Mellick. 1997. Reflex sympathetic dystrophy treated with gabapentin. *Archives of physical medicine and rehabilitation* 78:98-105.

Molyneaux, B.J., P. Arlotta, J.R. Menezes, and J.D. Macklis. 2007. Neuronal subtype specification in the cerebral cortex. *Nature reviews. Neuroscience* 8:427-437.

Moroni, R.F., B. Cipelletti, F. Inverardi, M.C. Regondi, R. Spreafico, and C. Frassoni. 2011. Development of cortical malformations in BCNU-treated rat, model of cortical dysplasia. *Neuroscience* 175:380-393.

Morris, G., P. Jiruska, J.G. Jefferys, and A.D. Powell. 2016. A New Approach of Modified Submerged Patch Clamp Recording Reveals Interneuronal Dynamics during Epileptiform Oscillations. *Frontiers in neuroscience* 10:519.

Mouri, G., E. Jimenez-Mateos, T. Engel, M. Dunleavy, S. Hatazaki, A. Paucard, S. Matsushima, W. Taki, and D.C. Henshall. 2008. Unilateral hippocampal CA3-predominant damage and short latency epileptogenesis after intra-amygdala microinjection of kainic acid in mice. *Brain research* 1213:140-151.

Narkilahti, S., J. Nissinen, and A. Pitkanen. 2003. Administration of caspase 3 inhibitor during and after status epilepticus in rat: effect on neuronal damage and epileptogenesis. *Neuropharmacology* 44:1068-1088.

Newton, R.A., S. Bingham, P.C. Case, G.J. Sanger, and S.N. Lawson. 2001. Dorsal root ganglion neurons show increased expression of the calcium channel alpha2delta-1 subunit following partial sciatic nerve injury. *Brain Res Mol Brain Res* 95:1-8.

Nieto-Rostro, M., G. Sandhu, C.S. Bauer, P. Jiruska, J.G. Jefferys, and A.C. Dolphin. 2014. Altered expression of the voltage-gated calcium channel subunit alpha(2)delta-1: a comparison between two experimental models of epilepsy and a sensory nerve ligation model of neuropathic pain. *Neuroscience* 283:124-137.

Ning, M., D.A. Sarracino, A.T. Kho, S. Guo, S.R. Lee, B. Krastins, F.S. Buonanno, J.A. Vizcaino, S. Orchard, D. McMullin, X. Wang, and E.H. Lo. 2011. Proteomic temporal profile of human brain endothelium after oxidative stress. *Stroke* 42:37-43.

O'Shea, K.S., L.H. Liu, and V.M. Dixit. 1991. Thrombospondin and a 140 kd fragment promote adhesion and neurite outgrowth from embryonic central and peripheral neurons and from PC12 cells. *Neuron* 7:231-237.

O'Shea, K.S., J.S. Rheinheimer, and V.M. Dixit. 1990. Deposition and role of thrombospondin in the histogenesis of the cerebellar cortex. *J Cell Biol* 110:1275-1283.

Openchowski, P. 1883. Sur l'action localisée du froid, appliqué à la surface de la région corticale du cerveau. *Comptes rendus des Séances et Mémoire de la Société de Biologie* 35:38-43.

Pang, T., R. Atefy, and V. Sheen. 2008. Malformations of cortical development. *Neurologist* 14:181-191.

Park, J., Y.P. Yu, C.Y. Zhou, K.W. Li, D. Wang, E. Chang, D.S. Kim, B. Vo, X. Zhang, N. Gong, K. Sharp, O. Steward, I. Vitko, E. Perez-Reyes, C. Eroglu, B. Barres, F. Zaucke, G. Feng, and Z.D. Luo. 2016. Central Mechanisms Mediating Thrombospondin-4-induced Pain States. *The Journal of biological chemistry* 291:13335-13348.

Parrini, E., V. Conti, W.B. Dobyns, and R. Guerrini. 2016. Genetic Basis of Brain Malformations. *Mol Syndromol* 7:220-233.

Patel, R., C.S. Bauer, M. Nieto-Rostro, W. Margas, L. Ferron, K. Chaggar, K. Crews, J.D. Ramirez, D.L. Bennett, A. Schwartz, A.H. Dickenson, and A.C. Dolphin. 2013. alpha2delta-1 gene deletion affects somatosensory neuron function and delays

mechanical hypersensitivity in response to peripheral nerve damage. *The Journal of neuroscience : the official journal of the Society for Neuroscience* 33:16412-16426.

Patrick, S.L., B.W. Connors, and C.E. Landisman. 2006. Developmental changes in somatostatin-positive interneurons in a freeze-lesion model of epilepsy. *Epilepsy research* 70:161-171.

Payne, J.A., C. Rivera, J. Voipio, and K. Kaila. 2003. Cation-chloride co-transporters in neuronal communication, development and trauma. *Trends in neurosciences* 26:199-206.

Peters, O., C. Redecker, G. Hagemann, C. Bruehl, H.J. Luhmann, and O.W. Witte. 2004. Impaired synaptic plasticity in the surround of perinatally acquired [correction of aquired] dysplasia in rat cerebral cortex. *Cerebral cortex* 14:1081-1087.

Pilz, D.T., N. Matsumoto, S. Minnerath, P. Mills, J.G. Gleeson, K.M. Allen, C.A. Walsh, A.J. Barkovich, W.B. Dobyns, D.H. Ledbetter, and M.E. Ross. 1998. LIS1 and XLIS (DCX) mutations cause most classical lissencephaly, but different patterns of malformation. *Hum Mol Genet* 7:2029-2037.

Rakhade, S.N., and J.A. Loeb. 2008. Focal reduction of neuronal glutamate transporters in human neocortical epilepsy. *Epilepsia* 49:226-236.

Rakic, P. 1974. Neurons in rhesus monkey visual cortex: systematic relation between time of origin and eventual disposition. *Science* 183:425-427.

Rakic, P., R.S. Cameron, and H. Komuro. 1994. Recognition, adhesion, transmembrane signaling and cell motility in guided neuronal migration. *Curr Opin Neurobiol* 4:63-69.

Raol, Y.S., E.C. Budreck, and A.R. Brooks-Kayal. 2003. Epilepsy after early-life seizures can be independent of hippocampal injury. *Annals of neurology* 53:503-511.

Ravizza, T., K. Boer, S. Redeker, W.G. Spliet, P.C. van Rijen, D. Troost, A. Vezzani, and E. Aronica. 2006. The IL-1beta system in epilepsy-associated malformations of cortical development. *Neurobiology of disease* 24:128-143.

Redecker, C., G. Hagemann, R. Kohling, H. Straub, O.W. Witte, and E.J. Speckmann. 2005. Optical imaging of epileptiform activity in experimentally induced cortical malformations. *Experimental neurology* 192:288-298.

Redecker, C., G. Hagemann, O.W. Witte, S. Marret, P. Evrard, and P. Gressens. 1998. Long-term evolution of excitotoxic cortical dysgenesis induced in the developing rat brain. *Brain research. Developmental brain research* 109:109-113.

Redecker, C., H.J. Luhmann, G. Hagemann, J.M. Fritschy, and O.W. Witte. 2000. Differential downregulation of GABAA receptor subunits in widespread brain regions in the freeze-lesion model of focal cortical malformations. *The Journal of neuroscience : the official journal of the Society for Neuroscience* 20:5045-5053.

Rosen, G.D., K.M. Jacobs, and D.A. Prince. 1998. Effects of neonatal freeze lesions on expression of parvalbumin in rat neocortex. *Cerebral cortex* 8:753-761.

Rosen, G.D., D.M. Press, G.F. Sherman, and A.M. Galaburda. 1992. The development of induced cerebrocortical microgyria in the rat. *Journal of neuropathology and experimental neurology* 51:601-611.

Rosen, G.D., E.A. Sigel, G.F. Sherman, and A.M. Galaburda. 1995. The neuroprotective effects of MK-801 on the induction of microgyria by freezing injury to the newborn rat neocortex. *Neuroscience* 69:107-114.

Rosner, H., L. Rubin, and A. Kestenbaum. 1996. Gabapentin adjunctive therapy in neuropathic pain states. *The Clinical journal of pain* 12:56-58.

Ryvlin, P., J.H. Cross, and S. Rheims. 2014. Epilepsy surgery in children and adults. *The Lancet. Neurology* 13:1114-1126.

Sakakibara, T., S. Sukigara, T. Otsuki, A. Takahashi, Y. Kaneko, T. Kaido, Y. Saito, N. Sato, E. Nakagawa, K. Sugai, M. Sasaki, Y. Goto, and M. Itoh. 2012. Imbalance of interneuron distribution between neocortex and basal ganglia: consideration of epileptogenesis of focal cortical dysplasia. *Journal of the neurological sciences* 323:128-133.

Sansregret, L., and A. Nepveu. 2008. The multiple roles of CUX1: insights from mouse models and cell-based assays. *Gene* 412:84-94.

Satzinger, G. 1994. Antiepileptics from gamma-aminobutyric acid. *Arzneimittel-Forschung* 44:261-266.

Scantlebury, M.H., P.L. Ouellet, C. Psarropoulou, and L. Carmant. 2004. Freeze lesion-induced focal cortical dysplasia predisposes to atypical hyperthermic seizures in the immature rat. *Epilepsia* 45:592-600.

Schumacher, T.B., H. Beck, C. Steinhauser, J. Schramm, and C.E. Elger. 1998. Effects of phenytoin, carbamazepine, and gabapentin on calcium channels in hippocampal granule cells from patients with temporal lobe epilepsy. *Epilepsia* 39:355-363.

Schwarz, P., C.C. Stichel, and H.J. Luhmann. 2000. Characterization of neuronal migration disorders in neocortical structures: loss or preservation of inhibitory interneurons? *Epilepsia* 41:781-787.

Segal, A.Z., and G. Rordorf. 1996. Gabapentin as a novel treatment for postherpetic neuralgia. *Neurology* 46:1175-1176.

Shah, M.M. 2014. Cortical HCN channels: function, trafficking and plasticity. *The Journal of physiology* 592:2711-2719.

Shain, C., S. Ramgopal, Z. Fallil, I. Parulkar, R. Alongi, R. Knowlton, A. Poduri, and E. Investigators. 2013. Polymicrogyria-associated epilepsy: a multicenter phenotypic study from the Epilepsy Phenome/Genome Project. *Epilepsia* 54:1368-1375.

Sheen, V.L., P.H. Dixon, J.W. Fox, S.E. Hong, L. Kinton, S.M. Sisodiya, J.S. Duncan, F. Dubeau, I.E. Scheffer, S.C. Schachter, A. Wilner, R. Henchy, P. Crino, K. Kamuro, F. DiMario, M. Berg, R. Kuzniecky, A.J. Cole, E. Bromfield, M. Biber, D. Schomer, J. Wheless, K. Silver, G.H. Mochida, S.F. Berkovic, F. Andermann, E. Andermann, W.B. Dobyns, N.W. Wood, and C.A. Walsh. 2001. Mutations in the X-linked filamin 1 gene cause periventricular nodular heterotopia in males as well as in females. *Hum Mol Genet* 10:1775-1783.

Shimizu-Okabe, C., A. Okabe, W. Kilb, K. Sato, H.J. Luhmann, and A. Fukuda. 2007. Changes in the expression of cation-Cl- cotransporters, NKCC1 and KCC2, during cortical malformation induced by neonatal freeze-lesion. *Neuroscience research* 59:288-295.

Sidman, R.L., and P. Rakic. 1973. Neuronal migration, with special reference to developing human brain: a review. *Brain research* 62:1-35.
Sisodiya, S.M. 2000. Surgery for malformations of cortical development causing epilepsy. *Brain : a journal of neurology* 123 (Pt 6):1075-1091.
Smith, T.G., Jr., and D.P. Purpura. 1960. Electrophysiological studies on epileptogenic lesions of cat cortex. *Electroencephalography and clinical neurophysiology* 12:59-82.
Squier, W., and A. Jansen. 2014. Polymicrogyria: pathology, fetal origins and mechanisms. *Acta neuropathologica communications* 2:80.
Stacey, B.R., J.A. Barrett, E. Whalen, K.F. Phillips, and M.C. Rowbotham. 2008. Pregabalin for postherpetic neuralgia: placebo-controlled trial of fixed and flexible dosing regimens on allodynia and time to onset of pain relief. *J Pain* 9:1006-1017.
Stalmaster, R.M., and G.R. Hanna. 1972. Epileptic phenomena of cortical freezing in the cat: persistent multifocal effects of discrete superficial lesions. *Epilepsia* 13:313-324.
Stanfa, L.C., L. Singh, R.G. Williams, and A.H. Dickenson. 1997. Gabapentin, ineffective in normal rats, markedly reduces C-fibre evoked responses after inflammation. *Neuroreport* 8:587-590.
Stefani, A., F. Spadoni, and G. Bernardi. 1998. Gabapentin inhibits calcium currents in isolated rat brain neurons. *Neuropharmacology* 37:83-91.
Steinhauser, C., G. Seifert, and P. Bedner. 2012. Astrocyte dysfunction in temporal lobe epilepsy: K+ channels and gap junction coupling. *Glia* 60:1192-1202.
Stutterd, C.A., and R.J. Leventer. 2014. Polymicrogyria: a common and heterogeneous malformation of cortical development. *American journal of medical genetics. Part C, Seminars in medical genetics* 166C:227-239.
Sun, Q.Q., J.R. Huguenard, and D.A. Prince. 2005. Reorganization of Barrel Circuits Leads to Thalamically-Evoked Cortical Epileptiform Activity. *Thalamus & related systems* 3:261-273.
Sun, Q.Q., C. Zhou, W. Yang, and D. Petrus. 2016. Continuous spike-waves during slow-wave sleep in a mouse model of focal cortical dysplasia. *Epilepsia* 57:1581-1593.
Takano, T., C. Sawai, and Y. Takeuchi. 2004. Radial and tangential neuronal migration disorder in ibotenate-induced cortical lesions in hamsters: immunohistochemical study of reelin, vimentin, and calretinin. *Journal of child neurology* 19:107-115.
Takase, K., H. Shigeto, S.O. Suzuki, H. Kikuchi, Y. Ohyagi, and J. Kira. 2008. Prenatal freeze lesioning produces epileptogenic focal cortical dysplasia. *Epilepsia* 49:997-1010.
Taylor, C.P., T. Angelotti, and E. Fauman. 2007. Pharmacology and mechanism of action of pregabalin: the calcium channel alpha2-delta (alpha2-delta) subunit as a target for antiepileptic drug discovery. *Epilepsy research* 73:137-150.
Taylor, C.P., and R. Garrido. 2008. Immunostaining of rat brain, spinal cord, sensory neurons and skeletal muscle for calcium channel alpha2-delta (alpha2-delta) type 1 protein. *Neuroscience* 155:510-521.

Taylor, C.P., M.G. Vartanian, R. Andruszkiewicz, and R.B. Silverman. 1992. 3-alkyl GABA and 3-alkylglutamic acid analogues: two new classes of anticonvulsant agents. *Epilepsy research* 11:103-110.

Taylor, D.C., M.A. Falconer, C.J. Bruton, and J.A. Corsellis. 1971. Focal dysplasia of the cerebral cortex in epilepsy. *Journal of neurology, neurosurgery, and psychiatry* 34:369-387.

Templin, C., J.R. Ghadri, J.S. Rougier, A. Baumer, V. Kaplan, M. Albesa, H. Sticht, A. Rauch, C. Puleo, D. Hu, H. Barajas-Martinez, C. Antzelevitch, T.F. Luscher, H. Abriel, and F. Duru. 2011. Identification of a novel loss-of-function calcium channel gene mutation in short QT syndrome (SQTS6). *Eur Heart J* 32:1077-1088.

Thornton, G.K., and C.G. Woods. 2009. Primary microcephaly: do all roads lead to Rome? *Trends Genet* 25:501-510.

Tomson, T., L. Nashef, and P. Ryvlin. 2008. Sudden unexpected death in epilepsy: current knowledge and future directions. *The Lancet. Neurology* 7:1021-1031.

Traa, B.S., J.D. Mulholland, S.D. Kadam, M.V. Johnston, and A.M. Comi. 2008. Gabapentin neuroprotection and seizure suppression in immature mouse brain ischemia. *Pediatric research* 64:81-85.

Tran-Van-Minh, A., and A.C. Dolphin. 2010. The alpha2delta ligand gabapentin inhibits the Rab11-dependent recycling of the calcium channel subunit alpha2delta-2. *The Journal of neuroscience : the official journal of the Society for Neuroscience* 30:12856-12867.

van Landeghem, F.K., T. Weiss, M. Oehmichen, and A. von Deimling. 2006. Decreased expression of glutamate transporters in astrocytes after human traumatic brain injury. *Journal of neurotrauma* 23:1518-1528.

Vergult, S., A. Dheedene, A. Meurs, F. Faes, B. Isidor, S. Janssens, A. Gautier, C. Le Caignec, and B. Menten. 2015. Genomic aberrations of the CACNA2D1 gene in three patients with epilepsy and intellectual disability. *Eur J Hum Genet* 23:628-632.

Wang, B., W. Guo, and Y. Huang. 2012. Thrombospondins and synaptogenesis. *Neural regeneration research* 7:1737-1743.

Wang, J.L., G.L. Jin, Z.G. Yuan, X.B. Yu, J.Q. Li, T.L. Qiu, and R.X. Dai. 2016. Plasma thrombospondin-1 and clinical outcomes in traumatic brain injury. *Acta neurologica Scandinavica* 134:189-196.

Wang, T., T. Kumada, T. Morishima, S. Iwata, T. Kaneko, Y. Yanagawa, S. Yoshida, and A. Fukuda. 2014. Accumulation of GABAergic neurons, causing a focal ambient GABA gradient, and downregulation of KCC2 are induced during microgyrus formation in a mouse model of polymicrogyria. *Cerebral cortex* 24:1088-1101.

Watanabe, M., and A. Fukuda. 2015. Development and regulation of chloride homeostasis in the central nervous system. *Frontiers in cellular neuroscience* 9:371.

Watanabe, M., M. Hitomi, K. van der Wee, F. Rothenberg, S.A. Fisher, R. Zucker, K.K. Svoboda, E.C. Goldsmith, K.M. Heiskanen, and A.L. Nieminen. 2002. The pros and cons of apoptosis assays for use in the study of cells, tissues, and organs. *Microscopy and microanalysis : the official journal of Microscopy Society of*

America, Microbeam Analysis Society, Microscopical Society of Canada 8:375-391.

Wheeler, G. 2002. Gabapentin. Pfizer. *Curr Opin Investig Drugs* 3:470-477.

Williams, A.J., C.C. Bautista, R.W. Chen, J.R. Dave, X.C. Lu, F.C. Tortella, and J.A. Hartings. 2006. Evaluation of gabapentin and ethosuximide for treatment of acute nonconvulsive seizures following ischemic brain injury in rats. *The Journal of pharmacology and experimental therapeutics* 318:947-955.

Williams, A.J., C. Zhou, and Q.Q. Sun. 2016. Enhanced Burst-Suppression and Disruption of Local Field Potential Synchrony in a Mouse Model of Focal Cortical Dysplasia Exhibiting Spike-Wave Seizures. *Frontiers in neural circuits* 10:93.

Wonders, C.P., and S.A. Anderson. 2006. The origin and specification of cortical interneurons. *Nature reviews. Neuroscience* 7:687-696.

Wong, M. 2008. Mechanisms of epileptogenesis in tuberous sclerosis complex and related malformations of cortical development with abnormal glioneuronal proliferation. *Epilepsia* 49:8-21.

Wong, M. 2009. Animal models of focal cortical dysplasia and tuberous sclerosis complex: recent progress toward clinical applications. *Epilepsia* 50 Suppl 9:34-44.

Wong, M., and S.N. Roper. 2016. Genetic animal models of malformations of cortical development and epilepsy. *Journal of neuroscience methods* 260:73-82.

Xiao, W., A. Boroujerdi, G.J. Bennett, and Z.D. Luo. 2007. Chemotherapy-evoked painful peripheral neuropathy: analgesic effects of gabapentin and effects on expression of the alpha-2-delta type-1 calcium channel subunit. *Neuroscience* 144:714-720.

Yang, R.H., W.T. Wang, J.Y. Chen, R.G. Xie, and S.J. Hu. 2009. Gabapentin selectively reduces persistent sodium current in injured type-A dorsal root ganglion neurons. *Pain* 143:48-55.

Yashiro, K., and B.D. Philpot. 2008. Regulation of NMDA receptor subunit expression and its implications for LTD, LTP, and metaplasticity. *Neuropharmacology* 55:1081-1094.

Yeh, C.Y., S.C. Chung, F.L. Tseng, Y.C. Tsai, and Y.C. Liu. 2011. Biphasic effects of chronic intrathecal gabapentin administration on the expression of protein kinase C gamma in the spinal cord of neuropathic pain rats. *Acta anaesthesiologica Taiwanica : official journal of the Taiwan Society of Anesthesiologists* 49:144-148.

Zeng, L.H., L. Xu, D.H. Gutmann, and M. Wong. 2008. Rapamycin prevents epilepsy in a mouse model of tuberous sclerosis complex. *Annals of neurology* 63:444-453.

Zhang, S., S. Khanna, and F.R. Tang. 2009. Patterns of hippocampal neuronal loss and axon reorganization of the dentate gyrus in the mouse pilocarpine model of temporal lobe epilepsy. *Journal of neuroscience research* 87:1135-1149.

Zhang, Y., K. Chen, S.A. Sloan, M.L. Bennett, A.R. Scholze, S. O'Keeffe, H.P. Phatnani, P. Guarnieri, C. Caneda, N. Ruderisch, S. Deng, S.A. Liddelow, C. Zhang, R. Daneman, T. Maniatis, B.A. Barres, and J.Q. Wu. 2014. An RNA-sequencing transcriptome and splicing database of glia, neurons, and vascular cells of the cerebral cortex. *The Journal of neuroscience : the official journal of the Society for Neuroscience* 34:11929-11947.

Zilles, K., M. Qu, A. Schleicher, and H.J. Luhmann. 1998. Characterization of neuronal migration disorders in neocortical structures: quantitative receptor autoradiography of ionotropic glutamate, GABA(A) and GABA(B) receptors. *The European journal of neuroscience* 10:3095-3106.

Zsombok, A., and K.M. Jacobs. 2007. Postsynaptic currents prior to onset of epileptiform activity in rat microgyria. *Journal of neurophysiology* 98:178-186.